A Study of Post-Combustion Point Source Carbon Capture by Chemical Absorption to Develop a Technology Selection Matrix

Jeppe W. Møller
Thermal Energy & Process Engineering, TEPE4-1008, 2025-06

4th M.Sc. Semester Project - Master Thesis

AAU Energy
Aalborg University
http://www.aau.dk

AALBORG UNIVERSITY
STUDENT REPORT

Title:
A Study of Post-Combustion Point Source Carbon Capture by Chemical Absorption to Develop a Technology Selection Matrix

Theme:
Master Thesis

Project Period:
Spring Semester 2025

Project Group:
TEPE4-1008

Participants:
Jeppe Winther Møller

Supervisor:
Thomas Helmer Pedersen

Number of Pages: 69

Date of Completion:
May 28th - 2025

Abstract:

This thesis presents a comparative study of three mature chemisorption-based *Carbon Capture* (CC) technologies: *Monoethanolamine* (MEA), *Potassium Carbonate with Carbonic Anhydrase* (PCCA), and *Chilled Ammonia Process* (CAP), for post-combustion point sources. A selection matrix tool was developed to evaluate these technologies across standardized flue gas compositions from waste incineration, biomass, and natural gas combustion. Equilibrium-based process models were created in Aspen Plus, and a parametric study identified optimal operating conditions. *Key Performance Indicators* (KPI)s such as CO_2 recovery, energy consumption, and solvent and water make-up were used to assess performance. The CAP demonstrated the lowest energy and water demands, while PCCA offered high adaptability through low-temperature regeneration. Heat integration analyses further extended the comparative overview of the CC technologies. A real-world case study on a waste-to-energy plant investigated the tools applicability to constraints. The updated net electricity output was determined to be -0.2, 5.0, 4.8, and 2.2 MW for MEA, PCCA, CAP, and PCCA with integrated high-temperature heat pump, respectively. The optimal CC technology was PCCA due to the lower penalty on electricity generation while upholding a district heating constraint. The study concludes that the selection matrix provides a robust screening framework for identifying the most suitable CC technology based on technical performance and integration potential, while including specific case constraints.

The content of this report is freely available and may be used in publications with reference. By accepting the request from the fellow student who uploads the study groups project report in Digital Exam System, you confirm that all group members have participated in the project work, and thereby all members are collectively liable for the contents of the report. Furthermore, all group members confirm that the report does not include plagiarism.

Summary

This thesis investigates the performance of three mature chemisorption-based *Carbon Capture* (CC) technologies. The three CC technologies are *Monoethanolamine* (MEA), *Potassium Carbonate with Carbonic Anhydrase* (PCCA), and *Chilled Ammonia Process* (CAP). This thesis revolves around post-combustion point sources. The study aims to develop a selection matrix for systematically comparing CC technologies across standardized point sources, reflecting industrial processes and heat and power production plants. The selection matrix is based on the technical performance of the CC technologies.

The motivation arises from the fast need to reduce CO_2 emissions from hard-to-abate sectors such as power generation and industrial processes. Post-combustion CC is particularly relevant due to the retrofitting potential for existing plants, avoiding the need to redesign or construct new plants. The study focuses on three representative flue gas sources: waste incineration, biomass combustion, and natural gas combustion. These sources were chosen to reflect a range of CO_2 concentrations and compositions, and to align with future decarbonization goals.

Each CC technology was modeled using Aspen Plus to obtain three adaptable process flowsheet models. These equilibrium-based models evaluate the thermodynamic and chemical performance of the CC technologies. The CC process models incorporate detailed process configurations from the flue gas inlet until the compressed CO_2 product. These configurations include an absorber, desorber, heat exchanger, and multi-stage compressor. The developed process models were investigated in a parametric study to determine the optimal operating conditions. The variables in focus were *Liquid-to-Gas ratio* (L/G), lean solvent temperature, flue gas temperature, and reboiler duty. The results showed that reboiler duty and L/G had the most significant impact on performance, while temperature variations had a lesser effect. The key takeaway from the parametric studies is the optimal L/G values of 3.3, 3.9, and 1.7 kg/kg for MEA, PCCA, and CAP, respectively, reflecting the difference in CO_2 absorption capacity between the solvents.

Key Performance Indicators (KPI)s were defined to systematically compare the technologies in the selection matrix. These included CO_2 recovery, *Specific Primary Energy Consumption per CO_2 Avoided* (SPECCA), *Electrical Work per Avoided CO_2* (EWA), water and solvent make-up, and the purity of the recovered CO_2. The CAP demonstrated the lowest SPECCA of 2.5 to 2.8 MJ/kgCO_2 and water make-up of 0.2 kg/kgCO_2 across the three standardized point sources, making it the optimal CC technology across the three technologies. MEA showed robust performance across all scenarios but required higher energy and water make-up. PCCA, while offering low regeneration temperatures and the potential for full electrification, was limited in CO_2 recovery and resulted in higher compression energy due to its low-pressure desorption, reflecting the EWA scores of 0.3, 0.4, and 0.2 to 0.3 for MEA, PCCA, and CAP, respectively. The variations for the CAP rose due to the chiller's work to maintain low operation temperatures.

Pinch analyses were performed to include the heat integration potentials, extending the selection matrix comparison of the CC technologies. These analyses demonstrated that MEA and CAP show unfavorable characteristics due to the need for steam at 130 and 150 °C, respectively, limiting the integration flexibility. In contrast, PCCA can operate with low-grade heat, making it more adaptable, especially when integrated with a high-temperature *Heat Pump* (HP). The PCCA-HP configuration eliminated the hot utility requirements, with the penalty being a 160 % increase in electricity demand. The utility requirements were normalized against avoided CO_2, where the hot utility requirement showed results of 3.6, 2.8, 2.5, and 0.0 MJ/kgCO_2 for MEA, PCCA, CAP, and PCCA-HP, respectively. The cold utility requirements were 5.0, 4.1, 4.8, and 2.1 MJ/kgCO_2, respectively. The extension of the selection matrix by the heat integration analyses provided a broader comparison.

A real-world case study involving a *Waste-to-Energy* (WtE) plant was used to validate the selection matrix. The study evaluated each CC technology's integration into the WtE plant. Steam was extracted to sustain the CC technologies, imposing penalties on the electricity and district heating production from the WtE plant. The district heating production was constrained to the original production. CAP emerged as the most favorable heat integration option due to its low process heat penalty and low hot utility requirement after integration. PCCA imposed no penalty on electricity generation but had the highest process heat penalty. Yet, PCCA showed the greatest net electrical output while meeting the district heating constraint. The PCCA-HP was unfavored over PCCA and CAP even without extracting steam, showing that heat integration benefits the CC implementation. The updated net electricity outputs were determined to be -0.2, 5.0, 4.8, and 2.2 MW for MEA, PCCA, CAP, and PCCA-HP, respectively, reflecting PCCA as the optimal CC technology in this conducted case study.

In conclusion, the selection matrix developed in this thesis provides a practical and adaptable tool for evaluating CC technologies based on technical and integration constraints. It enables process designers to make informed decisions tailored to specific plant conditions. While CAP generally performed best across the defined KPIs and showed the optimal heat integration possibility, the optimal choice remains case-dependent. Yet, the selection matrix tool developed provides a sharp analytical ability for comparing mature chemisorption CC technologies regarding thermodynamics and chemistry, and heat integration possibilities to determine an optimal one based on specific case constraints.

Preface

This master project is completed by Jeppe Winther Møller, the only student in the 4th semester M.Sc. group TEPE4-1008 from AAU Energy at Aalborg University. I want to acknowledge the supervisor of this project, Thomas Helmer Pedersen. Additionally, the help and guidance from Sebastian Bruhn Petersen from Aalborg University. A huge gratitude to Hazel Reardon and Jeppe Grue from Niras for supporting the project proposal for this thesis and guidance regarding the topic and decisions.

Expectations for the Reader

It is expected from the reader to have a general knowledge of thermodynamic and chemical principles to understand the perspectives from this thesis.

Reading Guide for the Project

The report is structured in chapters, sections, and subsections. Throughout the project report, figures, tables, equations, and reactions are used, which are numbered individually. The references implemented throughout the report are presented with the Harvard referencing method. An Appendix is attached after the bibliography, where figures, estimations, and additional contents of the report are included. The Appendix is an attached part of the project, and a printout is recommended.

The following software is used in the project:

- AspenTech - Aspen Plus V12.1
- F-Chart Software - Engineering Equation Solver (EES)
- Mathworks - MATLAB
- Microsoft - Office365
- Overleaf - LaTeX
- Draw.io AG & JGraph Ltd - Draw.io

Jeppe Winther Møller Signature: Jeppe Møller

Nomenclature

Abbriviation	Explanation
CA	Carbonic Anhydrase
CAP	Chilled Ammonia Process
CC	Carbon Capture
CCGT	Combined Cycle Gas Turbine
CCS	Carbon Capture and Storage
CCUS	Carbon Capture Utilization and Storage
CCC	Cold Composite Curve
CHP	Combined Heat and Power
CW	Cooling Water
DAC	Direct Air Capture
DEA	Danish Energy Agency
DH	District Heating
ELECNRTL	Electrolyte Non-Random Two-Liquid
GCC	Grand Composite Curve
GHG	Greenhouse Gas
HCC	Hot Composite Curve
HP	Heat Pump
HPW	Heat Pump Water
IEA	International Energy Agency
IPCC	Intergovernmental Panel on Climate Change
KPI	Key Performance Indicator
LMTD	Log-Mean Temperature Difference
LPS	Low-Pressure Steam
MEA	Monoethanolamine
MPS	Medium-Pressure Steam
MVR	Mechanical Vapor Recompression
PCCA	Potassium Carbonate with Carbonic Anhydrase
PCCA-HP	PCCA with integrated high-temperature Heat Pump
PSCC	Point Source Carbon Capture
TRL	Technological Readiness Level
WtE	Waste-to-Energy

Symbol	Explanation	Unit
COP	Coefficient of Performance	[-]
EWA	Electrical Work per Avoided CO_2	[MJ/kgCO_2]
H	Henry's constant	[Pa]
L/G	Liquid-to-Gas ratio	[kg/kg]
$\dot{m}$	Mass flow rate	[tonne/h]
$\dot{n}$	Molar flow rate	[kmol/h]
P	Pressure	[bar]
p	Partial pressure	[Pa]
$\dot{Q}$	Power	[W]
R_{CO_2}	CO_2 recovery	[%]
SPECCA	Specific Primary Energy Consumption per CO_2 Avoided	[MJ/kgCO_2]
T	Temperature	[°C]
U	Overall heat transfer coefficient	kW/m^2·K
$\dot{W}$	Work	[MW]
y	Molar fraction	[-]
γ	Solvent loading	[kmol/kmol]

Chemical	**Name**	**Molar weight** [g/mol]
CO_2	Carbon dioxide	44.01
CO_3^{2-}	Carbonate ion	60.01
H^+	Proton	1.01
H_2O	Water	18.02
HCO_3^-	Bicarbonate	61.02
K^+	Potassium ion	39.10
K_2CO_3	Potassium carbonate	138.21
MEA	Monoethanolamine	61.08
MEA^+	Protonated Monoethanolamine	62.09
$MEACOO^-$	Carbamate of Monoethanolamine	104.10
MEACOOH	Carbamate of Monoethanolamine	105.11
N_2	Nitrogen	28.01
NH_2COO^-	Carbamate	60.03
NH_2COONH_4	Ammonium carbamate	78.06
NH_3	Ammonia	17.03
NH_4^+	Ammonium	18.04
NH_4HCO_3	Ammonium bicarbonate	96.09
NO_2	Nitrogen dioxide	46.01
O_2	Oxygen	32.00
OH^-	Hydroxide	17.01
SO_2	Sulfur dioxide	64.07

Contents

List of Figures

List of Tables

Chapter 1

Introduction

Climate change results from human activity, more precisely deforestation and consumption of fossil fuels, causing the global temperature to increase [Friedlingstein et al., 2022]. Figure 1.1 displays the development of CO_2 concentration due to human activity from 1958 to the present.

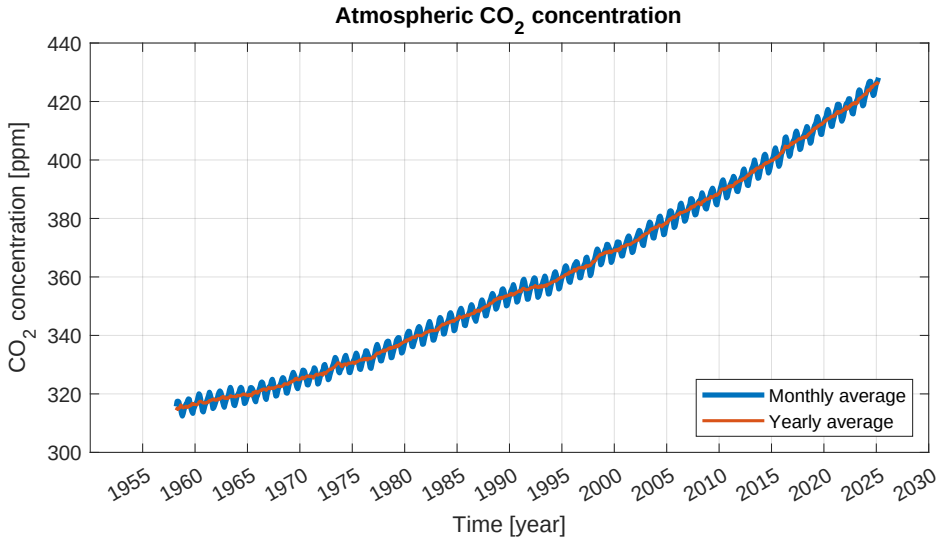

Figure 1.1: Development of CO_2 concentration in the atmosphere from 1958-2025 [NOAA, 2025].

The CO_2 concentration has drastically increased and is indicated to keep increasing unless action is taken. As a result, the Paris Agreement was signed by 196 countries in 2015 to ensure the global temperature increase is kept below 1.5 °C pre-industrial levels [UNFCCC, 2022]. This constitutes decreasing *Greenhouse Gas* (GHG) emissions and reaching the goal of net-zero CO_2 emissions by 2050.

The major CO_2-emitting sectors today are the production of electricity and heat and cooling for buildings, etc. (43.8 %), transportation (23.3 %), and industry (18.4 %) [IEA, 2025]. Out-phasing fossil fuels with renewable solutions to decarbonize the CO_2-emitting sectors has been a hot topic for decades. Yet, decarbonizing important industrial processes is difficult due to limited alternative options. This involves industries as cement, paper, metal/steel, and chemicals, which produce materials where CO_2 is a consequence. Additionally, electricity and heat production by coal and natural gas operating on a large scale is difficult to replace with renewable sources due to unstable production. The *Intergovernmental Panel on Climate Change* (IPCC) hereby states that to reach the international goals of net-zero CO_2 emissions, *Carbon Capture and Storage* (CCS) is necessary to compensate for these CO_2-emissions and reach the goals in time [Masson-Delmotte et al., 2018].

1.1 Carbon Capture Utilization and Storage

Carbon Capture Utilization and Storage (CCUS) involves capturing CO_2 and either utilizing it in producing fuels, chemicals, etc., or storing it underground away from the atmosphere. Utilization involves capturing CO_2 to utilize it for a product, replacing fossil fuels, thereby entering it into a carbon-neutral loop. Conversely, storage or sequestration enables the carbon-negative possibility necessary to remove the already lingering CO_2 emitted due to human activities since industrialization began. CCS concerns capturing CO_2 emission from a carbon source, compression and transportation of CO_2, and storing CO_2 underground, as in boreholes previously used to extract oil. Storing biogenic CO_2 in underground reservoirs is recognized as a carbon-negative option by the parties involved in the Paris Agreement. Storing non-biogenic CO_2 is only carbon-neutral. [Haszeldine et al., 2018]

CC can occur as *Point Source Carbon Capture* (PSCC) or *Direct Air Capture* (DAC). The easiest and quickest way to decrease CO_2 emission is by PSCC due to the CO_2 concentration at the point source being higher than in the atmosphere [Hekmatmehr et al., 2024, DEA, 2024].

Incorporating a CC system on a point source (flue gas) requires assessing the system in detail to understand which CC technology is best-suited for the process. Integrating CCUS demands planning, and each technology is difficult to compare due to differences in system, economy, and scalability. Furthermore, purification, compression, and transportation are other aspects that need attention. [Baker et al., 2022]

In literature, CC technologies with implementation on different point sources are widely researched, however, a decision-making tool to compare and rank technologies across point sources is lacking for determining which technology integrates best with the carbon-emitting process. [Baker et al., 2022, DEA, 2024, Hekmatmehr et al., 2024]

Utilization and sequestration have their demands in the purity of CO_2 depending on the specific process. Incentives from the IPCC and EU are made to reduce CO_2-emissions to reach the common goals of the Paris Agreement. Regardless of utilization or storage, the CO_2 purification, compression, and transportation are similar. The crucial aspect in determining the best CC technology requires evaluating the integration with the carbon-emitting source. As a result, this study aims to compare CC technologies across point sources to indicate which key parameters will determine the best-suited technology.

Chapter 2

State of the Art

2.1 Point Source Carbon Capture

PSCC concerns stripping CO_2 from flue gas. The flue gas can emerge from different kinds of processes such as pre-combustion, post-combustion, and oxy-fuel combustion, where the latter is fairly new and demands pure oxygen. The key difference is dependent on where the CO_2 is emitted in the process. Figure 2.1 illustrates the differences between these point sources.

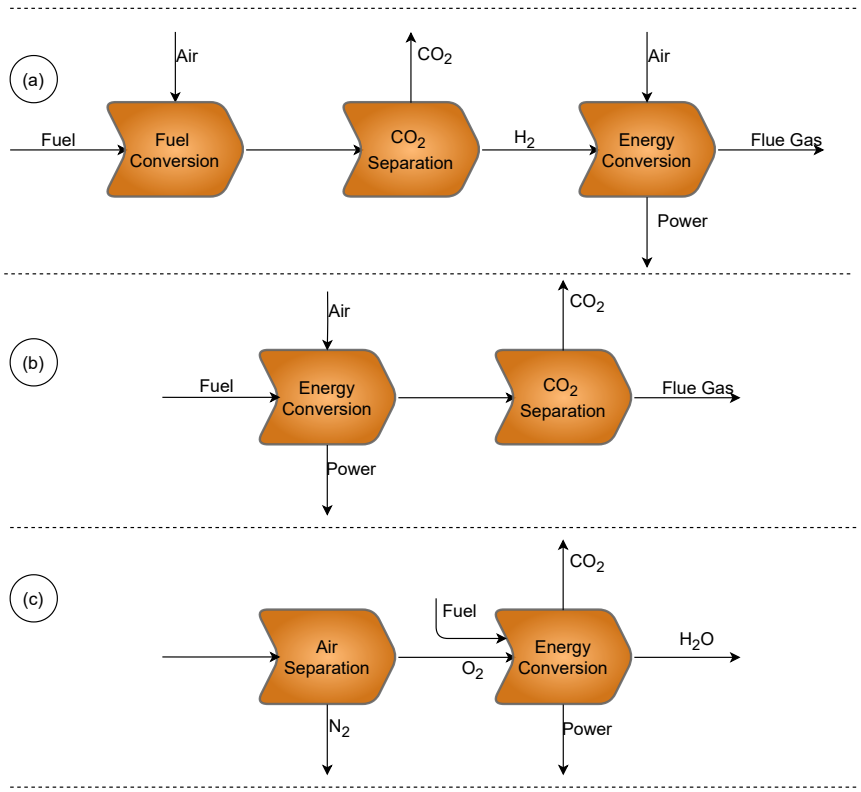

Figure 2.1: Flow diagrams of point source possibilities: (a): pre-combustion, (b): post-combustion, and (c): oxy-fuel combustion

Pre-combustion CC concerns the separation of CO_2 before an energy conversion. An example is natural gas sweetening, where natural gas is stripped of CO_2 before producing electricity, heat, or hydrogen. [Hekmatmehr et al., 2024].

Oxy-fuel combustion involves the combustion of hydrocarbon fuel with pure oxygen as

the oxidizer, in contrast to the typical air used in combustion, which contains nitrogen. Oxygen is typically obtained through cryogenic separation of air. The pure oxygen combustion results in a higher CO_2 concentration in the flue gas containing mostly water and CO_2, favoring the CC.

As embedded in the word, post-combustion CC concerns CO_2 removal from a flue gas after combustion or energy conversion. This includes not only power generation but also industrial processes, where combustion is used for purposes other than electricity and heat production. Post-combustion CC is a most needed process since re-designing processes to pre- or oxy-fuel combustion would require a large reconstruction of already existing industrial and energy-converting plants [Baker et al., 2022, Hekmatmehr et al., 2024]. The unfavored aspect of post-combustion flue gas is the lower CO_2 concentration than the other point sources. Table 2.1 presents the CO_2 concentration in flue gas for different point sources.

Table 2.1: Typical point source CO_2 concentrations [Hekmatmehr et al., 2024, Suleman et al., 2022, DEA, 2024].

Point source	CO_2 concentration [vol%]
Pre-combustion	Up to 60 %
Oxy-fuel combustion	Up to 98 %
Post-combustion	Coal-fired power plant = 7-14 %
	Waste-fired power plant = 9-14 %
	Biomass-fired power plant = 10-17 %
	Gas turbine = 2-4 %
	Cement plant = 20-30 %

While pre-combustion sources flue gas contains higher CO_2 concentrations, it requires expensive modifications of existing infrastructure, involving complex and expensive capital cost processes such as gasification or reforming. Oxy-fuel combustion, burning fuel on pure oxygen to produce a CO_2-rich flue gas, also demands capital-intensive equipment and technical challenges due to the energy-demanding oxygen production and new designs for combustion systems. [Bukar and Asif, 2024]

In contrast, post-combustion point sources indicate better possibilities for retrofitting existing plants and industrial processes for CC. These also account for the highest amount of global CO_2 emissions among the three combustion point sources. Therefore, post-combustion CC is seen as a critical component for decreasing CO_2 emission and allegedly the most market-realistic possibility, why post-combustion CC is considered in this study. [Hekmatmehr et al., 2024]

Three post-combustion point sources are chosen as standardized point sources to attain a

broad scope of possible point sources for CC implementation. The post-combustion point sources chosen in this study reflect *Combined Heat and Power* (CHP) plants or industrial process plants. These are a natural gas *Combined Cycle Gas Turbine* (CCGT) plant, biomass combustion plant, and *Waste-to-Energy* (WtE) plant. Coal CHP plants are the largest CO_2-emitters today, however, these are omitted in this study due to the ambition of 0 % electricity production by coal in 2040 by the EU, resulting in a non-beneficial lifetime of a CC plant before coal CHP plants shut down [IEA, 2021]. Biogenic CO_2 from biomass or biogas plants gives a realistic perspective regarding the future with a market for biogenic CO_2. Upgraded biogas has similarities to natural gas in combustion, containing primarily methane, and flue gas composition. The selected point sources reflect CO_2 emissions from existing plants necessary for decarbonization to reach net-zero CO_2 emissions.

Table 2.2 presents the flue gas compositions utilized in this study. The SO_x and NO_x concentrations are assumed to be the emission limits stated by EU law [EU, 2021]. This reflects the upper limits, hence the worst conditions for CC technologies. NO_2 and SO_2 are assumed to represent NO_x and SO_x, respectively [Gijlswijk et al., 2006].

Table 2.2: Flue gas compositions defined as standards in this study. *a*: no limit from EU [EU, 2021]

Compounds	Units	Waste incineration [AffaldPlus, 2023]	Biomass plant (wood chips) (Appendix A)	Natural gas CHP [Gijlswijk et al., 2006]
CO_2	[vol%]	12.2	11.1	4.0
O_2	[vol%]	7.7	5.8	12.4
H_2O	[vol%]	17.4	17.4	8.4
N_2	[vol%]	62.7	65.7	75.2
NO_2 limit	[mg/Nm^3]	225	165	55
SO_2 limit	[mg/Nm^3]	100	85	NaN^a
Temperature	[°C]	60	60	60
Pressure	[bara]	1.01	1.01	1.01

The biomass flue gas composition is determined in Appendix A, where the flue gas composition is based on the combustion of fir wood chips from the Phyllis database [TNO, 2025] with an assumed moisture content of 42.3 % [DEA, 2018]. The water content is equal for waste incineration and biomass combustion since the flue gas is saturated at 60 °C, but not for natural gas combustion. These flue gas compositions are determined with the Peng-Robinson equation of state by phase equilibrium at 60 °C.

The flue gas temperatures are assumed to be 60 °C from each point source [Carlsson, 2008], reflecting the cooled flue gas temperature post flue gas cleaning. In combustion plants today, flue gas cleaning is necessary to uphold the emission limits from the EU. Additionally, the pressure of the flue gas after gas cleaning is close to atmospheric pressure. The input

conditions to the process simulations for this study are the flue gas composition, temperature, and pressure, whereas the CC plant size will determine the flow rate.

2.2 Carbon Capture Technologies

Multiple CC technologies exist, with even more being researched and developed [DEA, 2024]. Depending on the combustion, different technologies can be used. The most common post-combustion CC technologies are absorption, adsorption, membrane, or cryogenic. Each capture technology includes numerous process steps that enable optimization when integrated with an industrial process. The difficulty of choosing a CC technology for a post-combustion point source arises due to the variety in flue gas characteristics and system configuration. [Baker et al., 2022]

Absorption methods are the most mature CC technologies, operating on large-scale commercial plants worldwide. Currently, two distinct absorption phenomena are employed within CC: physical or chemical. Physical absorption concerns the dissolution of CO_2 into a solvent without chemical reactions occurring. Most physical solvents demand a high CO_2 concentration since the dissolution of CO_2 into the solvent is directly proportional to the partial pressure of CO_2 as described by Henry's law in Equation (2.1). [Cengel and Ghajar, 2016]

$$y_{\text{liquid side}} = \frac{p_{\text{gas side}}}{H} \tag{2.1}$$

Where H is Henry's constant, P is the partial pressure of the solute in the gas phase, and y is the molar fraction of the solute in the liquid phase. Henry's law is only temperature dependent for low soluble species in a dilute gas-liquid solution under 5 bar and linearly behaves with temperature change. However, the relationship is not linear for highly soluble species such as ammonia in water and depends on pressure and temperature.

Today, large-scale physical absorption CC processes primarily operate on a pre-combustion process. Chemical absorption is a better-suited option for post-combustion CC due to the lower CO_2 concentration than pre- and oxy-fuel combustion. The absorption capacity against the CO_2 concentration of physical and chemical absorption is illustrated in Figure 2.2. [Hekmatmehr et al., 2024]

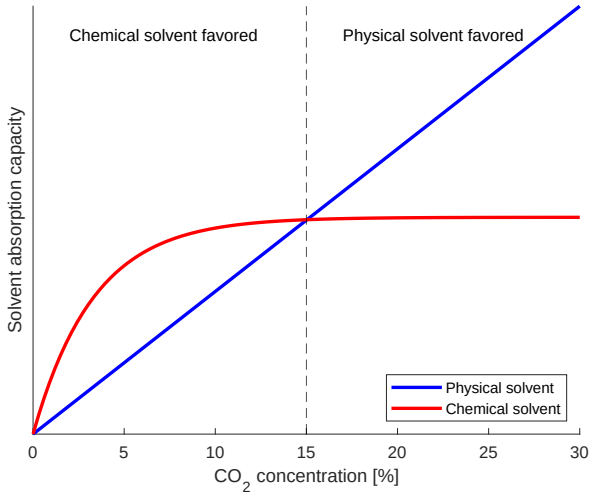

Figure 2.2: Absorption capacity concerning CO_2 concentration. (Inspired by [Cormos, 2017])

The figure indicates that chemical absorption is favored at low CO_2 concentrations, coinciding with the post-combustion point sources chosen. When chemical reactions are present, the dissolution of CO_2 into a solvent follows a nonlinear behaviour for the absorption capacity. Physical absorption is not economically beneficial for CO_2 concentration below 15 vol% [Chakravarti et al., 2001].

The benchmark technology for chemical absorption is *Monoethanolamine* (MEA), which has well-known thermodynamics and kinetics [Zhang and Lu, 2015]. MEA is commonly used today due to fast kinetics and mass transfer rates. Yet, capturing CO_2 with MEA is energy-intensive and costly, with literature showing approximately 4.0 MJ/kgCO_2 required. The energy intensity arises from the regeneration of the solvent. An increase in MEA concentration can reduce energy requirements, yet high MEA concentration raises corrosion and degradation rates. The major issues with MEA are thermal decomposition and degradation by O_2, SO_x, and NO_x. The degradation tends to form heat-stable salts and corrosive products by irreversible chemical reactions, resulting in added solvent replacement cost. [Hekmatmehr et al., 2024]

Alternatives to MEA have been widely researched for chemisorption CC to obtain more effective solvents with lower degradation rates and energy requirements, reflecting solvent performance to decrease the cost of CC. Two other chemisorption technologies are approaching *Technology Readiness Level* (TRL) similar to MEA. MEA is considered TRL 9, reflecting large-scale commercial level, where the alternatives *Potassium Carbonate with Carbonic Anhydrase* (PCCA) and *Chilled Ammonia Process* (CAP) are on the way up there with a TRL of 7-8 and expecting to reach full-commercial scale in this decade [DEA, 2024, Bukar and Asif, 2024].

While alternatives to MEA for post-combustion CC are extensively studied [Hu et al., 2017, Suleman et al., 2022, Darde et al., 2010], being able to assess the CC technologies across point sources and quickly evaluate the greater solution is lacking. Choosing a CC technology requires a system assessment regarding heat integration, process operation, energy penalty, plant efficiency reduction, and general cost for beneficial CC implementation. Previous studies developed a CC technology development decision tool for assessing necessary development in CC technologies [Baker et al., 2022], yet, the time for CC technologies to rise through the TRLs to a large commercial scale can be extensive, stalling the net-zero CO_2 emission goal by 2050. In favor of reaching net-zero emissions, this study aims to develop a tool to assess the beneficial CC technology chosen across multiple *Key Performance Indicators* (KPI)s. This can preferably provide a screening tool to decrease the determining period when choosing the optimal CC technology for implementing CC on large-scale point sources.

The thesis framework revolves around high TRL chemisorption CC technologies to evaluate present technology that is ready for implementation on large-scale point sources. The assessment tool chosen for development is a selection matrix. A selection or decision matrix is a tool for comparing suggested problem solutions across different criteria chosen. This enables systematic comparison to determine the optimal solution. Constraints or specific needs from the user can be implemented by subjective weighting of the criteria. The selection matrix utilizes CC technologies as solutions, enabling systematic comparison across KPIs as criteria. The KPIs are to be determined for this study, yet a greater understanding of the CC technologies is necessary before choosing the KPIs for the selection matrix evaluation.

2.3 Chemisorption Carbon Capture Technologies

Figure 2.3 presents a standard chemisorption CC process plant from the flue gas inlet until compression of captured CO_2.

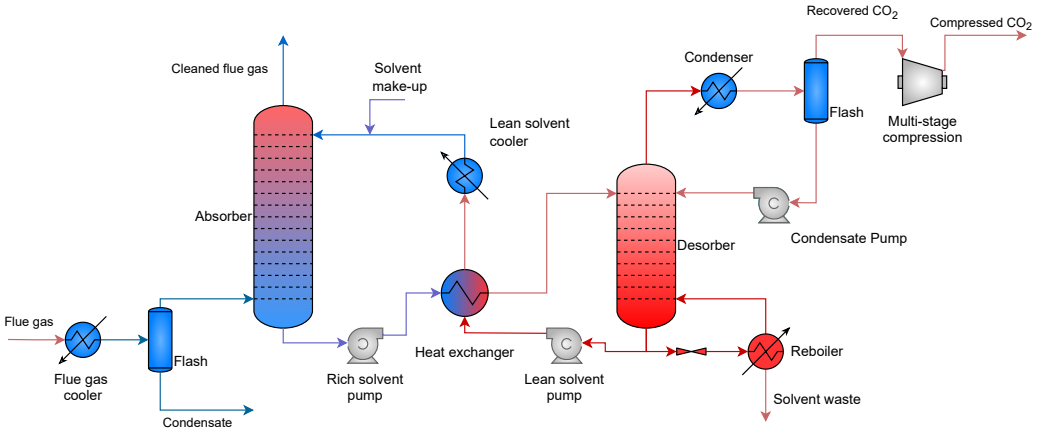

Figure 2.3: Illustration of typical chemisorption CC process

In the figure above, flue gas from a point source enters a flue gas cooler and flash tank as the flue gas is saturated with water. The cooled flue gas enters the absorber with sieve trays or packing material, to increase residence time and surface area, enhancing CO_2 capture. The absorber tower operates typically at low temperatures as CO_2 absorption is an exothermic process. A lean solvent entering the top of the absorber tower is washing the flue gas. The product streams from the absorber are a CO_2 rich solvent solution at the bottom and a cleaned flue gas from the top. The rich solvent is heated by the lean stream from the desorber in a heat exchanger before entering the top desorber stage as the condensate from the condenser above. The remaining gas above the desorber becomes the recovered CO_2, which undergoes multistage compression to reach transportation criteria. The desorber bottom stage is supplied with evaporated solvent from the reboiler pumparound. The lean stream exiting the desorber is cooled through the heat exchanger and lean solvent cooler before returning to the absorber. From this point, the temperature-swing cycle proceeds for the chemisorption CC process. [Suleman et al., 2022, Masson-Delmotte et al., 2018]

The CC technologies chosen follow the principle of the CC process from Figure 2.3. An overview of the CC technologies is conducted by a literature study [Hekmatmehr et al., 2024, Aouini et al., 2012, Qi et al., 2018, Hu et al., 2017, Lu et al., 2011, Darde et al., 2010, Sutter et al., 2016, Bukar and Asif, 2024]. This is presented in Table 2.3.

Table 2.3: Overview of the chosen chemisorption CC technologies.

CC Technology	MEA	PCCA	CAP
Advantages	Favorable kinetics High absorption rates	Low regeneration energy at 70-80 °C High thermo-stability Enzyme has high CO_2 selectivity Compounds formed are benign Non-volatile Low enthalpy of reaction $\approx$ 27 kJ/molCO_2	Lower energy penalty than MEA High absorption capacity > 5wt% Highly resistance to O_2, SO_X, and NO_X Low regeneration requirement
Disadvantages	Energy intensive Highly corrosive above 25 wt% Toxic compounds Highly degradative/oxidative Low CO_2 loading capacity	Enzyme degradation (not regenerateable) Low CO_2 loading capacity	Highly volatile Complex physicochemical phenomenas Solid formations hard to control
TRL	9	7	7
SPECCA	$\approx$ 4.0 MJ/kgCO_2	$\approx$ 3.0-3.5 MJ/kgCO_2	$\approx$ 2.5-3.0 MJ/kgCO_2

With a general overview of the CC technologies presented, chemistry and specific conditions for each technology will be evaluated.

2.3.1 Monoethanolamine - Carbon Capture

CO_2 absorptions by MEA are described in the literature by two different reaction mechanisms. Firstly the zwitterion reaction mechanism by Reactions (R1) and (R2) [Suleman et al., 2022, Zhang and Lu, 2015].

$$\mathrm{MEA} + \mathrm{CO_2} \rightleftharpoons \mathrm{MEACOOH} \tag{R1}$$

$$\mathrm{base} + \mathrm{MEACOOH} \rightleftharpoons \mathrm{MEACOO^-} + \mathrm{baseH^+} \tag{R2}$$

Reaction (R1) presents the production of the intermediate zwitterion (MEACOOH), followed by deprotonation in Reaction (R2) by a base. The base in an aqueous MEA solvent can be MEA, H_2O, or OH^- to produce carbamate $MEACOO^-$ and a protonated base. The second mechanism is termolecular, presented in Equation (R3).

$$\mathrm{MEA} + \mathrm{CO_2} + \mathrm{MEA} \rightleftharpoons \mathrm{MEACOO^-} + \mathrm{MEA^+} \tag{R3}$$

The termolecular reaction reflects the same reaction, yet with MEA as the base, resulting in three reactants (MEA, CO_2, and MEA) simultaneously reacting to form products (carbamate and protonated MEA). MEA is the dominant base in CO_2 absorption. H_2O and OH^- are also present, yet have minimal impact on the chemical absorption of CO_2. [Borhani et al., 2018]

CO_2 absorption with MEA is an exothermic reaction with a heat of absorption of approximately 85-90 kJ/molCO_2. The absorber typically operates at 40-60 °C and the desorber at 100-120 °C. The desorber is limited to 2 bar operational pressure due to thermal degradation occurring above 122 °C of MEA. [Pfaff et al., 2010]

Although MEA is the benchmark CC technology for chemisorption CC, utilizing MEA has disadvantages. Solvent degradation by flue gas contaminants O_2, SO_x, and NO_x results in the formation of toxic thermo-stable salts and corrosive products. The MEA degradation impacts the operation by increasing the solvent make-up as the degraded reactions are irreversible. The MEA degradation rate seen from Andrade et al was 1.5 g/kgCO_2 capture [de Andrade, 2014], yet this heavily depends on the flue gas compounds and solvent concentration. Alternatively, a more extensive flue gas pre-treatment can avoid these issues with MEA degradation, yet both scenarios increase the operational expenditures. The other aspect is increased cost due to waste handling of the toxic degraded compounds or material cost to avoid breakdown due to corrosion. The flue gas content can be vital for the cost of CC when utilizing MEA, however, the impact on performance in CO_2 recovery and energy requirement is insignificant if actions against MEA degradation are taken. [Aouini et al., 2012, DEA, 2024]

2.3.2 Potassium Carbonate with Carbon Anhydrase - Carbon Capture

In the PCCA process, an aqueous solution of potassium carbonate (K_2CO_3) is the solvent, where the enzyme *Carbonic Anhydrase* (CA) promotes the dissolution of CO_2 in the solvent.

The solvent without CA is an aqueous solution with K_2CO_3 promoting two Reactions (R4) and (R5). Firstly, the hydration of CO_2 to form carbonic acid (H_2CO_3) that then dissociates fast to bicarbonate (HCO_3^-) and a proton. Secondly, dissolved CO_2 with hydroxide ions. [Hu et al., 2017, Zhang and Lu, 2015]

$$CO_2 + H_2O \rightleftharpoons HCO_3^- + H^+ \tag{R4}$$

$$CO_2 + OH^- \rightleftharpoons HCO_3^- \tag{R5}$$

The heat of absorption for aqueous PC with CO_2 is lower than MEA ($\approx$ 27 kJ/molCO_2). The weak CO_2 affinity in aqueous solvent results in possible regeneration at lower temperatures (60-80 °C). [Lu et al., 2011]

The CC technology is similar to MEA, nevertheless, the absorption rate of CO_2 is significantly slower. This would result in a larger and more costly absorber column to obtain equal CO_2 recovery as a benchmark MEA absorber. The environmental impact is benign in contrast to MEA, which is an advantage. To enhance the CO_2 absorption rate, promoters can be added. The technology developed by CO_2 Solutions Inc. has been bought by Saipem, which utilizes the enzyme CA as a promoter [Saipem, 2025]. The enzyme functions as a biocatalyst in the dissolution of CO_2 presented in (R6)

$$CO_2 + H_2O + CA \rightleftharpoons HCO_3^- + H^+ + CA \tag{R6}$$

The enzyme participates as a catalyst in the CO_2 hydration seen above. Promoting the solvent with a biocatalyst results in an adsorption effect on the active site of the CA enzyme. CO_2 hydration is sped up by the catalytic effect. The regeneration in the PCCA process occurs in an integrated vacuum desorber. Here the pressure is 0.15-0.55 bar which enables evaporation of the rich solvent at low temperature (< 80 °C). PCCA regeneration is key to keep below 80 °C to avoid enzyme degradation, hence the need for makeup. [Qi et al., 2018]

In an experimental study by Lu et al, the enhancement of CO_2 dissolution was investigated, where the enhancement factor was found to be largest at low temperatures (25 °C) and high CA concentration (600 mg/L) due to the lower Henry's constant and lower activation energy of Reaction (R6). Additionally, the CA activity is not significantly affected by the CO_2 loading at high CA concentrations ($\geq$ 300 mg/L), indicating Reaction (R5) as the dominant reaction until sufficiently high CA concentration, whereafter Reaction (R6) will become the dominant reaction. Another aspect observed by Lu et al is that when Reaction (R6) is the dominant, CO_2 absorption rate is insignificantly changed with CO_2 loading in the solvent, reflecting constant capture behavior through an absorber column. [Lu et al., 2011]

The enzyme degradation occurs due to the deactivation of the active side of the biocatalyst. The degradation rates were observed by Lu et al, with less than 10.2 % loss in CA activity by the presence of NO_x and SO_x. This results in decreased absorption rates unless catalyst make-up is added, increasing the operational expenditure.

2.3.3 Chilled Ammonia Process - Carbon Capture

Two options using ammonia as a solvent for chemical absorption are utilized, chilled ammonia (0-20 °C) and at ambient conditions (25-40 °C). Due to the high volatility of ammonia, the CAP reduces ammonia slip from the absorber, decreasing the extensive water wash needed for the process at ambient conditions. The most mature process is the CAP, available from General Electric (developed by Alstom) [Bukar and Asif, 2024]. A risk of the CAP is precipitation in contradiction to the ambient process, however, the CAP developed by Alstom is a non-precipitating CAP on TRL 7. Based on the provided information, this study employs the CAP without solid formations to compare with the previously mentioned technologies. [Darde et al., 2010, Hanak et al., 2015]

Sutter et al. optimized the CAP on a coal-fired power plant. Reflecting the non-precipitating CAP, an energy requirement of approximately 3.0 MJ/kgCO_2 was observed. This was achieved with a solvent concentration of approximately 10 wt.% and a water-wash section recapturing above 97.5% of the ammonia slip from the absorber. [Sutter et al., 2016].

To operate the CAP absorber at sufficiently low temperature (<20 °C), the flue gas needs cooling by a direct contact cooler below 10 °C. Additionally, the lean stream entering the absorber will also need to be cooled to 10 °C. A chiller is necessary to reach these low temperatures for the flue gas. [Hanak et al., 2015]

The key chemical reactions in CC by NH_3 are presented in Reactions (R7), (R8), and (R9).

$$NH_3 + CO_2 \rightleftharpoons NH_2COO^- + H^+ \tag{R7}$$
$$NH_3 + H_2O \rightleftharpoons {NH_4}^+ + OH^- \tag{R8}$$
$$H_2O + CO_2 \rightleftharpoons {HCO_3}^- + H^+ \tag{R9}$$

Where *carbamate anion* (NH_2COO^-) and *ammonium* (${NH_4}^+$) can form the solid *ammonium carbamate* (NH_2COONH_4). Additionally, ${NH_4}^+$ and *bicarbonate* (${HCO_3}^-$) can form the solid *ammonium bicarbonate* (NH_4HCO_3). The key to avoiding these formations is keeping the ammonia concentration below 17.5 wt.% and avoiding the temperature from decreasing below 2 °C in the process. [Hanak et al., 2015, Sutter et al., 2015].

The extended research on CC with ammonia in contradiction to amine arises due to the potential of more cost-beneficial regeneration while observing high CO_2 absorption capacity. A few characteristics are the reason for this. Primarily, the heat of absorption of approximately 70 kJ/molCO_2 is lower than MEA, reducing the energy penalty for regeneration [Qin et al., 2011]. Regeneration can occur at higher pressure in the desorber in contrast to MEA, since thermal degradation of ammonia is almost non-existent. Additionally, interaction with flue gas impurities has an insignificant effect on ammonia degradation, enabling a multifunction capture with ammonia as a solvent. Especially O_2 concentration, a significant drawback with MEA due to corrosion and degradation, yet an insignificant impact on degradation and CO_2 capture with ammonia. [Sutter et al., 2015, Darde et al., 2010, Sutter et al., 2016]

A drawback of the CAP is relatively slow kinetics compared to MEA, affecting the equipment sizing. Another important aspect is the system configuration needed to avoid ammonia slip. The cleaned flue gas exiting the absorber is prone to contain toxic evaporated ammonia. A water wash system is typically installed to diminish the ammonia slip, which functions as another absorber/desorber system, yet in a significantly smaller size than the primary temperature swing. Figure 2.4 illustrates this CAP system configuration.

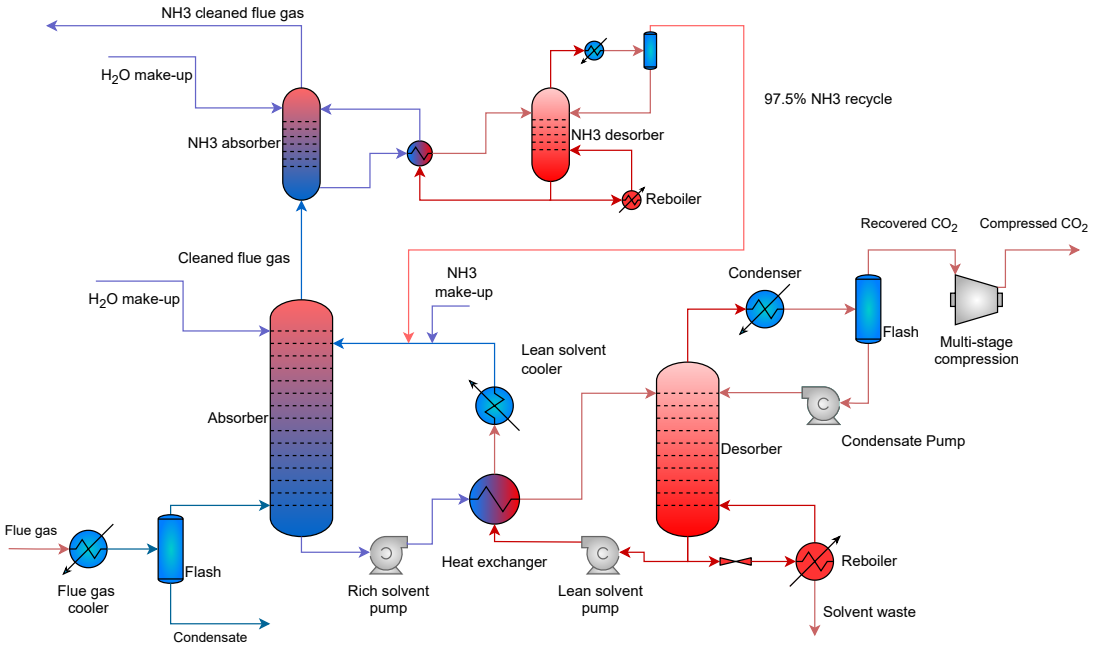

Figure 2.4: Illustration of the CAP system process including water wash.

As illustrated in the figure above, the water wash system is added to decrease ammonia slip with the CO_2 cleaned flue gas before going to the stack. The recovered ammonia is recycled back to the cooled lean solvent stream. The water make-up is added in the top absorber stage, where the lean solvent containing highly volatile ammonia enters the second top stage, decreasing the ammonia evaporation. Thus, enhancing the absorber CO_2 recovery. [Sutter et al., 2016, Hanak et al., 2015]

2.3.4 Summary of Carbon Capture Technologies

The benchmark chemisorption CC technology MEA has been introduced with two alternatives. These three technologies are deemed ready for large-scale commercial implementation as PSCC technologies. Determining the greater technology for each point source is case-dependent and requires evaluation across KPIs. Table 2.4 presents the operating conditions utilized in this study.

Table 2.4: Determined operating conditions for each chemisorption CC technology

	MEA [Okuno et al., 2019] [Hu et al., 2017] [Nakamura et al., 2013]	PCCA [Lu et al., 2011] [Thee et al., 2015] [Qi et al., 2018]	CAP [Hanak et al., 2015] [Sutter et al., 2016]	Unit
Absorber temperature	40-60	30-60	11-43	[°C]
Absorber pressure	1.013	1.013	1.013	[bar]
Desorber temperature	110-120	70-80	130-150	[°C]
Desorber pressure	2	0.25	10	[bar]
Inlet flue gas temperature	20	25	7	[°C]
Lean solvent temperature	20	25	10	[°C]
Desorber condenser temperature	25	18	68	[°C]
Technology provider	Fluor Ecoamines	Saipem (developed by CO_2 Solutions Inc.)	General Electric (developed by Alstom)	

The absorber pressure is assumed to be atmospheric pressure. Compressing a high volumetric flowrate flue gas, before entering the absorber, requires significant compressor power, as electrical energy further increases the already energy-demanding CC technology.

This study will utilize these operating conditions to conduct process simulations to determine the performance of each technology regarding the specific point sources previously presented.

2.4 Sizing the Chemisorption Carbon Capture System

A typical chemisorption CC plant system size is chosen to compare MEA, PCCA, and CAP across the waste incineration, biomass, and natural gas point sources. This is based on the modular CC plant solution from SLB Capturi Advanced Carbon Capture^{TM}. The technology is named Just Catch^{TM} 100, referring to the capturing capacity of 100 ktonne/year. Assuming 8000 operating hours each year results in a capture of 12.5 tonne/h. [SLB Capturi, 2025]

Assuming the flue gas operates with 12.2 vol% CO_2 concentration (from the waste incineration point source) and the CO_2 recovered from the inlet flue gas to exit downstream of the desorber is 90 %, the CO_2 mass flow rate can be determined to be 14.4 tonne/h. Using this, the total mass and molar flow can be determined. Table 2.5 presents the mass and molar composition and flow rates of each point source chosen.

Table 2.5: Standardized flue gas flow rates for the chosen point sources

	Waste incineration				**Biomass**				**Natural gas**			
Units	[vol%]	[kmol/hr]	[wt.%]	[tonne/h]	[vol%]	[kmol/hr]	[wt.%]	[tonne/h]	[vol%]	[kmol/hr]	[wt.%]	[tonne/h]
CO_2	12.2	327.0	18.8	14.4	11.1	300.2	17.3	13.2	4.0	107.5	6.2	4.7
O_2	7.7	206.4	8.6	6.6	5.8	156.9	6.6	5.0	12.4	335.6	14.0	10.7
H_2	17.4	466.4	11.0	8.4	17.4	470.6	11.1	8.5	8.4	227.8	5.4	4.1
N_2	62.7	1680.7	61.6	47.1	65.7	1776.7	65.1	49.8	75.2	2031.3	74.4	56.9
Sum	100.0	2680.5	100.0	76.5	100.0	2704.3	100.0	76.5	100.0	2702.3	100.0	76.5

The total mass flow is set to 76.5 tonne/h as the standard inlet condition for each flue gas to compare the CC technologies on equal terms.

2.5 Key Performance Indicators for Selection Matrix

The MEA, PCCA, and CAP technologies share a similar CC process system configuration, yet the thermodynamic and chemical aspects are different. These differences reflect the variation in operating conditions across the CC technologies. The KPIs are determined to investigate the impact on system performance due to these differences.

In the previously presented study by Baker et al. for the technology development matrix, the KPIs are defined in three categories: performance, cost, and lifetime [Baker et al., 2022]. Yet, this study neglects lifetime as a KPI due to the similar process operation between the CC technologies. While both performance and costs are critical in evaluating CC technologies for a point source, cost evaluations are highly case-specific and depend on the equipment sizing, point source site conditions, and the process designer's constraints for the individual process plant. This limits a consistent systematic comparison of the CC technologies across point sources. Therefore, this study focuses on performance-based KPIs to reflect differences between the CC technologies. Thus, a broad comparison of technical feasibility and process efficiency in the post-combustion CC context.

The main parameter in CC is the CO_2 recovery. This is chosen as a KPI to compare the CC technologies and evaluate the remaining KPIs. CO_2 recovery is vital to minimize emissions and cost penalties in the future. The CO_2 recovery is defined by Equation (2.2).

$$R_{CO_2} = \frac{\dot{n}_{CO_2,\text{recoverd}}}{\dot{n}_{CO_2,\text{in}}} \cdot 100 \quad [\%] \tag{2.2}$$

Where the $\dot{n}$ is the molar flow rate. The CO_2 recovery KPI is defined to monitor the CO_2 capture and emission post CC. Another aspect is the purity of the CO_2 recovered. A study by the European project DYNAMIS improved the CO_2 quality recommendation regarding CCUS, first proposed by the ENCAP project. The specified recommendations by the DYNAMIS project are presented in Table 2.6.

Table 2.6: DYNAMIS recommendation for CO_2 quality with regards to CCUS [SINTEF, 2009]. *a*: limitations for storage [ABS, 2025]

Component	Unit	Concentration	Reason
H_2O	[ppm]	< 500	water solubility limit in CO_2
O_2	[ppm]	< 100-1000	Knowlegde gap regarding underground consequences
N_2	[vol%]	< 4	From ENCAP project
SO_2	[ppm]	< 100	Safety and health hazards
NO_2	[ppm]	< 100	Safety and health hazards
Amine	[ppm]	$< 10^a$	Safety and health hazards
NH_3	[ppm]	$< 10^a$	Safety and health hazards
CO_2	[vol%]	> 95.5	By component balance

Based on the recommendations from the DYNAMIS study, the KPI is defined as above 95.5 vol% CO_2 purity to enable both utilization and storage post CC. Additionally, from the CO_2 recommendations, the O_2, N_2 and solvent content are added as KPIs.

The utility demand is a key aspect for a CC plant as it directly presents the technical feasibility of a CC technology. It presents the penalty to implement CC, decreasing the point source environmental impact by CO_2 emissions. Additionally, the utility demand reflects the thermodynamic and process efficiency of the CC technology. The reboiler duty is one of the major aspects in determining the utility demand for a CC technology. The *Specific Primary Energy Consumption for CO_2 Avoided* (SPECCA) is defined as a KPI. This corresponds to the total primary energy needed per kg CO_2 avoided. The SPECCA value is determined by Equation (2.3).

$$\text{SPECCA} = \frac{\dot{Q}_{\text{primary,energy}}}{\dot{m}_{\text{CO}_2,\text{avoided}}} \tag{2.3}$$

Where $\dot{Q}$ is the thermal heat power of the primary energy and $\dot{m}$ is the mass flow of CO_2 avoided. The primary energy in the CC technology itself is the reboiler duty as the only thermal heating demand in the system. Additionally, the electrical work required is measured against the avoided CO_2 defined as the *Electrical Work per Avoided CO_2* (EWA). Equation (2.4) shows the definition of the EWA KPI.

$$\text{EWA} = \frac{\dot{W}_{\text{pumps}} + \dot{W}_{\text{compressors}} + \dot{W}_{\text{chillers}}}{\dot{m}_{\text{CO}_2\text{avoided}}} \tag{2.4}$$

Where $\dot{W}$ is the present electrical work consumption for pumps, compressors, and chillers in the CC process. This is another KPI chosen to compare CC technologies. Solvent and water make-up are two other KPIs chosen. These define the operational demands, reflecting resource efficiency and long-term operational needs. It shows a different technology performance, which impacts the environmental sustainability of each CC technology. The make-ups are normalized according to recovered CO_2 to compare the CC technologies.

Table 2.7 summarizes the KPIs and their units.

Table 2.7: Overview of defined KPIs utilized in the selection matrix

KPI	Units
CO_2 recovered	[%]
SPECCA	[MJ/kgCO_2]
EWA	[MJ/kgCO_2]
Water makeup	[kg/kgCO_2]
Solvent makeup	[g/kgCO_2]
CO_2 purity	[vol%]
O_2 in recovered CO_2	[ppm]
N_2 in recovered CO_2	[ppm]
Solvent in recovered CO_2	[ppm]

The KPIs are chosen to evaluate the CC technology performances across point sources, reflecting the difference in effective CC and process operation.

Chapter 3

Objective

Post-combustion *Carbon Capture Utilization and Storage* (CCUS) is necessary to reach the common goal of net-zero CO_2 emissions, as industrial process plants and heat and power production from fossil fuels are emitting CO_2 are indispensable and difficult to replace otherwise before 2050.

To enable the decrease in CO_2 emissions from point sources quickly, the study revolves around three chemisorption *Carbon Capture* (CC) technologies on a high *Technological Readiness Level* (TRL) (Monoethanolamine, potassium carbonate with carbonic anhydrase, and chilled ammonia process). Additionally, these technologies are investigated across three standardized point sources, systematically comparing their performance regarding post-combustion CC.

This study aims to develop a selection matrix as an analysis tool to selectively determine an optimal chemisorption CC technology for real-world specific post-combustion point sources. The systematic comparison of CC technologies is based on *Key Performance Indicators* (KPI)s, which enables consistent evaluation of technical performance and process efficiencies.

Below is defined the research question as specific objectives to frame this master thesis main objective:

- How can an adaptable process model of each technology be developed to reflect a modular CC plant for systematically comparing the CC technologies on equal terms?
- Which of the operating parameters, liquid-to-gas ratio, lean stream temperature, flue gas temperature, and reboiler duty, most significantly impact CO_2 recovery and energy consumption per CO_2 avoided, based on a parametric study?
- What ranking between the chosen CC technologies can be determined based on the selection matrix KPI scores of the three standardized point sources?
- What assessments can be made regarding the selection matrix by extending it with heat integration analyses of the CC technologies?
- Which CC technology is optimal based on a real-world case, utilizing the extended selection matrix tool for comparing the technology integrations?

Chapter 4

Modeling Approach

This chapter aims to develop three adaptable process models, one for each CC technology, to evaluate the KPI scores and compare them in the selection matrix. Addionally, presenting how a heat integration analysis can be performed. Each model is an equilibrium-based model, with the main objective of comparing the technology performance due to their difference in thermodynamic and chemical capabilities. The operating conditions for each CC technology follow the conditions from Table 2.4.

4.1 Equilibrium Process Models Description

The equilibrium models for MEA, PCCA, and CAP feature an equilibrium-based absorber and desorber. Each process simulation will be carried out in the Aspen Plus software utilizing the *Electrolyte Non-Random Two-Liquid* (ELECNRTL) property model, an activity coefficient property model incorporating the Redlich-Kwong equation of state to evaluate the vapor phase fugacities. The ELECNRTL property method is commonly utilized in chemical processes where interactions between ions and solvents are key to determining the chemistry, as is the case for absorbers and desorbers. The property model provides precise calculations for activity coefficients in highly non-ideal solutions. [AspenTech, 2020]

The CC part of each process model involves the ELECNRTL property method, which calculates heat and material balances while determining thermodynamic, chemical, and phase equilibria. A difference between the process models is the compound species involved. Table 4.1 shows which compounds are present in each process simulation.

Table 4.1: Compounds present in each Aspen Plus process model. *α: specified Henry component*

Compounds	MEA	PCCA	CAP
$^{\alpha}CO_2$	✓	✓	✓
$^{\alpha}O_2$	✓	✓	✓
H_2O	✓	✓	✓
$^{\alpha}N_2$	✓	✓	✓
H^+	✓	✓	✓
HCO_3^-	✓	✓	✓
OH^-	✓	✓	✓
CO_3^{2-}	✓	✓	✓
MEA	✓	×	×
MEA^+	✓	×	×
$MEACOO^-$	✓	×	×
K_2CO_3	×	✓	×
K^+	×	✓	×
NH_3	×	×	✓
NH_4^+	×	×	✓
NH_2COO^-	×	×	✓

CO_2, O_2, and N_2 are Henry components in the process models as the vapor pressure for

ions is zero. The pollutant compounds NO_x and SO_x included in the point sources previously presented are omitted in the equilibrium models. The impact on CC and energy requirements across the CC technologies would be minor, as their presence will impact the operational parameters as additional solvent and water make-up [de Andrade, 2014].

Pressure losses are excluded in the process simulations since the important aspect is comparing system performance. The pressure loss across the processes depends on the specific equipment and sizing, why omitted in the process equilibrium models.

4.1.1 Absorber

The RadFrac column block in Aspen Plus is designed to model distillation or absorption processes. When operating in the software, the equilibrium-based specification is chosen, indicating that the software determines an equilibrium at each stage. The number of absorber stages reflects the separation efficiency, as each stage enables the vapor and liquid phases to reach equilibrium. This increases the vaporization efficiency, enhancing the purity of the separated compounds. As the number of stages increases, the absorber height increases, resulting in higher capital cost. Yet more stages enable a lower reflux ratio while maintaining high separation efficiency. The energy requirement also increases with the number of stages. However, as the absorber is without a reboiler or condenser, the number of stages is typically greater than in the desorber. The number of stages in the absorber has been investigated during process model setups, where 15 stages are deemed acceptable for separation efficiency [Awtry, 2013]. The determining process is the CAP model due to the most volatile solvent of the three. Each process model is specified with 15 absorber stages to enable comparison on equal terms. [Aromada and Øi, 2015].

The absorber in each process model is specified with the presented specifications from Table 4.2.

Table 4.2: Absorber operating conditions: *a* not a feed stream to the absorber.

Absorber specification	Unit	MEA	PCCA	CAP
Feed stage (flue gas)	[-]	15	15	15
Feed stage (lean stream)	[-]	1	1	2
Feed stage (make-up H_2O)	[-]	NaN[a]	NaN[a]	1
Product stage (rich stream)	[-]	15	15	15
Product stage (clean gas)	[-]	1	1	1
Column pressure	[bar]	1.013	1.013	1.013

The absorber specifications across the CC technologies are similar, however, the CAP has a water make-up feed into the absorber to diminish ammonia slip. Each process is specified with atmospheric pressure to reflect practical operation. The absorber tower typically is

the largest in both diameter and height, why increasing the pressure is expensive as it handles the largest volume flow in the system, the flue gas. [de Andrade, 2014]

4.1.2 Desorber

As the absorber, the desorber is modeled with a RadFrac model, however, a reboiler specification is added for solvent regeneration. The number of stages for the desorber is found to be sufficient at 10 during process model setups regarding separation efficiency. The separation efficiency is lower compared to the absorber. Yet, as the desorber includes a reboiler and condenser, the energy requirement is lower than if 15 stages were chosen. The desorber specifications are presented in Table 4.3. [Aromada and Øi, 2015]

Table 4.3: Desorber operating conditions.

Desorber specification	Unit	MEA	PCCA	CAP
Feed stage (Rich stream)	[-]	1	1	1
Feed stage (Condensate return)	[-]	1	1	1
Product stage (lean stream)	[-]	10	10	10
Product stage (CO_2 rich gas)	[-]	1	1	1
Column pressure	[bar]	2	0.25	10

The table above shows similar specifications to the absorber, however, the reboiler duty is another necessary specification. Due to this being a key parameter that is varied in search of system performance, it is not specified in the table. The column pressure of the desorber is different for each technology due to the allowed reboiler temperatre fo each solvent.

4.1.3 Heat Exchanger

A heat exchanger is added for the lean and rich streams to heat-integrate the CC plant, decreasing the amount of excess heat utility required. The heat exchanger is executed with the shortcut method, assuming a constant overall heat transfer coefficient. This results in uncertainties for the heat exchanger area calculation. The heat exchanger for each process is modeled as a countercurrent heat exchanger with the LMTD method approach, utilizing a constant overall heat transfer coefficient U of 0.85 kW/m^2·K and ΔT_{min} of 5 °C. [AspenTech, 2020]

A design approach is necessary to execute the shortcut heat exchanger model, where the hot outlet/cold inlet temperature of 5 °C is chosen. The lean stream has a lower mass flow than the rich stream, hence lower heat capacity, indicating the pinch point in the heat exchanger is on the cold side [Kothandaraman, 2010]. Providing a starting guess for the hot lean stream entering the heat exchanger aids the heat exchanger model towards convergence. This includes the stream temperature, pressure, mass flow, and composition.

The rich product stream from the absorber provides the inlet conditions for the cold stream entering the heat exchanger.

4.1.4 Multi-Stage Compression

The critical point for CO_2 is at 31.1 °C and 73.8 bar [Zhang et al., 2006]. The compressor is set to deliver 110 bar pressure to fulfill the demand for CO_2 transportation [Pfaff et al., 2010]. CO_2 compression is included in the CO_2 recovery to include the pressure difference between each CC technology, resulting in different electrical work needed to reach 110 bar.

The multi-stage compressor model in Aspen Plus is utilized. An 8-stage compression with intercooling between each stage is specified with the specified outlet pressure of 110 bar. Each compressor is assumed to have an isentropic efficiency of 85 % [Amara, 2021]. The cooling water temperature is set to 25 °C, from the calculation for a cooling tower presented in Appendix B. For the gas-liquid heat exchange at each intercooling, the pinch temperature is assumed to be 10 °C, resulting in a specified outlet temperature of 35 °C after each intercooling stage. This temperature is above the critical temperature (31.1 °C), avoiding liquefying the CO_2 between compressor stages as it becomes supercritical above 73.8 bar. A temperature limit of 150 °C after the final compressor is set, where an additional stage will be inserted if the temperature increases above this point [Wacker and Dittmer, 2014].

As the CO_2 compression operates around the supercritical point, the ELECNRTL property method is swapped with a Peng-Robinson property method [AspenTech, 2020]. The Peng-Robinson equation of state is generally preferred for predicting the behaviour of CO_2 near the critical point, as it shows greater accuracy compared to the Redlich-Kwong equation of state, which determines the gas phase properties in the ELECNRTL property method [Grunwald et al., 2012].

4.1.5 Auxiliary Components

The auxiliary components include heaters/coolers, flash drums, pumps, valves, splitters, and mixers. These are provided in the process simulations to reach the correct conditions of streams before entering the key components. Each calculates heat and material balances. Additionally, the chemical and phase equilibria are determined after each component to follow temperature and pressure changes. The pumps are assumed to have an efficiency of 80 %.

Another auxiliary component added is cooling demand from chillers in the CAP process model. The flue gas is cooled to 7 °C and the lean stream to 10 °C. A chilling *Coefficient Of Performance* (COP) of 6.55 is assumed to include the electrical power demand for a chiller in the CAP model [Sutter et al., 2016]. The COP of a chiller is defined in Equation (4.1).

$$\text{COP} = \frac{\dot{Q}_c}{\dot{W}} \tag{4.1}$$

Where $\dot{Q}_c$ is the thermal cooling demand to cool the flue gas or lean stream temperature to 7 or 10 °C, respectively. $\dot{W}$ is the electrical work needed to achieve the cooling demand. [Cengel and Ghajar, 2016]

4.1.6 Nesting Order and Design Specifications

Each process simulation is iterated based on a provided nesting order and design specifications. The design specifications control the solvent make-up to ensure a steady-state converged result. A design specification for both water and solvent make-up is included. The nesting order controls which iteration path is chosen first to ensure which order each loop is converged. The key nesting order is the outside (final) loop, which controls when a converged result is found.

The lean stream entering the absorber is set as the tear stream for the outer loop in the convergence order. As a result, this is where the simulations are initialized and end at a converged result. All three CC technology process simulations are iterated using the direct method, the most robust approach in Aspen Plus. The direct method is a convergence method that manually iterates based on a tear stream. [AspenTech, 2020]

The design specifications are converged with the secant method, converging one design specification at a time. This involves a target set to reach the mass balance of water and a variable to vary to meet this target. Additionally, a tolerance is specified for when the converged result is reached. Table 4.4 presents the tolerances specified for the tear streams and design specifications included in the process simulations.

Table 4.4: Loops and tolerances specified in process simulations

Loop	Solver	Tolerance
Outer loop (lean entering absorber tear stream)	Direct method	1e-5
Inner loop (condensate return to desorber tear stream)	Direct method	1e-5
Design spec. H_2O	Secant method	1e-5
Design spec. solvent (MEA, K_2CO_3, or NH_3)	Secant method	1e-5

The table above shows that each process simulation is incorporated with two tear streams and two design specifications, and specified with the same tolerance to ensure mass balances for all loops are not skewed by the tolerance levels.

The following sections define the chemistry and process conditions for the individual equilibrium models.

4.2 Monoethanolamine - Equilibrium Model

The setup of components and chemistry is the first step in developing an Aspen Plus process model. The ELECNRTL property method includes ion interactions. The CO_2-H_2O-MEA equilibrium for chemical reactions is specified. This defines the global chemistry for the MEA process model. The chemistry is presented in Reactions (R10), (R11), (R12), (R13), and (R14).

$$H_2O \rightleftharpoons OH^- + H^+ \tag{R10}$$
$$HCO_3^- \rightleftharpoons CO_3^{2-} + H^+ \tag{R11}$$
$$H_2O + CO_2 \rightleftharpoons HCO_3^- + H^+ \tag{R12}$$
$$MEA + HCO_3^- \rightleftharpoons H_2O + MEACOO^- \tag{R13}$$
$$MEA + H^+ \rightleftharpoons MEA^+ \tag{R14}$$

Where water dissociation and CO_2 dissolution are included. A parameter investigated across studies of chemisorption CO_2 capture is the CO_2 loading in the liquid solvent streams [Aspen Technology, 2014]. The defined CO_2 loading utilized in this study for MEA is seen in Equation (4.2).

$$\gamma_{MEA} = \frac{[CO_2] + [HCO_3^-] + [CO_3^{2-}] + [MEACOO^-]}{[MEA] + [MEA^+] + [MEACOO^-]} \tag{4.2}$$

Where the square brackets indicate the concentration of each compound. The solvent CO_2 loading is defined as the number of moles of CO_2 in the liquid divided by the number of moles of solvent (MEA). The process flowsheet and iteration order for the MEA model are found in Appendix C. The important tear stream in this process model is the lean stream ("LEAN-ABS") entering the absorber. Table 4.5 presents an overview of key operating specifications in the MEA process model.

Table 4.5: Key input specification for the MEA process model

Specification	Value	Unit
Cooled flue gas temperature	20	[°C]
Lean stream cooler temperature	20	[°C]
Condenser temperature	25	[°C]
Initial guesses		
MEA solvent concentration	30	[wt.%]
Lean CO_2 loading	0.254	[-]
Lean stream inlet ("HEX")	120	[°C]

The initial guesses for solvent concentration and lean stream loading are necessary to initialize the process model. The CO_2 loading and MEA concentration are found in literature

comparing process simulations to experimental data from a pilot plant [Aouini et al., 2012, Aspen Technology, 2014].

4.3 Potassium Carbonate with Carbonic Anhydrase - Equilibrium Model

For the PCCA process model, the solvent consists of K_2CO_3 and the enzyme CA. The extensive Aspen library does not include this enzyme, as it is a complex biological compound. As previously introduced, the CA enzyme functions as a biocatalyst in the CO_2 absorption. The kinetic absorption rates are enhanced due to the active sides favoring CO_2 hydration. Yet, a catalyst lowers the activation energy of a reaction, increasing the forward and reverse reaction rates equally. This means the equilibrium between reactants and products remains the same, yet it is reached quicker. As a result, modeling in equilibrium with or without the catalyst will leave the outcome unchanged regarding the CO_2 absorption.

Reactions (R15), (R16), (R17), and (R15) represent the chemistry of the PCCA process model without the CA enzyme.

$$HCO_3^- \rightleftharpoons CO_3^{2-} + H^+ \tag{R15}$$

$$H_2O + CO_2 \rightleftharpoons HCO_3^- + H^+ \tag{R16}$$

$$H_2O \rightleftharpoons OH^- + H^+ \tag{R17}$$

$$K_2CO_3 \rightleftharpoons CO_3^{2-} + 2\,K^+ \tag{R18}$$

The dissolution of CO_2 in water defines the chemistry in the PCCA model, yet the solvent dissociation K_2CO_3 into $2\,K^+$ and CO_3^{2-} is also important to reflect the pH changes and dissolved inorganic carbon equilibrium. This is illustrated in Figure 4.1.

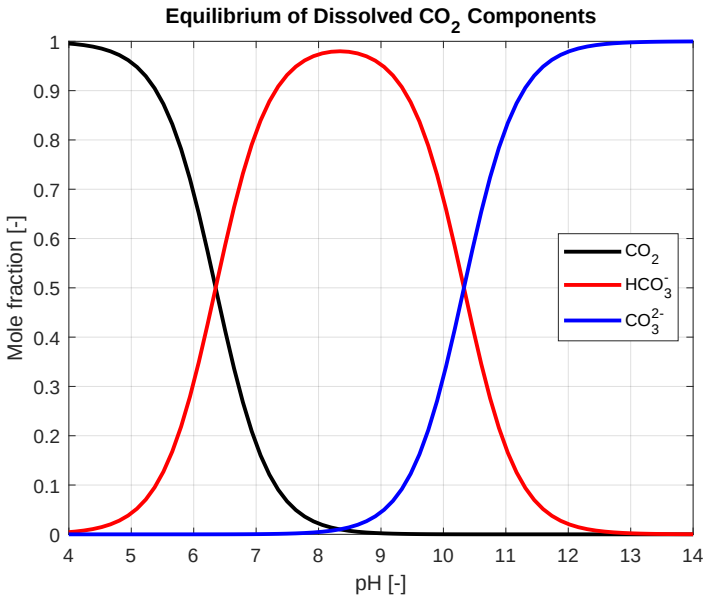

Figure 4.1: Dissolved inorganic carbon equilibrium [Pankow, 2020]

By the presence of K_2CO_3 the dissolved *carbonate ions* (CO_3^{2-}) shifts the equilibrium in Reaction (R15) toward HCO_3^-. The alkaline environment effectively increases the CO_2 absorption capacity due to the higher concentration of CO_3^{2-}, favoring the dissolution of CO_2 into the aqueous solvent. The increased pH obtained by dissolving K_2CO_3 reflects a higher concentration of HCO_3^- relating to the higher CO_2 absorption capacity. [Pankow, 2020].

The CO_2 loading in liquid solvent streams for PCCA is defined by Equation (4.3).

$$\gamma_{\text{PCCA}} = \frac{[CO_2] + [HCO_3-] + [CO_3^{2-}]}{[2\,K^+]} \tag{4.3}$$

Where the solvent is defined from the amount of *potassium ions* (K^+) present, since no other compounds including K^+ ion are present in the liquid. The solid salt K_2CO_3 is not present in the process model as it is dissolved to ions in the aqueous solution.

The process model flowsheet and iteration order for the PCCA model are found in Appendix C. In the PCCA process model, the desorber operates at a lower pressure than the absorber, which is the opposite of MEA and CAP. In the process model, the rich stream expands to 0.25 bar pressure through a valve before entering the desorber, ensuring the boiling temperature in the reboiler is below 80 °C to avoid the CA enzyme degrading. Practically, the desorber operates as an integrated vacuum desorber, with a vacuum pump removing gas at the top of the desorber to decrease CO_2 partial pressure in the desorber. This allows for solvent regeneration of the rich solvent at temperatures below 80 °C, as

the phase equilibrium changes. In the study by Lu et al., a vacuum pump integrated with a desorber in a PCCA process showed an approximately electrical cost of 0.1 MJ/kgCO_2 captured, corresponding to 25 % of the total compressor work [Lu et al., 2012]. Additionally, the electrical work and desorber size increased significantly when the pressure was decreased below 0.2 bar. [Lu et al., 2012]. It is worth noting that the vacuum pump can impact the EWA of the PCCA process, yet it is not included in the KPI scores, as the vacuum pump is not modeled in the Aspen Plus process model. The EWA scores for PCCA might be underestimated due to this assumption.

The remaining components are similar to the ones from the MEA process simulation. Table 4.6 presents the input specifications and initial guesses provided to the PCCA model.

Table 4.6: Key input specification for the PCCA process model

Specification	Value	Unit
Cooled flue gas temperature	25	[°C]
Lean stream cooler temperature	25	[°C]
Condenser temperature	18	[°C]
Initial guesses	Value	Unit
PCCA solvent concentration	30	[wt.%]
Lean CO_2 loading	0.61	[-]
Lean stream inlet ("HEX")	78	[°C]

The flue gas and lean stream temperature is 5 °C higher than that of the MEA model, due to a lower heat of absorption for CO_2 into PCCA than for MEA. Yet, the condenser temperature is decreased to 18 °C due to the lower pressure in the desorber. The initial guesses for PCCA solvent concentration and lean CO_2 loading are found in literature comparing simulations and experimental data [Qi et al., 2018, Hu et al., 2017].

4.4 Chilled Ammonia Process - Equilibrium Model

For the CAP model, the chemistry involves the highly volatile solvent NH_3. The chemical equilibrium reactions are presented in Reactions (R19), (R20), (R21), (R22), and (R23).

$$NH_3 + HCO_3^- \rightleftharpoons H_2O + NH_2COO^- \quad \text{(R19)}$$

$$NH_3 + H_2O \rightleftharpoons OH^- + NH_4^+ \quad \text{(R20)}$$

$$HCO_3^- \rightleftharpoons CO_3^{2-} + H^+ \quad \text{(R21)}$$

$$H_2O + CO_2 \rightleftharpoons HCO_3^- + H^+ \quad \text{(R22)}$$

$$H_2O \rightleftharpoons OH^- + H^+ \quad \text{(R23)}$$

As with the other process models, CO_2 dissociation in water is present to account for the CO_2 dissolution. As previously mentioned, the solid formation risk is not included in the equilibrium model for CAP due to stable operation without solid formation being witnessed from the literature [Sutter et al., 2016].

The CO_2 loading in the liquid solvent streams for CAP is defined by Equation (4.4).

$$\gamma_{NH_3} = \frac{[CO_2] + [HCO_3-] + [{CO_3}^{2-}] + [NH_2COO-]}{[NH_3] + [{NH_4}^{+}] + [NH_2COO-]} \tag{4.4}$$

Similarly to the MEA model, the CO_2 loading is determined by the number of moles of all CO_2 forms divided by the number of moles of all the solvent forms.

For the CAP model in Aspen Plus the process model flowsheet and iteration order are presented in Appendix C. Due to previously explained NH_3 volatility, it is worth noting that the process system configuration is of greater complexity than MEA and PCCA. The CAP consists of a separator component ("NH3-SPLI), recycling 97.5 % of the NH_3 escaping with the cleaned flue gas. This simplifies the process model, significantly reducing the need for a second temperature swing system. As a result, uncertainties occur for the water make-up scores due to the omission of the water wash section for NH_3 capture.

Through developing the CAP process model, an additional CO_2 water-wash column is added, removing most of the NH_3 exiting the desorber in the recovered CO_2 stream. This results in a minor increase in water consumption. Yet, it was found necessary to meet the CO_2 quality recommendation of below 10 ppm NH_3 in the pure CO_2 stream. Table 4.7 provides an overview of the key inputs to the CAP model.

Table 4.7: Key input specification for the CAP process model

Specification	Value	Unit
Cooled flue gas temperature	7	[°C]
Lean stream cooler temperature	10	[°C]
Condenser temperature	68	[°C]
Initial guesses	Value	Unit
NH_3 solvent concentration	10	[wt.%]
Lean CO_2 loading	0.21	[-]
Lean stream inlet ("HEX")	138	[°C]

The column pressure is set to 10 bar at the regeneration section and condenser temperature to 68 °C, avoiding the risks of solid formation [Sutter et al., 2016, Amara, 2021]. The initial guesses for NH_3 solvent concentration and lean CO_2 loading are based on literature, which compares simulation and experimental data for the CAP [Hanak et al., 2015]. As previously specified, a NH_3 concentration above 17.5 wt.% risks solid formation, which is

why the 10 wt.% concentration of NH_3 is chosen.

4.5 Heat Integration Analysis Approach

The heat integration analyses are performed to understand the energy requirements and heat integration possibilities while considering the temperature levels. The optimization by heat integration is vital for beneficial CC and can be a deciding factor for the optimal CC technology.

The pinch analysis is the method utilized for these analyses, with the key assumptions being steady-state operation, no heat losses, and constant heat capacity flows. The analysis uses simple thermodynamics in a practical approach, as the target is investigating process design and operation at the system level. This reflects a simple ideal overview of the energy penalty of CO_2 capture for each CC technology while indicating possible options for heat integration to reduce the energy requirement. Additionally, the pinch analysis shows which thermodynamic losses are inevitable and which can be avoided on a simplified system level. It allows the process designer to work practically with the process to diminish energy requirements. Further, it is a tool for investigating heat exchanger networks, optimizing the process, where the designer can specify constraints to distinguish between what is practically possible and ideal solutions. [Kemp, 2019]

The pinch tool uses the analogy that hot streams need cooling and cold streams need heating. The necessary information for the pinch analysis is supply and demand temperatures for each stream and the individual heat flow corresponding to these temperatures. With this information, the problem table method generates the heat cascade using a minimum temperature approach to determine the hot and cold utility requirements and the pinch point. Drawing composite curves illustrates where heat integration is possible and excess utility is needed. [Kemp, 2019]

Chapter 5

Parametric Study - Process Models

The parametric study investigates the impact on system performance and sensitivity to parameter change. The aim is to analyze the CC technologies and determine optimal operation conditions for comparing them for the selection matrix. A set of parameters will be varied to investigate each CC technology. The main parameter is chosen as the reboiler duty, with the rest being *Liquid-to-Gas ratio* (L/G), lean stream cooled temperature, and cooled flue gas temperature. The performance parameters evaluated in the parametric study are the SPECCA KPI value and CO_2 recovery.

The L/G represents the change in liquid mass flow rate, as the flue gas flow rate is kept constant. It is varied by adjusting the initial guesses for the lean tear stream of each process simulation. The lean stream temperature is controlled by the cooler after the heat exchanger, fixing the temperature of the lean stream before entering the absorber. Lastly, the flue gas temperature is adjusted in the direct contact cooler, which fixes the flue gas temperature entering the absorber.

The parametric studies in Aspen Plus consist of multiple process simulations varying the reboiler duty in a series. A series represents a test range of reboiler duties for a fixed value of the other investigated parameters. The parametric study is conducted on the standardized waste incineration point source flue gas compositions. Table 5.1 shows the baseline for each process model regarding the series parameters.

Table 5.1: Parametric study baseline for process models

Parameter	Unit	MEA	PCCA	CAP
L/G	[kg/kg]	2.61	3.26	1.57
T_{lean}	[°C]	20	25	10
T_{flue}	[°C]	20	25	7

The L/G is based on the absorption capacity of each solvent, why CAP has the lowest and PCCA the highest. The temperatures are defined as minimum temperatures by the CC technology specifications in Chapter 2. The temperature series is increased from here to reflect days where the cooling temperature will be insufficient to cover the baseline values.

5.1 Monoethanolamine Parametric Study

The L/G of 2.61 kg/kg baseline corresponds to a liquid mass flow rate of 200 tonne/h. The first round of the series tested the change in L/G. This is presented in Figure 5.1.

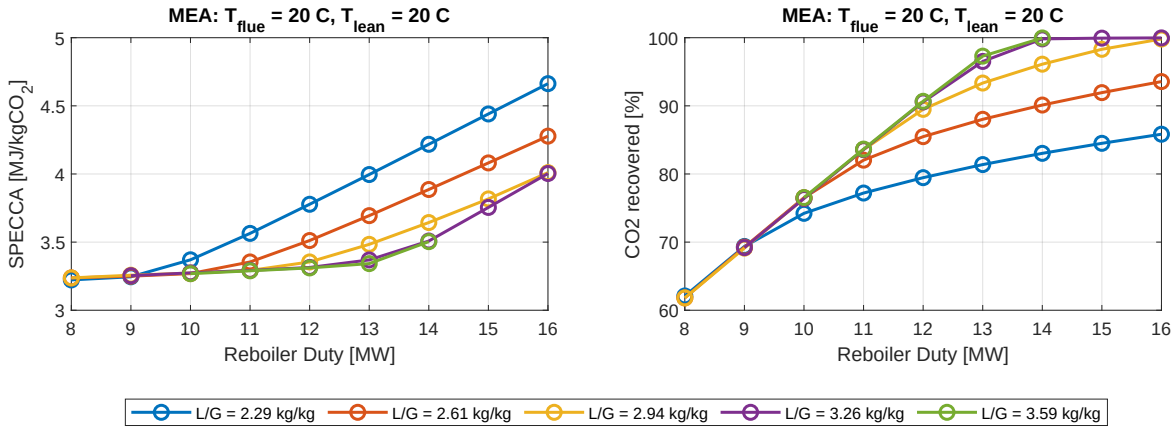

Figure 5.1: Parametric study of MEA model - lean stream massflow rate L/G

In the figure above, the y-axis on the left presents the SPECCA value with the units $MJ/kgCO_2$, and to the right, CO_2 recovered in percentage. The x-axis for both figures shows the reboiler duty range tested for each series. Omitted points are the result of failed simulations. Increasing the L/G results in a lower SPECCA value, corresponding with a higher CO_2 recovery. Yet, above the L/G of 3.26 kg/kg, the change is insignificant, indicating that the change in L/G will result in a larger system size without increasing the CO_2 recovery or energy requirement. As a result, the L/G is needed sufficiently high to decrease the SPECCA value and ensure high CO_2 recovery. Based on the L/G series, the L/G value of 3.26 kg/kg is chosen as the optimal value for the MEA process model. Figure 5.2 shows the lean stream temperature series tested.

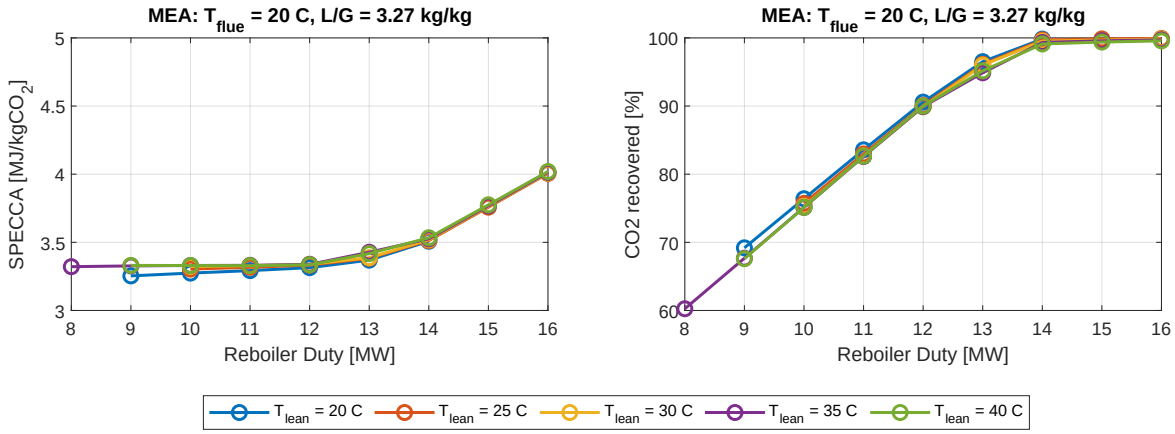

Figure 5.2: Parametric study of MEA model - lean stream temperature

Limited change is observed with the variation in lean temperature. The only significant changes are seen at the lower part of the reboiler range, where the temperature for the lean stream is desired to be low. Yet, the difference in SPECCA value and CO_2 recovery is

insignificant. The series for the flue gas temperature is presented in Figure 5.3.

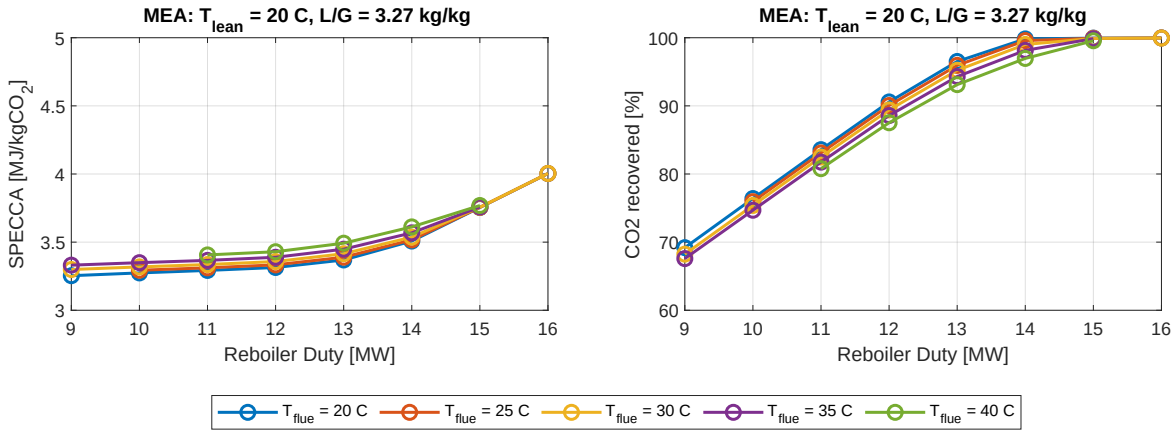

Figure 5.3: Parametric study of MEA model - flue gas temperature

Changing the flue gas temperature shows an insignificant effect on the SPECCA and CO_2 recovery. Even as the tendency is similar between all series across the tested reboiler duty range, the flue gas temperature is desired as 20 °C to reduce the temperature in the absorber, hence water carryover to the vapor phase.

For the MEA technology, the reboiler duty, followed by the L/G, has the greatest impact on the investigated parameters. The lean stream and flue gas temperature show an insignificant impact in the range tested. Yet, keeping the temperatures low is important for decreasing water consumption. The parametric study on MEA shows the need for a sufficiently high L/G if a CO_2 recovery above 90 % is desired. Based on the parametric study, the operating conditions of the MEA equilibrium utilized further on are a L/G of 3.26 kg/kg and cooled lean stream and flue gas temperature of 20 and 20 °C, respectively.

5.2 Potassium Carbonate with Carbonic Anhydrase Parametric Study

As for the MEA parametric study, the L/G, lean stream temperature, and flue gas temperature are varied in series for the PCCA process model. The baseline L/G of 3.26 kg/kg corresponds to a liquid mass flow rate of 250 tonne/h as the initial guess for the lean tear stream. The L/G series for PCCA is displayed in Figure 5.4.

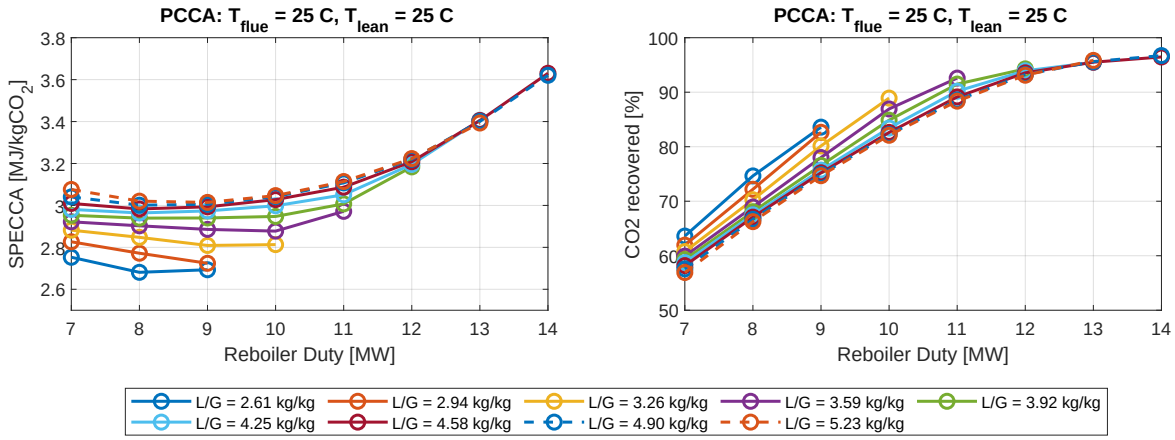

Figure 5.4: Parametric study of PCCA model - lean stream massflow rate L/G

The left figure above indicates an optimum for SPECCA value across the reboiler duty range for each L/G series. Between the L/G series, decreasing the L/G has a proportional effect on the SPECCA value. This shows that the CO_2 absorption capacity change between each series is insignificant. Yet, obtaining a converged simulation for the entire reboiler duty range becomes difficult for the low L/G series, as the temperature in the absorber increases, resulting in increased water evaporation into the clean gas. A sufficiently high L/G is needed to ensure a CO_2 recovery of 90 % or above. The tendency for the CO_2 recovery figure indicates a maximum CO_2 recovery of approximately 95 %. Thus, the solvent regeneration is limited in contrast to MEA, where 100 % recovery was observed.

The L/G value of 3.92 kg/kg is chosen as increasing the L/G further would result in a larger system than necessary. Yet, decreasing below this value shows difficulties in obtaining converged simulations. Figure 5.5 presents the variation in the lean stream temperature.

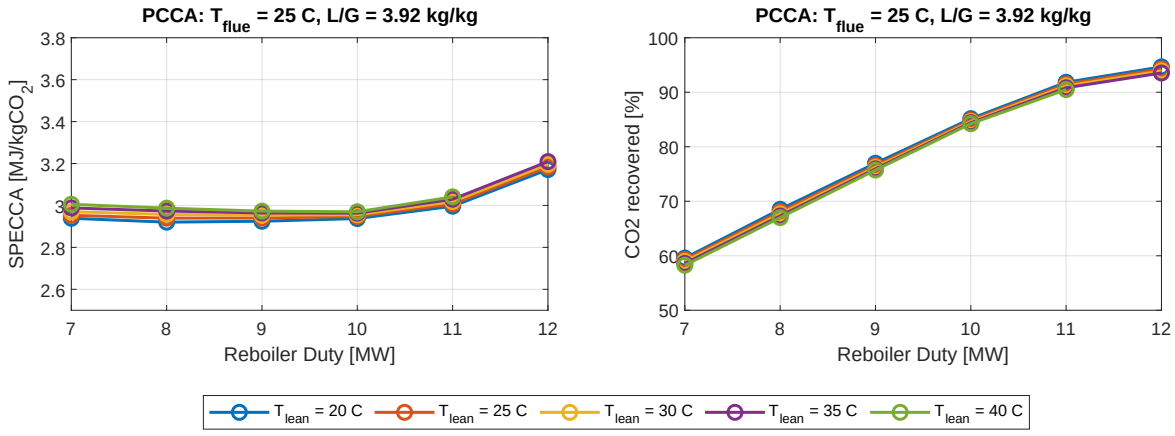

Figure 5.5: Parametric study of PCCA model - lean stream temperature

Decreasing the lean stream temperature shows insignificant changes in SPECCA and CO_2 recovery for PCCA. The reboiler duty follows the CO_2 recovery linearly until 90 % is reached. Increasing the above results in penalizing the SPECCA value, again showing the tendency of a maximum CO_2 recovery for PCCA. Figure 5.6 presents the series of flue gas temperatures.

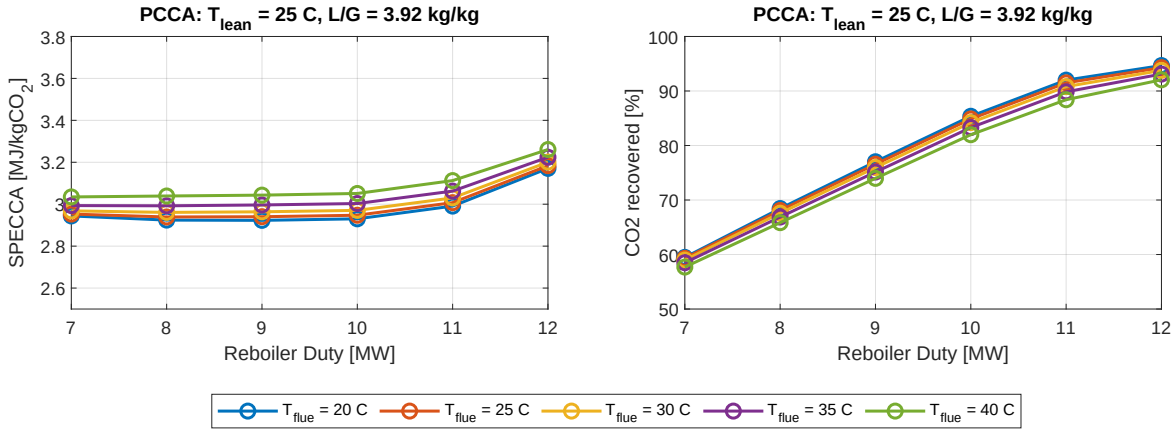

Figure 5.6: Parametric study of PCCA model - flue gas temperature

The flue gas temperature is desired as low as possible to reduce the SPECCA value and enhance the CO_2 recovery. The impact difference from 40 to 35 °C is more significant than from 35 to 30 °C and keeps decreasing. Yet, the impact of the flue gas temperature tested is insignificant.

The tendency of a capped CO_2 recovery of approximately 95 % is observed for PCCA, indicating 100 % is unachievable by increasing the reboiler duty. The absorption capacity and regeneration are robust to changes in the parameters tested. Yet, the tendency for L/G observed is different, becoming a trade-off between high CO_2 recovery and SPECCA value. Difficulties in obtaining a converged simulation are observed at too low L/G ratios, as for MEA, due to high absorber temperatures. The optimal operating conditions for further analysis are chosen with a L/G value of 3.92 kg/kg and cooled lean stream and flue gas temperatures of 25 and 25 °C, respectively, indicating the best trade-off between the SPECCA value and CO_2 recovery, while ensuring a converged result.

5.3 Chilled Ammonia Process Parametric Study

The CAP baseline L/G value of 1.57 kg/kg corresponds to a liquid mass flow rate of 120 tonne/h, nearly half of the other models. This reflects the CO_2 absorption capacity NH_3 possesses compared to MEA and PCCA. Additionally, the lower energy regeneration for NH_3 compared to MEA is a factor in the lower L/G value [Darde et al., 2010,

Sutter et al., 2015]. The parametric study for the L/G series is presented in Figure 5.7.

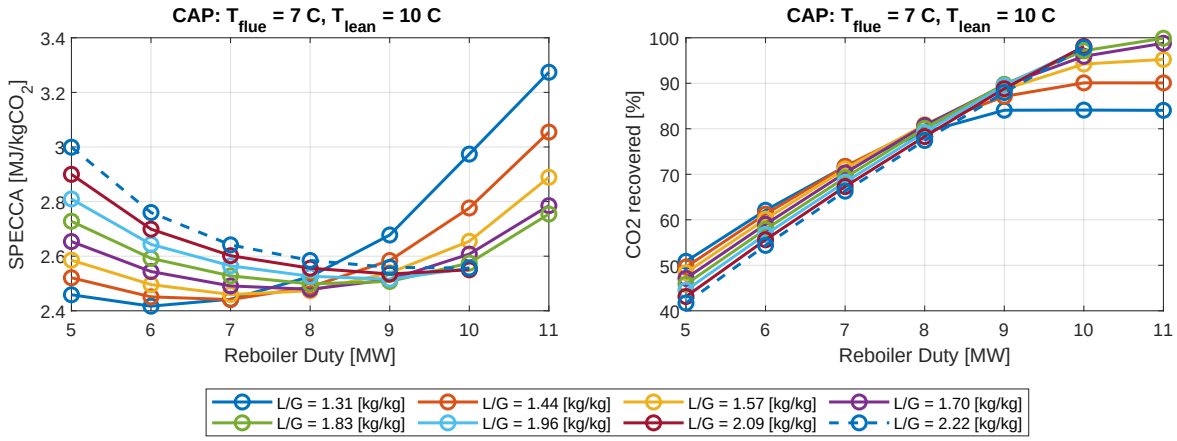

Figure 5.7: Parametric study of CAP model - lean stream massflow rate L/G

At high L/G, SPECCA decreases with increasing reboiler duty. Conversely, at low L/G, the reboiler duty shows the opposite effect. The high volatility of NH_3 reflects the variations in SPECCA. At high L/G above 10 MW in reboiler duty, failed simulations are seen, as a significant amount of NH_3 fails to return to the absorber due to accumulation in the condenser loop. This results in a lower NH_3 concentration, hence a lower rich stream temperature, causing the heat exchanger to fail. A high L/G shows promising high CO_2 with corresponding low SPECCA values, yet with the risk of increased NH_3 slip in the recovered CO_2 stream and lower capture rates.

For CO_2 recovery, an absorption capacity limit is reached for the low L/G series. These are optimal at low reboiler duties, yet limit the CO_2 recovery. This is undesired as it leaves a limited margin for a process designer when designing a CC plant. The optimal value of 1.70 kg/kg is chosen by a trade-off between low SPECCA value, high CO_2 recovery possibility, and robust operation within the reboiler duty range tested. Figure 5.8 represents the lean stream temperature series.

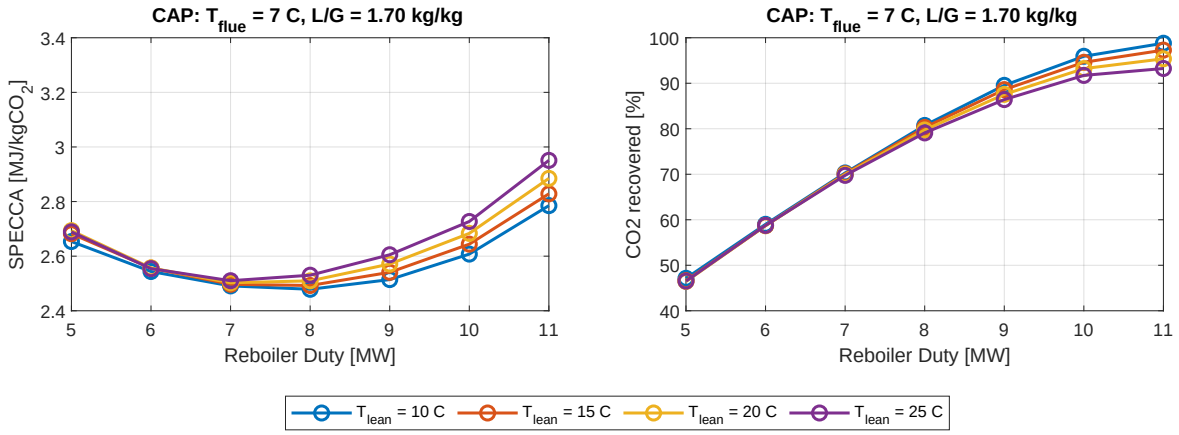

Figure 5.8: Parametric study of CAP model - lean stream temperature

Minor variations are observed by changing the lean stream temperature in the low reboiler duty range, yet become more significant when the reboiler range increases above 7 MW. Thus, the lean stream temperature is desired to be low based on the results above, while it is necessary to minimize NH_3 slip. Figure 5.9 presents the series for flue gas temperature from the CAP model.

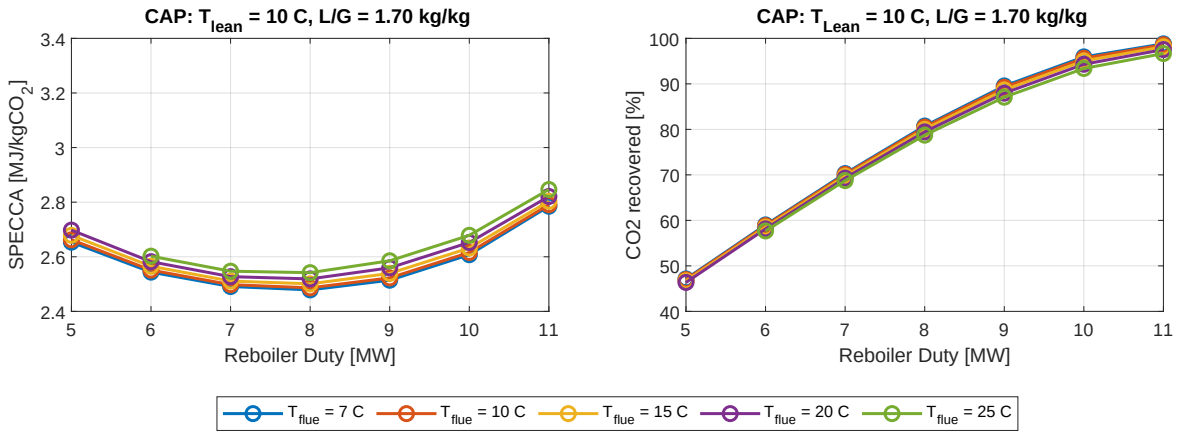

Figure 5.9: Parametric study of CAP model - flue gas temperature

The flue gas temperature shows an insignificant impact on SPECCA value and CO_2 recovery. Varying the reboiler duty results in a greater impact observed with an indicated optimum for the SPECCA value around 8 MW, resulting in a CO_2 recovery of approximately 80 %. Yet, the flue gas temperature is important to keep low to decrease NH_3 slip, as for the lean stream temperature.

The parametric studies show that the CAP CC performance is more sensitive to changes in the L/G than MEA and PCCA, indicating that the highly volatile NH_3 solvent significantly

impacts the system performance by minor variations. Thus, the optimal operating condition for evaluating the selection matrix KPIs is chosen to a L/G of 1.70 kg/kg and cooled lean stream and flue gas temperature of 10 and 7 °C, respectively. Table 5.2 summarizes the optimal operating conditions chosen for each CC technology.

Table 5.2: Optimal operating conditions retrieved from parametric studies

Parameter	Unit	MEA	PCCA	CAP
L/G	[kg/kg]	3.26	3.92	1.70
T_{lean}	[°C]	20	25	10
T_{Flue}	[°C]	20	25	7

The L/G values reflect the difference in absorption capacity between the three technologies. Across the temperature series, insignificant changes are observed. Yet the reboiler duty is vital for SPECCA value and CO_2 recovery. Increasing the L/G for MEA results in increased SPECCA value. Yet, for PCCA and CAP, an opposite tendency is observed, showing that the high heat of absorption regarding MEA controls the energy penalty. The chosen operating conditions become the new baseline for each CC technology to evaluate the selection matrix KPIs defined in Chapter 2.

Chapter 6

Selection Matrix and Heat Integration Analysis

The selection matrix tool enables a systematic comparison between the CC technologies. This governing chapter evaluates the KPI scores for each previously defined point source. Additionally, a heat integration analysis is performed to assess the difference in utility requirements between the CC technologies.

6.1 Selection Matrix Analysis with Fixed CO_2 Recovery

The CO_2 recovery KPI is fixed to compare the CC technologies systematically across the remaining KPIs. Thus, the reboiler duty in the desorber is varied for each case tested, ensuring a fixed CO_2 recovery. Each CC technology is evaluated for the standardized point sources, extending the comparison spectrum to flue gas compositions. The CO_2 recovery is fixed to 85, 90, and 95 % for each technology across each point source, resulting in 27 conducted cases.

The L/G remains constant for each CC technology at the waste incineration and biomass point sources due to similar CO_2 concentration. Yet for the natural gas point source, the L/G is decreased due to the lower CO_2 concentration, resulting in a lower L/G ratio for each CC technology for this point source.

6.1.1 Results of Fixed CO_2 Recovery Cases

The selection matrix KPI scores are extracted for all 27 simulated cases. Bar graphs are constructed, which show the difference in KPI scores for the CC technologies across the 27 cases conducted. In Appendix D, the stream results for the 90 % fixed CO_2 recovery case on the waste incineration points are presented. Additionally, in Appendix E, all KPI scores attained from the 27 cases are presented in a heat map. The fixed CO_2 recovery cases are displayed for the individual KPIs. Figure 6.1 presents the matrix scores for the SPECCA KPI.

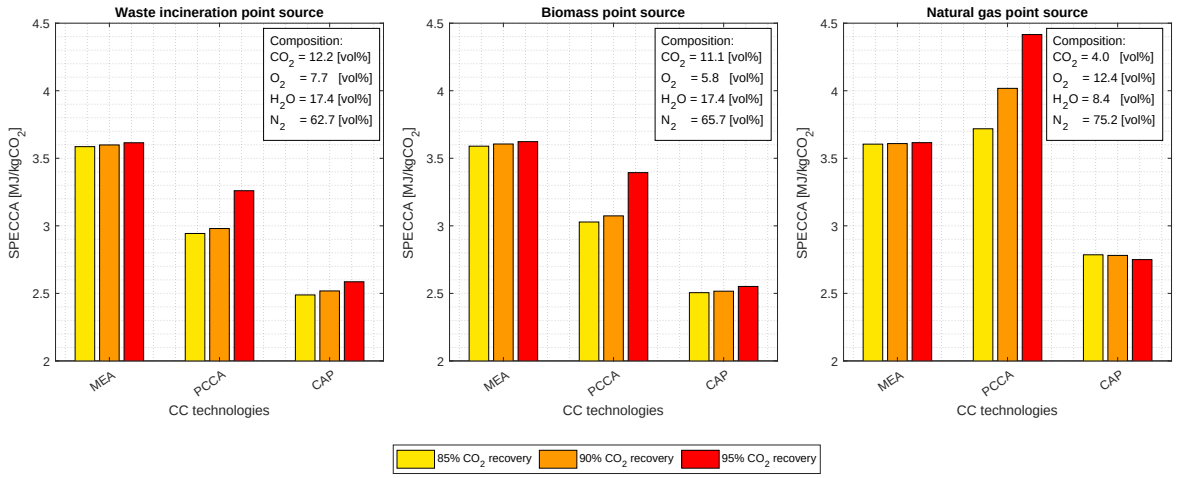

Figure 6.1: SPECCA KPI scores for conducted fixed CO_2 recovery cases

The preferred CC technology tendency across the SPECCA scores is the CAP, PCCA, and MEA, respectively, except for the natural gas point source, as PCCA exceeds MEA. The limitation of approximately 95 % CO_2 recovery case for PCCA is indicated as it spikes in SPECCA value, indicating a significantly more energy-intensive CC process than MEA and CAP above 90 % CO_2 recovery. MEA is the most robust regarding SPECCA score across the point sources, indicating that the CO_2 concentration and fixed recovery have an insignificant impact on the SPECCA value. The CAP is a clear favorite based on the SPECCA KPI scores between 2.5 and 2.8 across the conducted cases. Figure 6.2 compares the water make-up scores for the fixed CO_2 recovery cases across point sources.

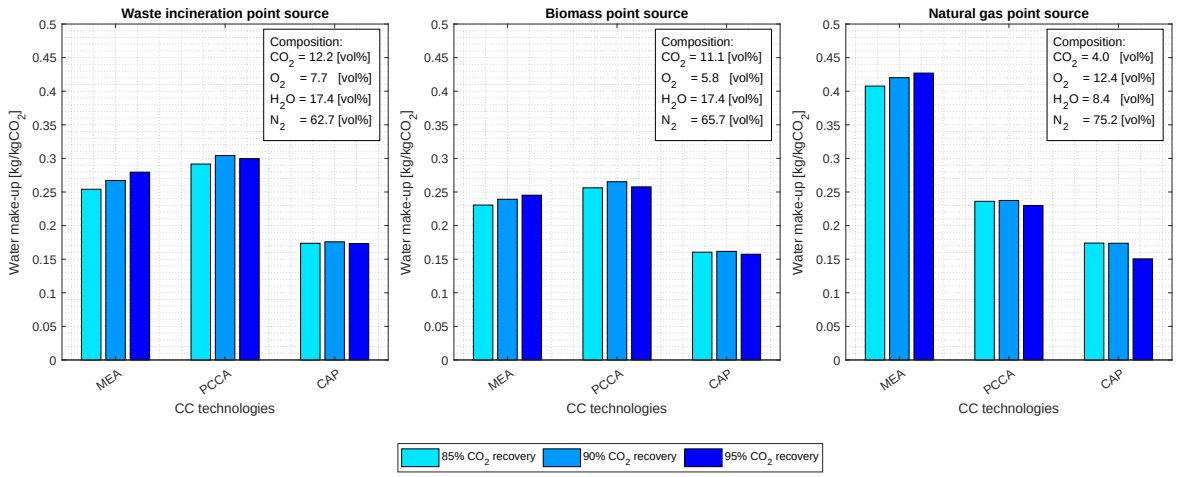

Figure 6.2: Water make-up KPI scores for conducted fixed CO_2 recovery cases

The tendency observed is that CAP requires less water make-up than MEA and PCCA. The water make-up for MEA is lowest at the biomass point source and highest at the natural

gas point source, due to the L/G at each point source. The L/G for waste incineration and biomass is equal, causing a higher absorber temperature due to the higher absorption heat in the waste incineration point source, as the CO_2 concentration is higher in the flue gas. The MEA water make-up is significantly higher for the natural gas point source, as the dry gas flow through the absorber is greater, reducing the separation effect and increasing the water loss. Yet, water make-up for PCCA and CAP is decreased at the natural gas point source, showing water is less likely to evaporate from the K_2CO_3 and NH_3 solvent than for MEA.

A tendency to lower water make-up per avoided CO_2 is observed for CAP and PCCA at 95 % compared to 90 % CO_2 recovery. Increasing the reboiler duty leads to a greater desorber distillate rate, reducing the water carryover to the absorber for PCCA and CAP. Yet for MEA, increasing the reboiler duty results in a lower lean loading returning to the absorber, increasing the absorber temperature, hence a greater need for water make-up per avoided CO_2. This shows the difference in thermodynamic and chemical capabilities of the solvents. The water make-up per avoided CO_2 is lowest for the CAP across all cases, even with the added water wash of the recovered CO_2 to minimize NH_3 slip. This indicates that the highest fraction of water escape occurs in the absorber due to the temperature of the cleaned flue gas. The water cycle above the absorber reducing the NH_3 slip is not included, resulting in an uncertainty for the water make-up for the CAP. Yet, the temperature in flue gas is not increasing by being washed with water when recapturing NH_3, hence no significant water make-up is expected due to this recapture.

Figure 6.3 presents the solvent make-up KPI scores.

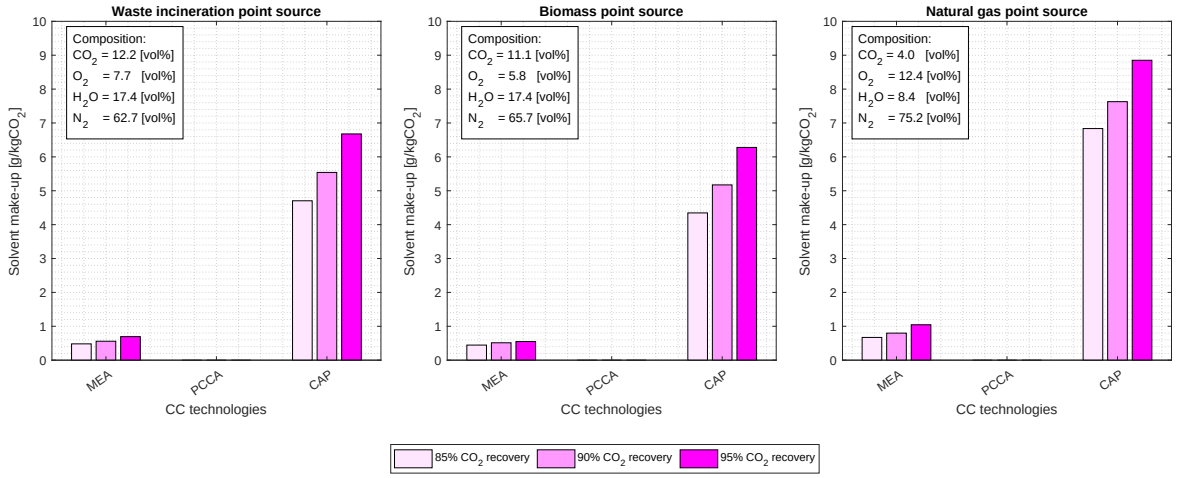

Figure 6.3: Solvent make-up KPI scores for conducted fixed CO_2 recovery cases

The solvent make-up KPI scores present similar tendencies for each CC technology across the cases. Increasing the fixed CO_2 recovery has a proportional effect on solvent make-

up per avoided CO_2 across all point sources. The solvent make-up per avoided CO_2 for the process models only includes the gas phase escape of solvents, why PCCA is zero. According to the presented results, CAP is the most solvent-expensive compared to MEA, with the absolute values for MEA and CAP below 10 g per kg avoided CO_2. Figure 6.4 presents the EWA KPI scores for the conducted cases.

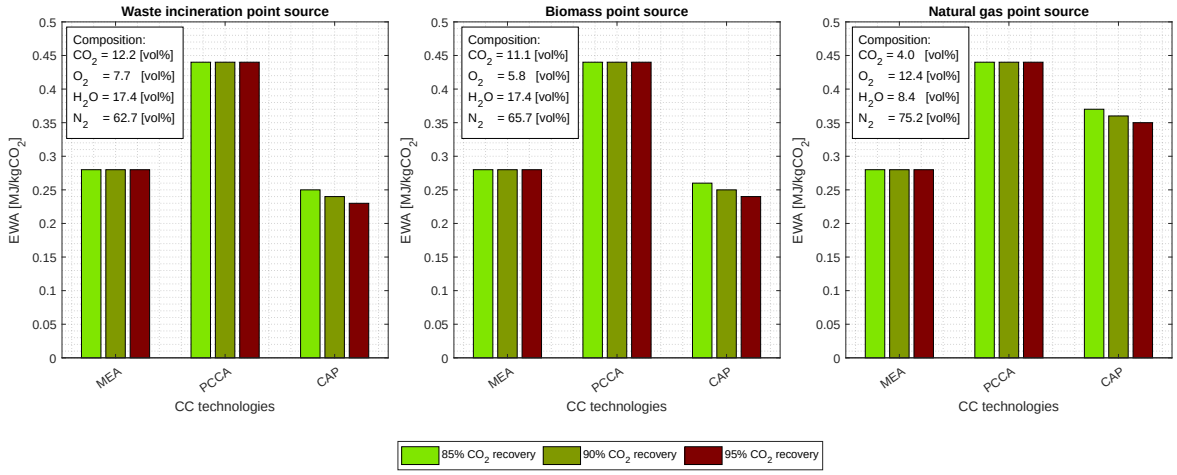

Figure 6.4: EWA KPI scores for conducted fixed CO_2 recovery cases

The EWA scores indicate PCCA as the technology requiring the highest electrical power per avoided CO_2. The desorber pressure determines the pressure of the recovered CO_2 stream, why the CO_2 compression unit for PCCA requires significantly more electrical work than MEA or CAP. Yet, a lower difference is observed between PCCA and CAP for the natural gas point source. Here, the CAP requires more electrical power than MEA, reflecting the chiller work needed to maintain the cold temperatures. The EWA scores show CAP as the better-suited option at high CO_2 concentration, indicating a turning point to MEA when decreasing the CO_2 concentration, even with a higher net compressor work for MEA than for CAP. Figure 6.5 shows the O_2 content in the capture CO_2, where the recommendation from DYNAMIS is below 100-1000 ppm [SINTEF, 2009].

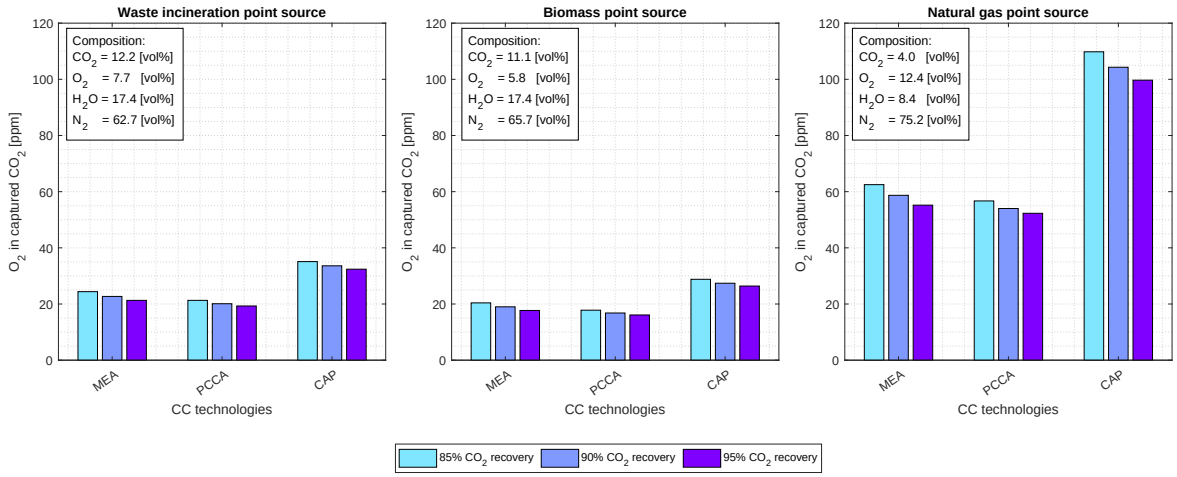

Figure 6.5: O_2 KPI scores for conducted fixed CO_2 recovery cases

The differences in CO_2 scores reflect the Henry constants for O_2 in each solvent. The O_2 dissolution is greater in NH_3 than for MEA and PCCA. PCCA scores lowest of the three, lower than 65 ppm for the natural gas point source containing 12.4 vol% O_2. Increasing the reboiler duty decreases the O_2 concentration in the recovered CO_2, indicating less evaporation of O_2 compared to CO_2 as the fixed CO_2 recovery is increased from 85 to 95 %. The main drawback is observed for the CAP, as the O_2 concentration increases in the flue gas, the O_2 content increases in the recovered CO_2. Even with the robust NH_3 solvent, where O_2 content is irrelevant for CO_2 absorption, too high a concentration of O_2 in the flue gas may result in the need for O_2 removal before the CO_2 quality is sufficient for storage or transport. Figure 6.6 displays the N_2 content KPI for the recovered CO_2 stream.

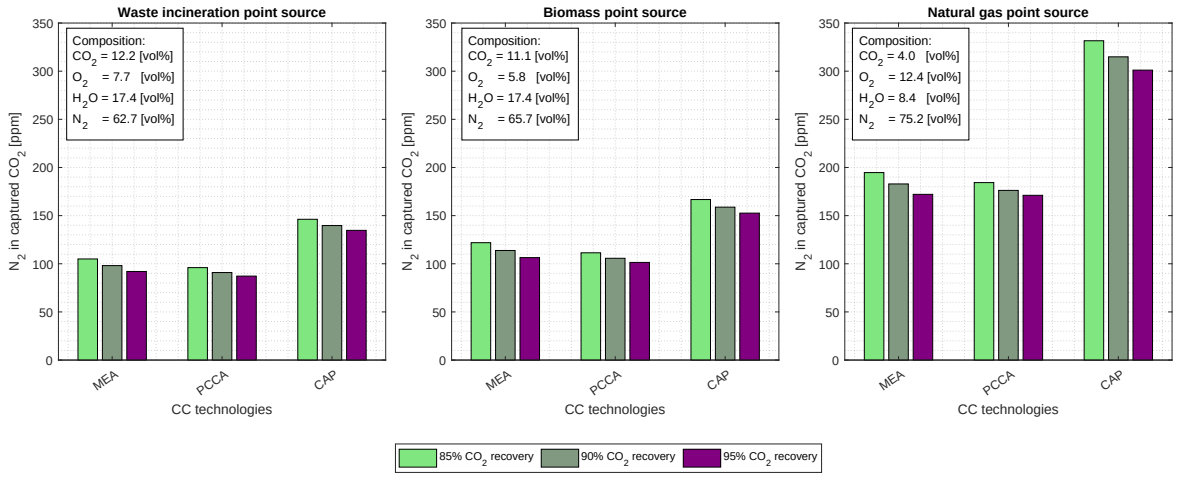

Figure 6.6: N_2 KPI scores for conducted fixed CO_2 recovery cases

N_2 content recommendation from the DYNAMIS project is below 4 vol%, where each KPI

scores significantly below that threshold. The Henry constant for N_2 regarding each solvent shows similar tendencies as O_2, where the CAP is inclined to have a greater dissolution of N_2 compared to MEA and PCCA. Conversely, PCCA shows the lowest dissolution amongst the CC technologies. N_2 has the largest volume fraction of the compounds in each flue gas. Yet, the gas N_2 concentration and content in the recovered CO_2 show that the Henry component is significantly lower than that of O_2. Additionally, increasing the reboiler duty for each CC technology decreases the N_2 content in the recovered CO_2, showing a similar tendency observed for the O_2 content. Figure 6.7 presents the KPI scores for solvent content in the recovered CO_2 stream. As MEA shows negligible solvent content and PCCA none, the solvent content is presented for CAP with and without water wash of the recovered CO_2 stream.

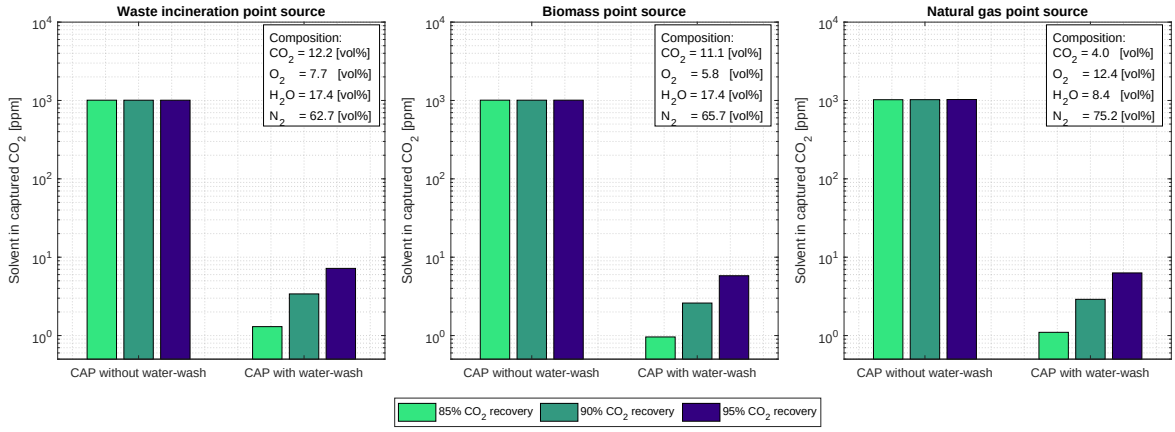

Figure 6.7: Solvent content KPI scores for conducted fixed CO_2 recovery cases

It is worth noting that the y-axis is logarithmic to display the magnitude difference between with and without water wash. The solvent content in the CO_2 recovered stream increases with the reboiler duty, showing that the reboiler duty is proportional to NH_3 slip. As the CO_2 water-wash column is added to the CAP process model, the fraction is kept below the 10 ppm threshold for the CO_2 quality recommendations. Yet, adding the water wash increases system complexity with additional wastewater, increasing both capital and operational costs.

The selection matrix case studies determine the CAP as an overall favorite for the KPIs. Yet, the CAP is not the best-performing on the solvent make-up, solvent content, and EWA at low CO_2 concentration in the flue gas (4 vol%). Even with the CAP as the best overall-performing technology, it is also the CC process with the greatest complexity due to added water wash, chillers, and high reboiler temperatures.

Heat integration between the CC technology and the host plant is important in evaluating the CC process and impacts the decision on which technology is preferred. Therefore, a

pinch analysis of each CC technology is conducted to expand the selection matrix comparison of the CC technologies with the minimum energy requirements. The SPECCA scores previously presented for each CC technology omit the energy quality. A pinch analysis is performed to include the temperature levels in determining the minimum energy requirements for each process, enabling an extended comparison of the CC technologies.

6.2 Heat Integration Analysis

The pinch analysis is performed for each CC technology on the 90 % fixed recovery case for the waste incineration point source.

The CC plants are seen as a stand-alone industrial process. Yet, practically, the process is attached to an industrial process where heat integration includes all hot and cold streams to evaluate beneficial CC. The degree of excess heat or cooling from the process plant to the CC plant is case-specific. As this study seeks to compare the CC technologies, the pinch analysis is conducted for each CC process, providing insight into the heat integration possibilities within the CC plant and the necessary energy requirement from outside the CC plant to compare differences across the CC technologies. The data extracted from each CC technology process model is presented in Table 6.1.

Table 6.1: Pinch analysis data from CC process model

Technology		**MEA**			**PCCA**			**CAP**		
Stream	Hot/Cold	T_1 [°C]	T_2 [°C]	$\dot{Q}$ [MW]	T_1 [°C]	T_2 [°C]	$\dot{Q}$ [MW]	T_1 [°C]	T_2 [°C]	$\dot{Q}$ [MW]
Flue gas	Hot	60	20	6.0	60	25	5.6	60	7	6.7
Lean stream	Hot	122	20	24.2	78	25	5.1	143	10	20.7
Gas desorber	Hot	103	25	3.9	65	18	3.8	115	68	1.6
Intercoolers (total)	Hot	80	35	1.9	100	35	2.7	70	35	1.5
Rich stream	Cold	42	104	18.1	59	70	1.5	26	138	15.3
Reboiler	Cold	122	122.1	12.9	78	78.1	10.7	143	143.1	9.1

The table above shows the hot and cold stream conditions for each CC technology utilized in the pinch analyses. A rule of thumb for the pinch point is that when processes include latent heat exchange, as the CC processes do, the bubble/dewpoints usually determine the pinch point. Additionally, for the reboiler, a pure latent heat exchanger, the boiling temperature would be constant, yet to avoid division by zero, a temperature difference of the cold stream of 0.1 °C is assumed to include the energy demand for evaporation. This represents the bubblepoint temperature, why the pinch point is expected here. [Kemp, 2019]

The *Grand Composite Curve* (GCC) is constructed by the problem table method [Kemp, 2019]. Additionally, the individual *Hot Composite Curve* (HCC) and *Cold Composite Curve* (CCC) are determined to present the differences in minimum required utility and the possibilities for heat integration. The pinch analysis is conducted with a global minimum temperature of 10 and 2 °C to compare the difference in utility requirement for a simple low capital

cost process and a complex high energy efficient process. This is assessed as possible due to the heat transfer processes in the CC plants. These include latent evaporation/condensation, direct contact cooling, and liquid-to-liquid heat exchange, which all involve high heat transfer coefficients.

A set of arbitrary utility sources is included on the GCCs to illustrate the difference in necessary utilities across the CC technologies. Yet, practically, all the utility sources depend on the type of industrial process plant and location, as it determines the excess heat temperature and heat flow available and the cooling water temperature. Additionally, the possibility of delivering to district heating. Table 6.2 shows the defined utilities utilized in this study.

Table 6.2: Arbitrary hot and cold utility sources chosen for pinch analysis.

Utility	Abbriviation	T_{in} [°C]	T_{out} [°C]
Medium-pressure steam	MPS	150	150
Low-pressure steam	LPS	130	130
Heat pump water	HPW	95	85
District heating	DH	45	80
Cooling water	CW1	20	25
Cooling water	CW2	10	15
Chiller	CH	2	2

Where medium and low-pressure steam utilities are at constant temperature, reflecting condensation to supply heat. The *Heat Pump* (HP) water presents a heat source that can deliver heat without steam, resulting in a lower-cost heat utility than steam. The district heating utility presents a third-generation district heating temperature level. The chiller operates at constant temperature, reflecting the evaporator in a refrigeration cycle. Figure 6.8 presents the GCC for each CC technology at the 90 % fixed CO_2 recovery case for the waste incineration point source with added utility sources to cover the requirements.

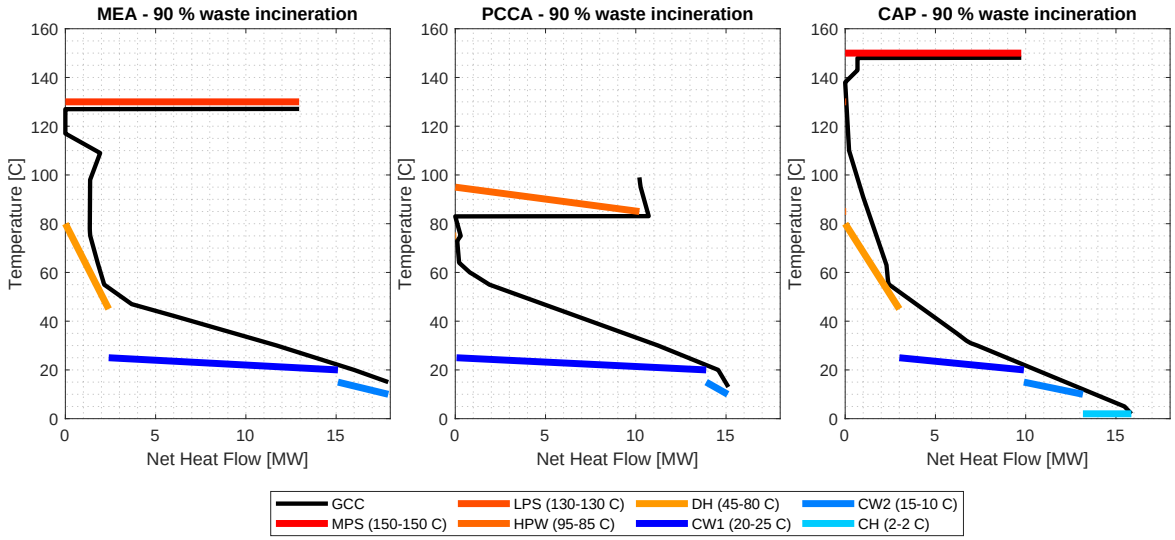

Figure 6.8: Grand composite curves for 10 °C global minimum temperature

In the figure above, the difference in GCC is seen across the three technologies. The pinch point is seen at the intersection with the y-axis. MEA shows a pinch region due to zero heat flow between 117 and 122 °C, where a pinch point at 80 and 138 °C is seen for PCCA and CAP, respectively. The temperature levels necessary to cover the reboiler duty are favored in the PCCA process. Additionally, a minor possible heat integration is observed from the "right pointed nose" in the PCCA GCC. The MEA GCC shows a minor heat integration possibility below the pinch point.

Part of the cooling requirement for MEA and CAP can be cooled by the district heating source, indicating a reduction in operational expenses. The temperature level for PCCA is too low to be cooled with district heating when the global minimum temperature is 10 °C. Yet, a high-temperature HP can cover the heating requirement for PCCA, which is why utility heat costs for MEA and CAP are considerably greater compared to PCCA. For the hot utility above the pinch point, the temperature level is directly proportional to the price of each utility, reflecting the latent evaporation energy for water. From the GCC in the figure above, the PCCA indicates the cheapest CC technology to implement regarding temperature levels and energy requirements.

Figure 6.9 shows the HCC and CCC with shaded areas for necessary hot and cold utilities when the global minimum temperature is set to 10 °C.

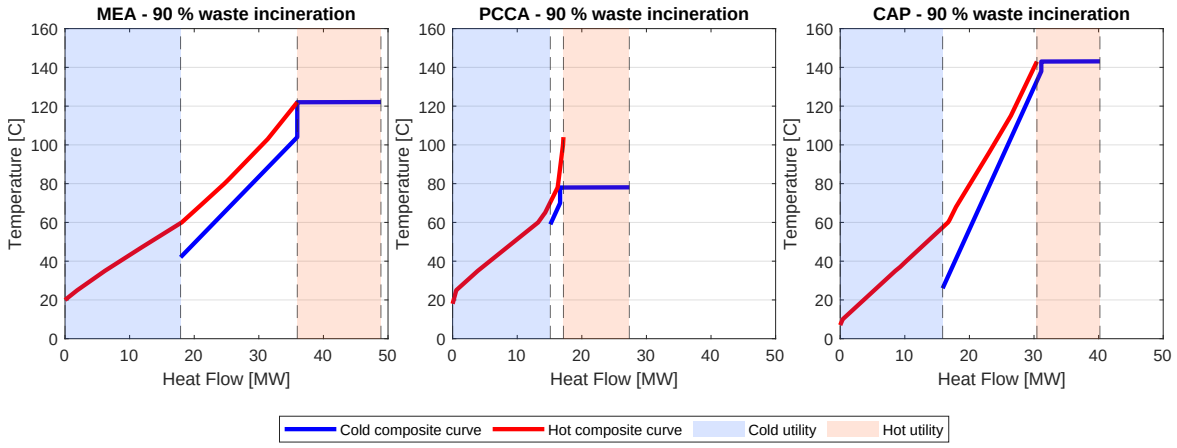

Figure 6.9: Hot and cold composite curves 10 °C global minimum temperature

The areas between the required hot and cold utilities show the option for heat integration, where the hot and cold composite curves can exchange heat. The heat exchangers from each CC technology primarily represent this area, showing a beneficial heat integration solution. For PCCA, a minor heat integration for the intercoolers with the reboiler is seen, yet the heat flow is significantly low to heat integrate. The significance of the heat exchangers is highest for MEA, even when it has the highest hot and cold utility-demanding process. The heat exchanger for PCCA covers a minor part of the utility requirement, indicating a smaller heat exchanger area, hence a lower heat exchanger cost.

A pinch analysis for each CC technology with a global minimum temperature of 2 °C is performed equally for the waste incineration case to investigate the change in utility requirement from the 10 °C analyses. Practically, larger heat exchangers are required to decrease the global minimum temperature approach, increasing the capital investment of the CC process. Yet, with the processes in the CC plant, a low global minimum temperature is not unrealistic.

For the 2 °C case, a possible high-temperature HP configuration is added to the PCCA GCC with condenser and evaporator heat flows. This illustrates a PCCA process where the heat utility requirement is replaced by electrical compressor work to sustain the CC process. The high-temperature HP has a COP of 3.9, utilizing ammonia as refrigerant. Appendix F presents a more detailed description of the HP utilized. Figure 6.10 shows the GCC from these analyses.

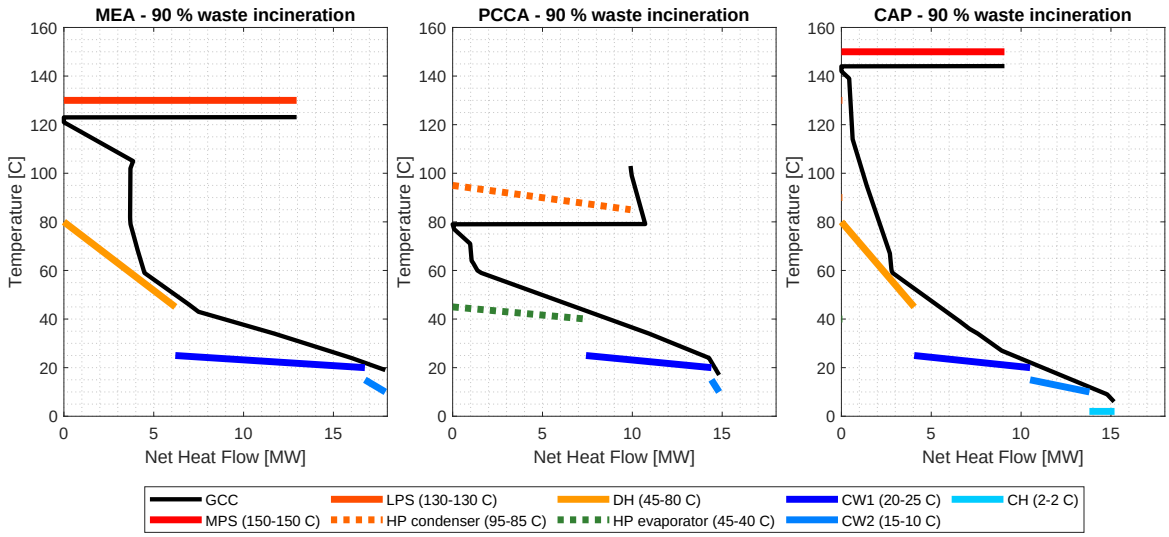

Figure 6.10: Grand composite curves for 2 °C global temperature

The 2 °C GCC shows a scenario for each CC technology with a higher energy-efficient process resulting in increased district heating possibilities for MEA and CAP. This shows that optimizing each CC process to a 2 °C global minimum temperature decreases the expenditures for cooling. This results in approximately half of the chiller heat flow necessary for cooling the CAP. For PCCA, the added HP evaporator replaces a fraction of the cooling water needed. Additionally, the hot utility requirement of 9.9 MW from PCCA can be covered by 2.6 MW of electrical compressor work, resulting in decreased cold utility requirement due to the evaporator. Figure 6.11 illustrates how the PCCA CC process can be implemented with a high-temperature HP to meet the hot utility requirement while decrease the cold utility requirement.

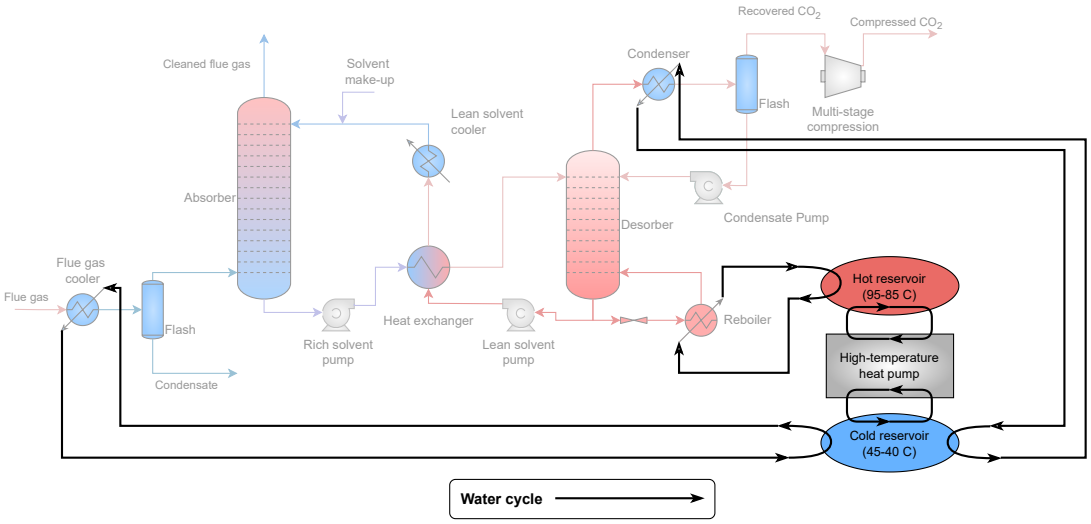

Figure 6.11: Process flow diagram of PCCA process with heat integrated heat pump

The dotted lines above show expected water cycles to cover the heat flows. The exchange between the HP and reservoirs demands a temperature difference, and equally, the exchange between the hot and cold reservoirs and the CC system components demands a temperature difference. This results in a larger temperature difference in the HP, decreasing the COP. The system configuration introduces this penalty due to the water cycles between the reservoirs and the CC process components. It is worth noting that the water cycle between the cold reservoir and the flue gas cooler and condenser only covers a fraction of the cold utility requirement for these components, due to the temperature level and heat flow seen on the GCC above. Figure 6.12 shows the HCC and CCC for the 2 °C global minimum temperature pinch analyses.

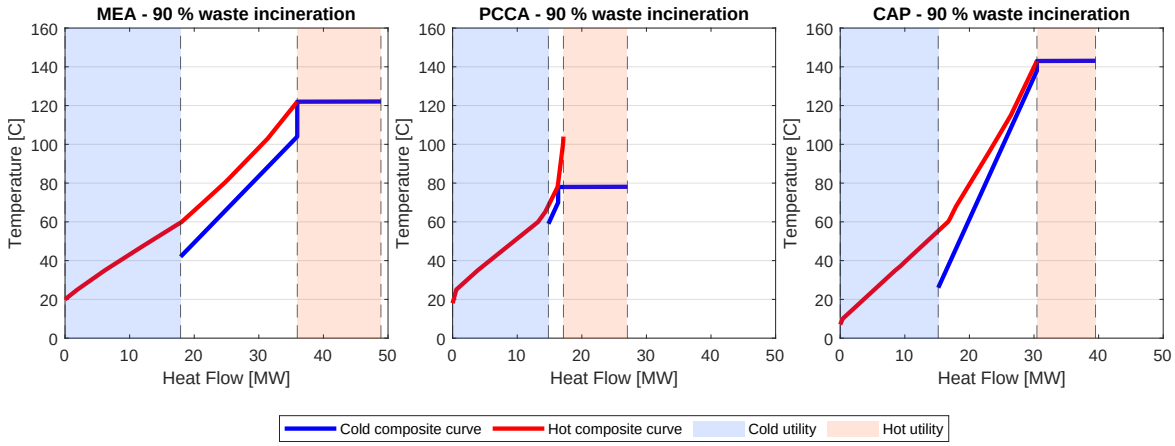

Figure 6.12: Hot and cold composite curves for 2 °C global minimum temperature

The figure above shows minor differences to the 10 °C global minimum temperature HCC and CCC figures, seen by the temperature levels and a decrease in hot and cold utility requirements. For the PCCA, the hot utility requirement can be met entirely by a high-temperature HP, resulting in an integrated process with increased electrical compressor power being the penalty.

6.2.1 Utility Supply Options

The utility supply options are vital in determining the most suitable CC technology for an industrial process plant. Table 6.3 shows the electrical work and utilities each process requires, with the integrated HP process for PCCA for comparison.

Table 6.3: Utility requirements for each CC technology from pinch analyses. *a*: *updated from HP coverage*

Electrical work	Unit	MEA	PCCA	CAP	PCCA-HP
From CC process	[MW]	1.0	1.6	0.8	1.6
HP replacement	[MW]	0	0	0	2.6
Total	[MW]	1.0	1.6	0.8	4.2
Hot utility requirement	[MW]	13.0	9.9	9.1	0.0^a
Cold utility requirement	[MW]	17.9	14.8	17.2	7.4^a

The table above shows an increase in electrical work by approximately 160 % for the PCCA when the high-temperature HP covers the hot utility requirement. Comparing the technologies with the updated utility requirements, the PCCA shows an almost complete electrical-driven process. Additionally, 50 % of the cold utility demand is covered by the high-temperature HP for PCCA-HP.

The hot utility requirements for MEA and CAP demand low or medium-pressure steam to run the process. Effective heat integration is essential to optimize the energy efficiency and reduce the utility demands. One strategy involves utilizing thermal energy from the host industrial plant. Rarely is any thermal heat from the host plant available as excess energy. It serves as a penalty for supplying the CC process. The thermal energy can be met through extracting steam and utilizing the latent heat from condensation. External heat must be provided when internal sources are insufficient or unavailable. This can be met with electricity-based as an electric heater or a HP, offering precise control and rapid response to changes in load. Another solution is combustion-based sources like gas-fired, biomass, and biogas boilers, which provide a steady thermal output and are compatible with various process configurations. The choice of heat sources and integration strategy becomes case dependent. Table 6.4 shows the hierarchy of assessed process heating sources in the two categories. [Olsson and Schipfer, 2022]

Table 6.4: Hierarchy of process heating sources

Hierarchy	Electricity-based	Combustion-based
1	Heat pump	Biomass/Biogas
2	Electric heater	Natural gas
3	Green Hydrogen	Coal

Electricity-based sources are expected to be driven by renewable energy sources. The HP is a clear favorite due to the high obtainable COP for electricity-based sources [Bauer et al., 2023], yet the specific value depends on the heat source and sink. High-temperature HP reaching 150 °C is possible, however, the complexity in HP configuration is proportional to investment cost [Dumont et al., 2023]. An electric heater is approximately a direct conversion from electrical to thermal energy. Green hydrogen is used through combustion, reflecting an electrical energy carrier. The conversion efficiency from electrical energy to hydrogen lies between 60 and 97 %, depending on the electrolyzer type [Pashchenko, 2024]. Yet, storage capacity is beneficial compared to batteries, resulting in a trade-off between an electric heater and green hydrogen, depending on the variation in electricity price. [Olsson and Schipfer, 2022]

Biomass and biogas are favored combustion-based sources, due to the possibility of being carbon-neutral. Natural gas is a fossil fuel, but is favored over coal due to the flue gas composition. Generally, sustaining a CC process by emitting CO_2 through combustion presents a paradox regarding the process. Increasing the CC plant size to capture the additional CO_2 emission from the process heat generation reduces the penalty concerning added CO_2 emissions, yet the CC plant is overdimensioned compared to its initial purpose. [Olsson and Schipfer, 2022]

Mechanical Vapor Recompression

The *Mechanical Vapor Recompression* (MVR) concept, as the HP, reduces hot utility requirement by electrical work as a replacement. The reboiler duty requirement decreases through heat recovery. Figure 6.13 illustrates the concept of the MVR used in CC processes.

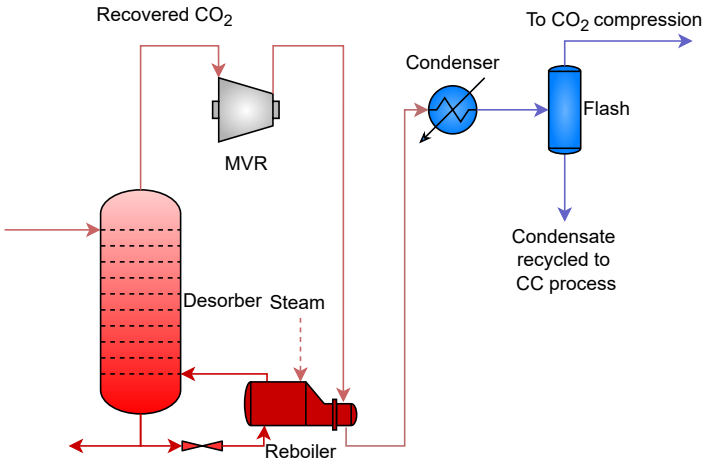

Figure 6.13: Illustration of mechanical vapor recompression in a CC process

A compressor is inserted after the desorber, pressurizing the vapor stream, increasing the stream temperature and pressure. The compressed vapor stream then delivers heat to the reboiler before moving through the condenser. The stream is then cooled and condensed to separate the CO_2 and condensate, which is recycled to the CC process. This reduces the hot utility requirement with electrical compressor work as a consequence. A study by Fischer et al investigated the impact of the MVR method in a techno-economic analysis of a MEA CC process regarding a coal power plant. From the study, a decrease in reboiler duty of 18 to 39 % was observed. Yet, the impact of MEA degradation above 122 °C is not included in the study. Thus, the risk of MEA thermal degradation increases, as the condensate post-reboiler heat exchanger is recycled to the CC process. This would increase the MEA make-up, risk of emitting toxic components, and corrosion, hence operational expenditures for the CC process. [Fisher et al., 2005]

Another advantage of the MVR method is that the compressor generally functions as the first stage of the CO_2 multi-stage compression, resulting in less compressor power to reach 110 bar for the CO_2 recovered stream. Yet, the gross compressor work might increase as the compression in the MVR handles a greater mass flow. Conversely, the reduced reboiler duty requirement may be a beneficial solution. Thus, the MVR heat recovery is another electrification method, reducing the hot utility requirement as a HP. Yet, the heat recovery is at a higher temperature, which can cover part of the steam generation demand of MEA and CAP. MVR increases system complexity and investment cost, but can be a solution if insufficient excess heat is available. [Fisher et al., 2005]

6.3 Results of Case Studies and Heat Integration Analysis

The heat integration analyses investigated the differences in minimum utility requirements for the CC technologies. The selection matrix scores for SPECCA and WEA are presented with the additional hot and cold utilities normalized against avoided CO_2 to include the results from the pinch analyses in comparing the CC technologies. Figure 6.14 presents a heat map with a column color scaling, hence each column is scaled for each KPI score. Additionally, the PCCA-HP proposed technology is included in the matrix.

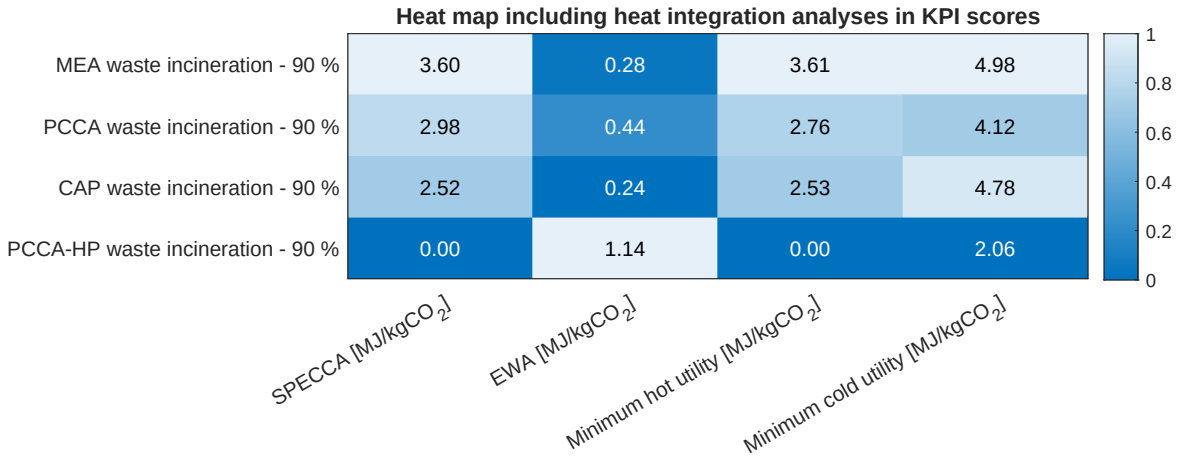

Figure 6.14: Heat map results based on heat integration analyses

The spectrum from light to dark blue reflects the worst to the best score concerning the individual KPI. For SPECCA, the CAP previously showed the best-scoring technology, and omitting the PCCA-HP shows the same results except for the minimum cold utility requirement. A takeaway from the matrix scores is that MEA indicates the worst heat integration possibility of all 4, with the highest minimum utility requirements. Yet, as the hot utility requirement of the PCCA-HP process is met with the high-temperature HP, the SPECCA value is set to zero. Thus, PCCA becomes the best-scoring technology for the SPECCA KPI with the penalty of electricity demand increasing by 160 %. The remaining KPIs are previously discussed, with CAP as the overall best compared to MEA and PCCA, only lacking in solvent make-up and solvent content in the CO_2 recovered stream. Yet, the absolute values are low for a CC process and uphold CO_2 quality recommendations.

When incorporating the heat integration analyses into the matrix evaluation, the CAP emerges as a potential overall optimal technology compared to MEA and PCCA. Yet, the CAP shows certain integration challenges due to the temperature range within the CC process, demanding medium pressure steam at 150 °C and chiller work at temperatures below 5 °C. MEA follows closely, demanding 130 °C. This points to a disadvantage for CAP and MEA compared to PCCA, where low-grade heat is more readily available. This

makes CAP and MEA less adaptable than PCCA in such contexts. PCCA-HP shows a solution, reflecting the greater adaptability of PCCA integration with the host plant.

The EWA scores for the CAP include the chiller work, and the associated cooling duty can significantly influence the overall energy integration strategy, which can be a determining factor in choosing or disregarding this CC technology. The difference in SPECCA value between MEA and CAP is significantly higher than EWA. The CAP shows a better trade-off than MEA due to similar reboiler temperature but a lower SPECCA value. This includes the consideration of the chiller work sensitivity concerning chiller size and efficiency.

Ultimately, while CAP shows the greatest promise in heat integration with the host CC plant, the optimal decision becomes case-specific. The need for medium-pressure stream or low chilling temperature can be a deal breaker. Thus, the optimal decision will come down to the techno-economic evaluation from the CC plant design perspective, which considers energy integration potential and broader system design constraints.

While the KPI scores provide a high-level comparison between the CC technology performance, the heat integration analyses show a broader comparison of the technologies, providing the user with an additional overview. This shows the importance of the temperature levels and utility requirements, hence heat integration metrics, in determining the optimal CC technology. The selection matrix tool serves as a structured screening overview tool for the CC technologies, enabling the application of specific constraints as the availability of the excess heat, which can shift the relative rankings from the observed results from this study. This underlines that the optimal CC technology depends on the host industrial plant and heat integration possibilities.

Chapter 7

Case Study on Waste-to-Energy Plant

A case with a CHP WtE plant is presented by the collaborating company in this study, Niras, to test the developed selection matrix tool [Grue and Reardon, 2025]. The objective of testing the selection matrix tool on this real-world case is to evaluate the penalties on the WtE plant associated with attaching a CC process. Additionally, comparing these penalties across the CC technologies to determine which CC technology is optimal for the WtE plant. Table 7.1 presents the conditions of the WtE plant, including flue gas composition, energy output, and efficiency.

Table 7.1: WtE plant case data

Flue gas	Value
CO_2	10.3 [vol%]
O_2	7.6 [vol%]
H_2O	5.2 [vol%]
N_2	76.9 [vol%]
Temperature	34.2 [°C]
Pressure	1.0 [bar]

Plant outputs	Value
Gross power	19.1 [MW]
Net power	12.3 [MW]
Process heat	83.5 [MW]
CHP efficiency	99.41 [%]
Flue gas mass flow	202.5 [tonne/h]
Fuel power	96.4 [MW]

The flue gas composition and mass flow rate are used to extract the selection matrix KPI results, utilizing the equilibrium technology models. Figure 7.1 presents the heat map scores at 90 % CO_2 recovery. The colors are again normalized for each KPI to indicate the worst and best scores.

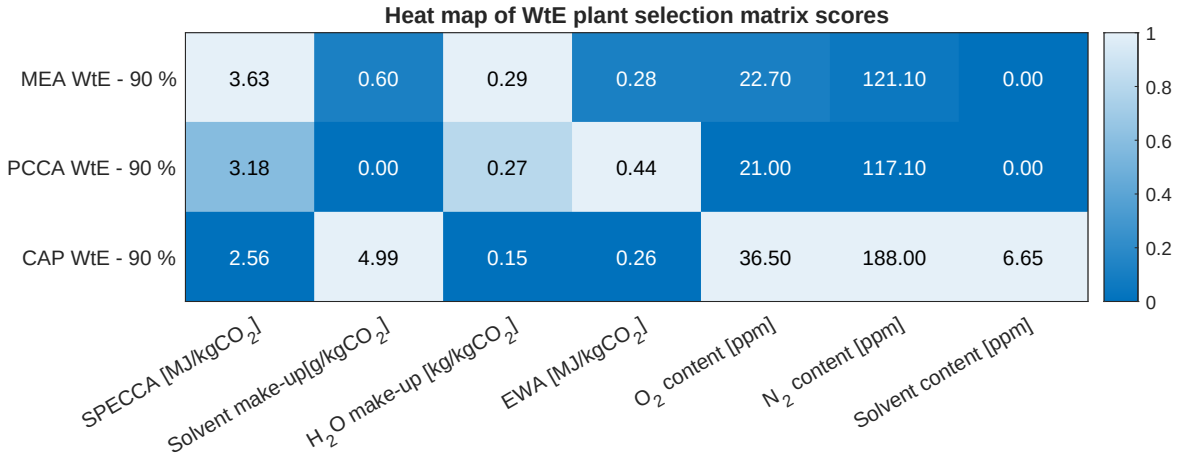

Figure 7.1: Heat map KPI scores from WtE flue gas data

The CAP scores best in SPECCA, water make-up, and EWA, indicating the overall optimal technology for the WtE plant flue gas composition. The O_2, N_2, and solvent contents align

with the CO_2 quality recommendation, so these are neglected when comparing the three technologies. Figure 7.2 shows a simplified process flow diagram of the WtE process.

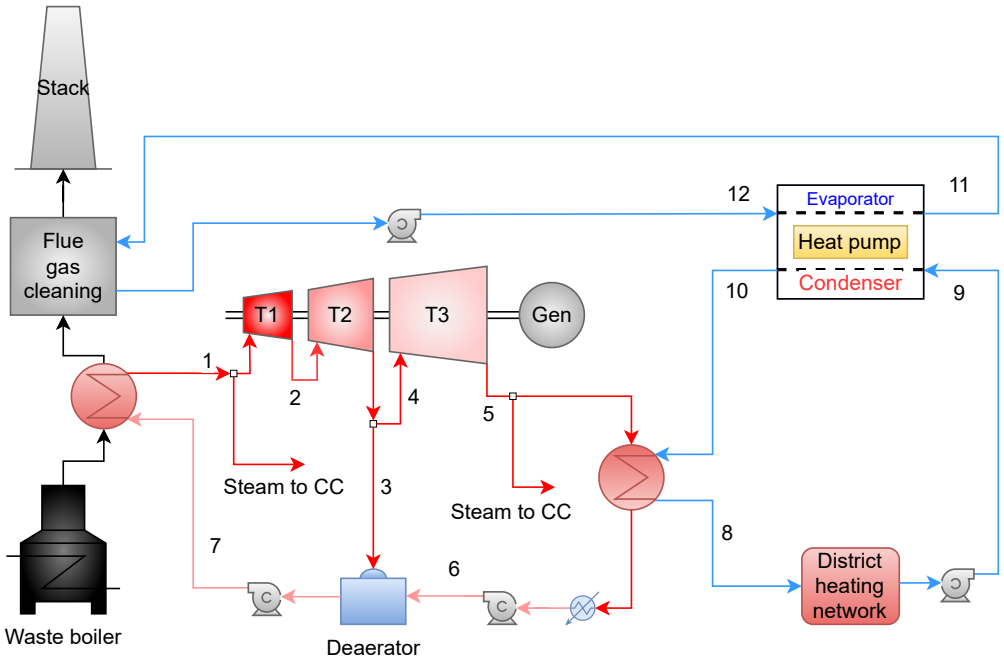

Figure 7.2: WtE simplified process flow diagram

The waste combustion produces steam for a steam cycle, generating power. After the turbine, with 3 steps, the steam is saturated and condenses to deliver energy to the district heating. A HP cycle cools a water cycle, which is heated through flue gas cleaning, and heats the district heating return water to ensure 90 °C delivery temperature for the district heating network. The HP is attached before the latent heat exchanger to attain a higher COP. The condensed water is cooled and mixed with approximately a 10 % fraction of the steam from the T2 turbine step in the deaerator, before being pressurized to generate steam again. The deaerator serves the purposes of heating the condensed water, venting non-condensable gases as O_2, and having a buffer storage for the water cycle.

The waste boiler, steam-generating heat exchangers, and flue gas cleaning are designed to generate steam at 400 °C and clean the flue gas to emission approval. These components are constrained to their design conditions to avoid re-design. The primary product of the WtE plant is the process heat to deliver district heating. The electricity generation is a byproduct, why the process heat delivery is constrained. Steam can be extracted before entering or after exiting the turbine system. These are considered the possibilities for meeting the hot utility requirements in the CC processes. Table 7.2 presents the stream

conditions in the numbered water streams on the process flow diagram above.

Table 7.2: Water stream data from WtE plant

	Streams	1	2	3	4	5	6	7	8	9	10	11	12
T	[°C]	399.9	378.1	121.6	121.6	94.0	64.3	121.4	90.0	59.4	50.1	24.0	34.0
P	[bar]	40	30.8	2.1	2.1	0.82	4.3	43.5	11.0	13.41	12.72	2.8	2.2
$\dot{m}$	[tonne/h]	110.9	109.6	10.9	98.7	99.9	100.7	108.3	1791.3	1791.3	1791.3	1352.4	1352.4

For MEA and CAP, steam must be extracted before the turbine, yet for PCCA, the steam temperature after the turbine is sufficient. The district heating cycle is a constraint for the plant designer, why when steam is taken from the process to sustain CC, a gap to cover the district heating demand occurs. Pinch analyses are performed to investigate the penalty and new utility requirements obtained by attaching the CC technologies to the WtE plant. Figure 7.3 illustrates the integration proposed for MEA and CAP.

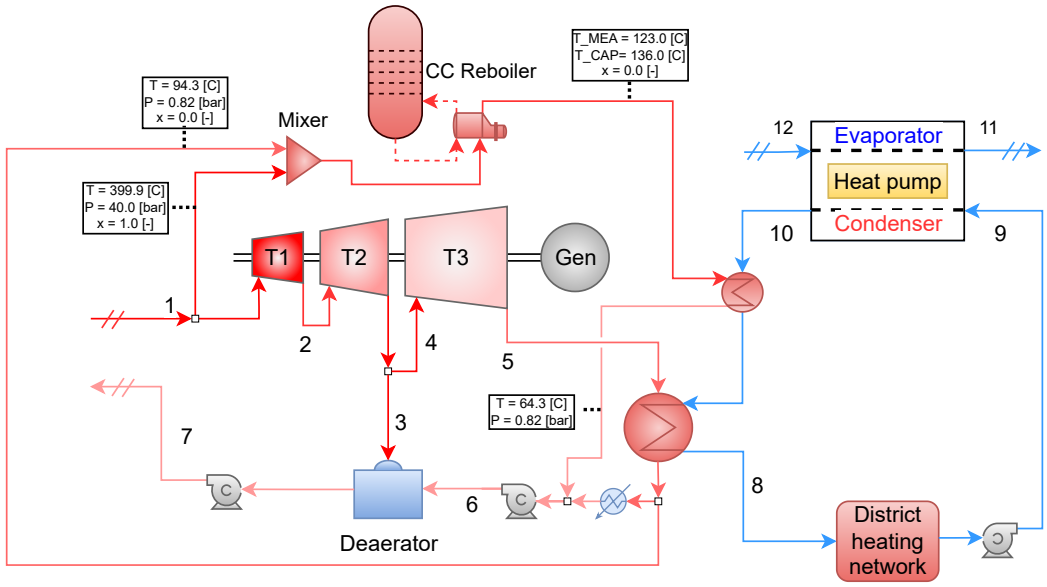

Figure 7.3: WtE attached to MEA and CAP technologies process flow diagram

Here, steam is extracted from stream 1 and mixed with water extracted after the district heating condenser. This expands the steam to the saturation pressure, coinciding with the reboiler temperature for MEA or CAP. The reboiler exit is water that can deliver heat to the district heating network. The water cycles are recycled back to the process before the deaerator to keep the mass balance for steam generation. Figure 7.4 shows the process flow diagram, integrating PCCA with the WtE plant.

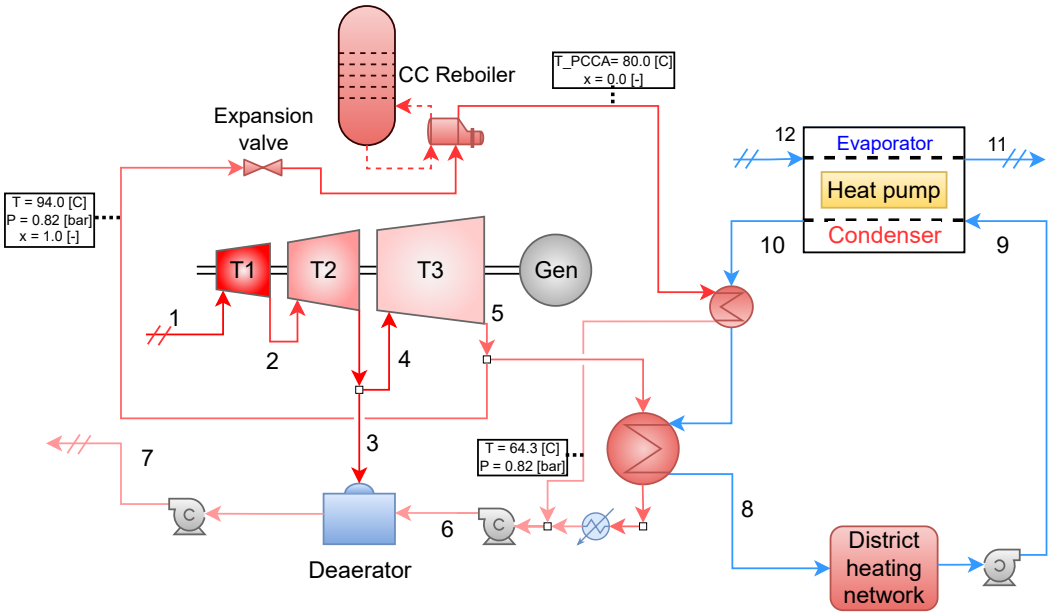

Figure 7.4: WtE attached to PCCA technology process flow diagram

For the PCCA integration, the steam is extracted after the turbine at the saturation point, where it is expanded to decrease the saturation temperature. A lower saturation temperature extends the distance across the saturation curve, hence a greater condensation energy. The exit water from the reboiler can heat stream 10 before the district heating cycle, before the condenser. The water is again returned before the deaerator to ensure mass balance in the steam generation.

Heat and mass balances are performed to quantify the required steam extraction mass flow for each CC technology integration. These calculations determine the resulting hot and cold streams associated with sustaining the CC technologies. The identified streams are incorporated into the pinch analyses to account for the consequence of maintaining the district heat delivery of the WtE plant. Table 7.3 presents the hot and cold streams conditions utilized in the pinch analyses based on the calculated heat and mass balances and process simulations on the WtE flue gas composition and mass flow rate.

Table 7.3: Pinch analysis data WtE real case

CC plant		MEA			PCCA			CAP		
Stream	Hot/Cold	T_1 [°C]	T_2 [°C]	$\dot{Q}$ [MW]	T_1 [°C]	T_2 [°C]	$\dot{Q}$ [MW]	T_1 [°C]	T_2 [°C]	$\dot{Q}$ [MW]
Flue gas	Hot	34.2	20.0	3.3	34.2	25.0	2.2	34.2	7.0	5.1
Lean stream	Hot	121.0	20.0	57.6	78.0	25.0	13.1	134.0	10.0	51.5
Gas desorber	Hot	103.0	25.0	8.2	66.0	18.0	9.5	111.0	68.0	2.8
Intercoolers (total)	Hot	80.0	35.0	4.0	100.0	35.0	5.8	70.0	35.0	3.2
Rich stream	Cold	38.0	103.0	44.7	57.0	66.0	4.5	24.0	129.0	38.5
Reboiler	Cold	121.0	121.1	28.1	78.0	78.1	24.8	134.0	134.1	19.9
Integrated Streams										
Reboiler steam	Hot	123.1	123.0	28.1	80.1	80.0	24.8	134.1	134.0	19.9
Reboiler exit	Hot	123.0	64.3	3.2	80.0	64.3	0.7	136.0	64.3	2.8
Steam turbine exit	Hot	94.0	64.3	41.3	94.0	64.3	42.6	94.0	64.3	48.2
District heating	Cold	59.4	90.0	63.6	59.4	90.0	63.6	59.4	90.0	63.6

The table shows that a reboiler steam hot stream is added to cancel the reboiler demand from the CC processes. The heat flow difference between the steam turbine exit hot stream and the district heating cold stream shows the penalty in extracting steam from the WtE plant to sustain each CC technology. The table values above are utilized to determine the GCC, HCC, and CCC. Figure 7.5 shows the GCC for each CC technology integration. An ammonia HP is modeled as presented in Appendix F, yet with different temperature levels to meet the hot utilities requirements and utilize part of the cold utility of each CC technology while upholding a global minimum temperature of 2 °C. The remaining cold utility requirement is cooled by the arbitrary utilities previously defined.

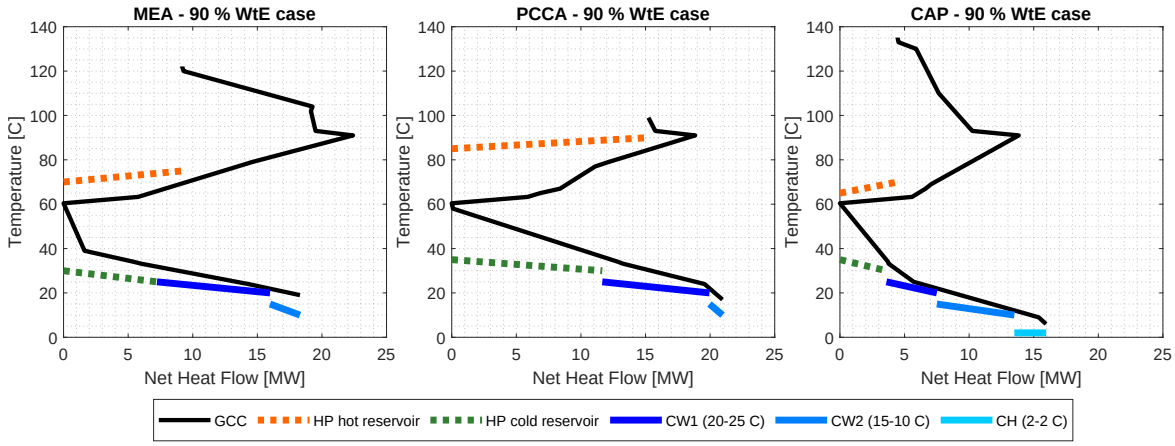

Figure 7.5: GCC from each CC technology integrated with WtE plant

Each CC technology's reboiler requirements are met, resulting in GCC figures canceling out heat flow. The heat flows in the 60-90 °C range are increased due to the district heating constraint. Yet, the heat flow is highest for MEA, reflecting the greater steam extraction to cover the reboiler duty. Extracting the steam after the turbine for PCCA shows a greater hot utility requirement, while MEA and CAP show great heat integration potential for the district heating demand. This shows the specific case delivering excess heat to district

heating has greater heat recovery options with MEA and CAP due to the high temperature levels. Additionally, the hot utility for PCCA is needed at a higher temperature than MEA and CAP, reflecting the possible heat recovery from the desorber condensers. The heat flows are further compared in Figure 7.6, showing the HCC and CCC for the integrated technologies.

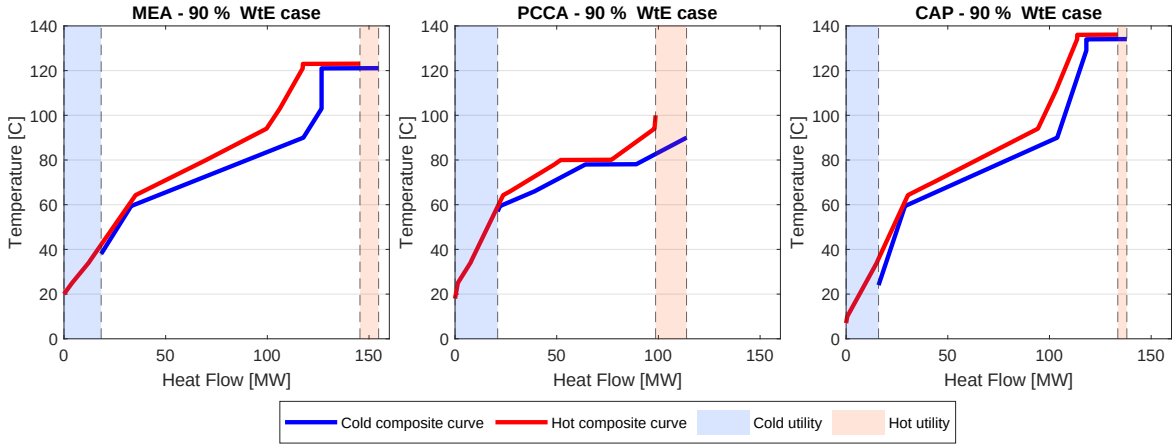

Figure 7.6: HCC and CCC for each CC technology integrated with WtE plant

The heat integration possibility is significant for each CC. The hot and cold utilities are low compared to the total heat flows, indicating great optimization possibilities for each CC technology with the WtE plant. The highest net utility is required in PCCA. Yet, it is worth noting that the PCCA does not affect the WtE electricity production as steam is extracted afterwards.

Each CC technology integration shows a hot utility requirement in the 60-80 °C range from the GCC. The beneficial solution for each would be to increase the district heating cycle temperature before entering the condenser between streams 8 and 10. A HP can cover this. There is a difference in the hot utility requirement favoring the CAP over MEA and PCCA.

Figure 7.7 presents an illustration of the heat integration of PCCA CC technology to cover the hot utility requirement with the new HP. This includes a water cycle above and below the pinch point (60.4 °C). The CC integration for MEA and CAP is found in Appendix G, yet the illustrated water cycles are similar for PCCA, even as the steam extraction is after the turbine.

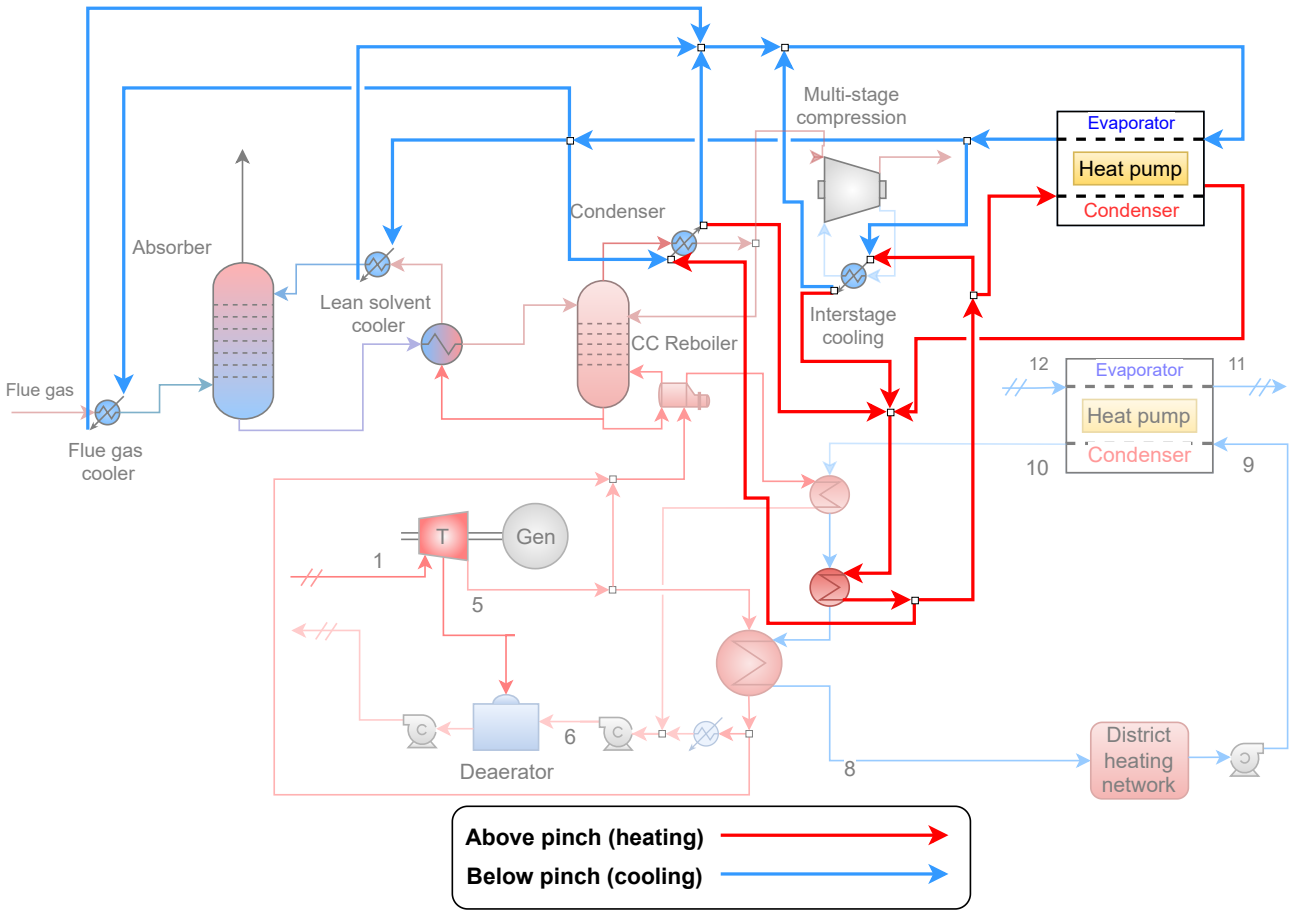

Figure 7.7: Illustration of HP with water cycle integration to cover updated hot utility demand for PCCA

The figure shows that the condenser and interstage cooler heat exchanges across the pinch point, why the cooling is divided into two heat exchanges (above and below pinch). The temperatures above the pinch point can directly exchange heat with the district heating stream 10. Yet, the below pinch cycles need to be boosted by the new HP. It is worth noting that the cold utility requirements for all three CC technologies are insufficiently met by the water cycles below the pinch point presented in the figure above. Thus, additional cooling water is expected for the flue gas cooler, lean solvent condenser, interstage color, and condenser, except for the CAP due to 68 °C condenser temperature. Additionally, the CAP needs chilling duty for flue gas and lean stream, why the configuration is even more advanced practically than presented in Figure G.2 in Appendix G.

The penalties for process heat and electricity production are evaluated under the assumption of linear scaling of turbine performance with respect to mass flow rate. This simpli-

fication assumes that the inlet and outlet states regarding thermodynamic properties as enthalpy, temperature, and pressure, remain constant. As a result, the reduction in power output is solely affected by the decrease in mass flow, not accounting for part-load operation effects or deviations. Additionally, this neglects the potential variation in turbine efficiencies that typically occurs under off-design or part-load conditions. Practically, turbine efficiency often decreases at lower mass flow rates due to changes in flow velocity profiles, incidence angles, and Reynolds number effects. These factors may lead to underestimating the electricity penalty, Thus, the energy and process penalties are simplified penalties associated with the reduced load. Table 7.4 presents the determined penalties for process heat and electricity output. This includes the PCCA-HP case, which can be driven separately with an auxiliary penalty due to the high-temperature HP.

Table 7.4: Process heat and electricity penalties from the WtE cases

Process heat output	Unit	MEA	PCCA	CAP	PCCA-HP
Process heat penalty	[MW]	22.0	23.2	15.5	0
Steam condensation loss	[%]	37.9	35.9	27.6	0
Updated hot utility requirement	[MW]	9.2	15.2	4.5	0
Electrical output					
Original net electricity	[MW]	12.3	12.3	12.3	12.3
CC process penalty	[MW]	2.2	3.4	2.0	10.1
Generation penalty	[MW]	8.3	0.0	6.7	0.0
Hot utility HP penalty	[MW]	2.0	3.9	0.8	0.0
HP COP calculated	[-]	4.7	3.9	5.8	3.8
Updated net electricity	[MW]	-0.2	5.0	4.8	2.2

The process heat penalty from the original production is greatest for the PCCA process, as it has the lowest potential for heat recovery due to the desorber temperature. The lower SPECCA value for CAP reflects the lower steam condensation loss and lower electricity generation penalty than MEA. The greater HP COP is also a result of this. Thus, MEA is unfavored over CAP due to higher process penalty and electrical penalty. For MEA, the updated net electricity becomes negative, resulting in a deficit of electricity from the WtE plant integration. The integrated PCCA process indicates the lowest updated net electricity, indicating the optimal CC solution for this WtE case. The CAP is a close second due to the better heat integration option. The PCCA-HP solution without steam extraction shows a greater integration penalty than PCCA and CAP, indicating that the heat integration provides more beneficial CC. It is worth noting that these results are based on the electricity generation penalty can be underestimated due to the assumption of linear scaling between turbine output and steam mass flow.

In summary, comparing the selection matrix scores aligns well with the trends observed from the standardized point source cases. The most significant influence on the optimal

decision comes from the integration of the CC technologies with the WtE plant. This resulted in a shift in ranking from CAP to PCCA, due to the lowest heat integration penalty on electricity production while meeting the constraint district heating demand of the original WtE plant. The CAP imposes the best overall matrix scores and greatest heat integration possibilities to minimize energy requirements. The PCCA solution imposes no penalty on the turbine electricity generation part of the WtE plant, resulting in a lower updated net electricity, even with a greater hot utility requirement than CAP. While the PCCA and CAP show great promise from the integration standpoint, the selection matrix tool proves a great comparison framework to interpret the influence of constraints from the specific plant on how suitable each CC technology is. The district heating constraint presents PCCA as the favored solution in the WtE plant case.

Chapter 8

Conclusion

This study investigated three mature chemisorption *Carbon Capture* (CC) technologies for post-combustion CC, *Monoethanolamine* (MEA), *Potassium Carbonate with Carbonic Anhydrase* (PCCA), and *Chilled Ammonia Process* (CAP). Three standardized flue gas compositions were defined from different point sources. These were waste incineration, biomass combustion, and natural gas combustion. A selection matrix tool was developed systematically comparing *Key Performance Indicators* (KPIs) scores across the CC technologies. These matrix scores were based on adaptable equilibrium process models developed in Aspen Plus for each CC technology, reflecting a modular CC plant. The flowsheet models were based on gathered research from the literature. Thus, the process configuration between the CC sources was similar

A parametric study was performed for each CC technology, testing CO_2 recovery and *Specific Primary Energy Consumption per CO_2 Avoided* (SPECCA). The operating parameters tested were liquid-to-gas ratio, lean stream temperature, flue gas temperature, and reboiler duty. Changing the reboiler duty showed the greatest sensitivity on CO_2 recovery and SPECCA across the CC technologies, followed by the liquid-to-gas ratio. The temperature showed minor variance in performance parameters across the technologies. The PCCA technology showed limitations in CO_2 recovery of approximately 95 %. Conversely, MEA and CAP indicated 100 % recovery was possible without a significant increase in reboiler duty. The main takeaway from the parametric studies is the optimal L/G values determined to be 3.3, 3.9, and 1.7 kg/kg for MEA, PCCA, and CAP, respectively. This reflects the variations in CO_2 absorption capacities between the solvents. The optimal operating parameters were chosen for each CC technology, except for the reboiler duty. This was chosen as a case parameter.

The selection matrix KPIs were tested on 27 cases based on fixed CO_2 recovery from 85 to 95 %. The SPECCA KPI score values were observed as 3.6-3.6, 2.9-4.4, and 2.5-2.8 MJ/kgCO_2 for MEA, PCCA, and CAP across the cases, respectively. The *Electrical Work per Avoided CO_2* (EWA) scores were approximately constant across the cases for MEA and PCCA at 0.3 and 0.4 MJ/kgCO_2, respectively, yet for the CAP, the flue gas composition impacted the chiller work, varying the EWA scores from 0.2 to 0.3 MJ/kgCO_2 across the cases. From the case studies, the overall best-scoring technology was deemed the CAP due to the lowest scores across the tested KPIs. The CAP system was necessary to increase in complexity by adding a water wash column to meet the recommendations for CO_2 quality. Yet, the water consumption and SPECCA scores indicate a strong advantage over MEA and PCCA. MEA showed the best robustness across the point sources. PCCA has the worst score regarding EWA due to the low-pressure desorber resulting in high CO_2 compression work. The selection matrix tool showed that the ranking of each CC technology differs

from each tested point source, which shows how the tool provides a screening insight into the CC technologies for a case-specific source.

Heat integration analyses were performed for the 90 % fixed CO_2 recovery case for waste incineration by pinch analyses. Including the influence of temperature levels on minimum utility requirements in the selection matrix evaluation provided a broader view of the individual CC technologies, concerning the technologies in post-combustion point sources. The minimum utility requirements and possible heat utility supplies between the CC technologies provided heat integration aspects into the evaluation. By incorporating utility supply options, the overall utility requirement for PCCA was decreased significantly by implementing a high-temperature *Heat Pump* (HP), covering the entire hot utility requirement. The SPECCA then decreased to 0.0 MJ/kgCO_2 for PCCA, while the EWA increased by 160 % to 1.1 MJ/kgCO_2, resulting in a PCCA-HP technology. After including the pinch analyses, the minimum hot utility requirement showed a value of 3.6, 2.8, 2.5, and 0.0 MJ/kgCO_2 for MEA, PCCA, CAP, and PCCA-HP, respectively. The minimum cold utility requirement was observed to be 5.0, 4.1, 4.8, and 2.1 MJ/kgCO_2 for MEA, PCCA, CAP, and PCCA-HP, respectively. Extending the selection matrix with the heat integration provided a broader comparison and overview.

The extended selection matrix tool was tested for a real-case waste-to-energy plant producing process heat for district heating and the byproduct electricity. Integrating the CC technologies by steam extraction showed that the optimal solution for the most efficient heat integration was the CAP, as the hot utility requirement penalty was lower than MEA and PCCA. Yet, district heating was constrained, and HP configurations were suggested to meet this constraint. This presented that the PCCA was the optimal CC technology implementation for this real case, due to the lowest updated net electricity output. The updated net electricity output was found to be -0.2, 5.0, 4.8, and 2.2 MW for MEA, PCCA, CAP, and PCCA-HP, respectively. The PCCA-HP omitted steam extraction, yet was unfavored to PCCA and CAP, showing the importance of heat integration on CC. The selection matrix KPI scores resembled the CAP as optimal due to the best heat integration option from the lowest SPECCA value, which was also seen from the heat integration analyses on this real case. Yet, the optimal CC integration showed PCCA based on the district heating constraint from this case study, due to the highest net electricity output for the tested CC technologies implemented on the waste-to-energy plant.

The findings from this study showed that the selection matrix, including heat integration analyses, enabled a multi-criteria evaluation across CC technologies, with an overview of system performance for each CC technology. The broad overview from the systematic comparison provides a simple screening process of the CC technologies with the option of applying specific case constraints, enabling an optimal decision for the process designer. The technology selection process comes down to a techno-economic evaluation. In con-

clusion, the tool developed in this study analyzes the CC technology performances from the perspective of thermodynamic and chemical capabilities and heat integration possibilities, providing insight into which mature technology is optimal for the specific case and applied constraints.

Chapter 9

Future Work

9.1 Increasing the Selection Matrix Tool Range

The selection matrix developed in this study focuses on post-combustion CC for mature CC technologies. Yet, the development of other chemisorption CC technologies is slowly climbing the TRLs towards mature commercial technologies. Thus, the screening capability of the selection matrix can be extended, incorporating these technologies when ready, providing a wider range of technology options and potentially resulting in higher optimality for the governing case.

The selection matrix could even be extended beyond chemisorption CC technologies to adsorption, cryogenic, and membrane CC, yet complexity might result in difficulties in systematically comparing the technologies as modular CC technologies. Thus, the screening process might be too complex to keep a broad perspective while observing the individual CC technology performances.

9.2 Impact of Kinetics on Technology Ranking

This study investigated the thermodynamic and chemical capabilities in equilibrium process models. Thus, the kinetics determining the specific sizing of the absorber and desorber are omitted. The kinetics are another aspect of the chemical capabilities determining the dynamics in CO_2 absorption and desorption. The residence time during which liquid and gas interact is a key factor for absorption and desorption. The absorber and desorber tower height and diameter will practically be determined by the necessary residence time to reach a specific CO_2 recovery while accounting for the gas and liquid flow rates to avoid flooding and excessive pressure losses. Flooding causes entrainment, significantly lowering the separation efficiency of the column stages. Flooding occurs when the gas flow is too high compared to the liquid flow, resulting in liquid being carried with the vapor instead of countercurrent flow. [Minhas, 2025]

Thus, solvent kinetics significantly impacts the capital investment for each CC technology, which might shift the ranking based on economic analyses. Yet, the capital investment in a CC plant is important in the initial design and research phase, operational expenditures tend to exceed this over the plant lifetime. Thus, the levelized cost of CO_2 is vital, as this is a fast-growing market sensitive to what will happen in the near future concerning incentives, breakthrough technologies, etc.

9.3 Impurities Impact on Technology Ranking

The selection matrix KPI scores omit the impact of flue gas impurities such as NO_x and SO_x as these were deemed insignificant in system performance regarding CO_2 recovery and energy requirements. Yet, these impurities can be a deal-breaker due to irreversible chemical reactions. For MEA, degraded products are toxic and require expensive waste treatment. The flue gas cleaning can be intensified with the penalty being increased cost for pre-treatment.

The practical impact of the pollutants is necessary to include when designing the process due to the toxic degraded compounds from the presence of NO_x and SO_x. The pollutants impact the capital and operational costs, possibly shifting the ranking between the CC technologies, due to the disposal of the toxic compounds, the risk of corrosion, or added process complexity to avoid emitting the toxic degraded compounds. Thus, the can pollutants influence the perspective and possible ranking between the CC technologies.

9.4 Techno-Economic Analysis Impact on Technology Ranking

A techno-economic analysis will determine the optimal CC technology for a given industrial application in the end, when all aspects are included. While the KPIs provide valuable insights, they do not quite get the big picture. Techno-economic evaluation integrates KPIs with the economic aspects as capital and operational expenditures, maintenance requirements, and potential revenue streams. This overview approach allows for a realistic assessment of feasibility in the specific case with constraints. It also highlights trade-offs between energy penalties and infrastructure costs. Thus, a technology with higher energy efficiency may require more complex integration or higher upfront investment. Furthermore, the availability of excess heat, electricity price variation, and incentives can shift the balance between options. In conclusion, techno-economic analysis ensures that the selected CC solution is both technically and economically sustainable. It is an essential step in CCUS planning and designing.

Bibliography

[ABS, 2025] ABS, A. B. o. S. (2025). Co2 impurities and lco2 carrier design: Practical considerations. https://ww2.eagle.org/content/dam/eagle/publications/knowledgecenter/CO2%20Impurities%20and%20LCO2%20Carrier%20Design-Practical%20Considerations.pdf. Accessed: 2025-04-29.

[AffaldPlus, 2023] AffaldPlus (2023). Dagsorden til bestyrelsesmøde 27. januar 2023. https://affaldplus.dk/sites/default/files/2023-01/Dagsorden%20til%20bestyrelsesm%C3%B8de%2027.%20januar%202023%20version%202.pdf.

[Amara, 2021] Amara, S. (2021). Co2 capture in industry using chilled ammonia process. https://kth.diva-portal.org/smash/record.jsf?pid=diva2%3A1542310&dswid=-6078. Last accessed: 22-04-2025.

[Aouini et al., 2012] Aouini, I., Ledoux, A., Estel, L., Mary, S., Evrard, P., and Valognes, B. (2012). Experimental study of carbon dioxide capture from synthetic industrial incinerator flue gas with a pilot and laboratory measurements. http://dx.doi.org/10.1016/j.proeng.2012.07.463.

[Aromada and Øi, 2015] Aromada, S. and Øi, L. (2015). Simulation of improved absorption configurations for co2 capture. http://dx.doi.org/10.3384/ecp1511921.

[Aspen Technology, 2014] Aspen Technology, I. (2014). Rate-based model of the co2 capture process by mea using aspen plus. http://www.aspentech.com. Aspen Plus Version 7.3.2.

[AspenTech, 2020] AspenTech (2020). Aspen plus 11.1 user guide. https://esupport.aspentech.com/S_Article?id=000064720. Accessed: 2025-02-26.

[Awtry, 2013] Awtry, A. (2013). Status of the carbon-dioxide absorber retrofit equipment (care) program. https://www.netl.doe.gov/sites/default/files/event-proceedings/2013/co2%20capture/A-Awtry-NSG-Status-of-the-CARE-Program.pdf. 2013 CO2 Capture Technology Meeting.

[Baker et al., 2022] Baker, R., Alizadeh Sahraei, O., Dal-Cin, M. M., and Bensebaa, F. (2022). A technology development matrix for carbon capture: Technology status and rd gap assessment. https://www.frontiersin.org/journals/energy-research/articles/10.3389/fenrg.2022.908658.

[Bauer et al., 2023] Bauer, H., Ehrmaier, J., Gigliotti, L., Liebach, F., Schleyer, T., and Simoncini, A. (2023). Industrial heat pumps: Five considerations for future growth. https://www.mckinsey.com/industries/industrials-and-electronics/our-insights/industrial-heat-pumps-five-considerations-for-future-growth.

[Borhani et al., 2018] Borhani, T. N., Oko, E., and Wang, M. (2018). Process modelling and analysis of intensified co2 capture using monoethanolamine (mea) in rotating packed bed absorber. https://www.sciencedirect.com/science/article/pii/S0959652618328099.

[Bukar and Asif, 2024] Bukar, A. M. and Asif, M. (2024). Technology readiness level assessment of carbon capture and storage technologies. https://doi.org/10.1016/j.rser.2024.114578.

[Carlsson, 2008] Carlsson, K. (2008). Gas cleaning in flue gas from combustion of biomass. https://www.bioenergy.org.nz/documents/resource/thermalnet-gas-cleaning-in-flue-gas-from-combustion-of-biomass.pdf. Paper prepared for the EU project ThermalNet.

[Cengel and Ghajar, 2016] Cengel, Y. A. and Ghajar, A. J. (2016). *Heat and Mass Transfer Fundamentals & Applications*. McGraw-Hill Education - Europa. ISBN: 9879813158964.

[Chakravarti et al., 2001] Chakravarti, S., Gupta, A., and Hunek, B. (2001). Advanced technology for the capture of carbon dioxide from flue gases. In *First National Conference on Carbon Sequestration, Washington, DC*, volume 2001, pages 15–17. Citeseer.

[Cormos, 2017] Cormos, C.-C. (2017). Igcc with carbon capture and storage. https://doi.org/10.1016/B978-0-12-409548-9.10139-3.

[Darde et al., 2010] Darde, V., Thomsen, K., van Well, W. J., and Stenby, E. H. (2010). Chilled ammonia process for co2 capture. https://doi.org/10.1016/j.ijggc.2009.10.005. The Ninth International Conference on Greenhouse Gas Control Technologies.

[de Andrade, 2014] de Andrade, A. J. R. (2014). Design and operation optimisation of a mea-based co2 capture unit. https://fenix.tecnico.ulisboa.pt/downloadFile/563345090413438/Extended_abstract_67962.pdf. Supervisors: Prof. Dr. Carla Pinheiro; Dr. Javier Rodriguez.

[DEA, 2018] DEA (2018). Biomass statistics: Wood chips. https://ens.dk/media/3907/download. Last accessed: 03-03-2025.

[DEA, 2024] DEA (2024). Technology data for carbon capture, transport and storage. https://ens.dk/en/analyses-and-statistics/technology-data-carbon-capture-transport-and-storage. Last accessed: 12-02-2025.

[Dumont et al., 2023] Dumont, M., Wang, R., Wenzke, D., Blok, K., and Heijungs, R. (2023). The techno-economic integrability of high-temperature heat pumps for decarbonizing process heat in the food and beverages industry. https://doi.org/10.1016/j.resconrec.2022.106605.

[EU, 2021] EU (2021). Commission implementing decision (eu) 2021/2326 of 16 december 2021 on the harmonised standards for machinery drafted in support of directive 2006/42/ec of the european parliament and of the council. https://eur-lex.europa.eu/legal-content/DA/TXT/?uri=CELEX:32021D2326#pbl_1. Last accessed: 12-02-2025.

[Fisher et al., 2005] Fisher, K. S., Beitler, C., Rueter, C., Searcy, K., Rochelle, G., and Jassim, M. (2005). Integrating mea regeneration with co2 compression and peaking to reduce co2 capture costs. https://www.trimeric.com/assets/integrating-mea-regeneration-with-co2-compression-and-peaking-to-reduce-co2-capture-cos pdf.

[Friedlingstein et al., 2022] Friedlingstein, P., Jones, M. W., O'Sullivan, M., Andrew, R. M., Bakker, D. C., Hauck, J., and et al (2022). Global carbon budget 2021. https://essd.copernicus.org/articles/14/1917/2022/.

[Gijlswijk et al., 2006] Gijlswijk, R. V., Feron, P., Oonk, H., and Brouwer, P. (2006). Environmental impact of solvent scrubbing of co2. https://ieaghg.org/publications/environmental-impact-of-solvent-scrubbing-of-co2/.

[Grue and Reardon, 2025] Grue, J. and Reardon, H. (2025). Chp waste-to-energy plant with turbine and district heating system. External supervisors from Niras.

[Grunwald et al., 2012] Grunwald, N., Taron, J., Kolditz, O., Liedl, R., and Park, C.-H. (2012). Comparison of equations of state for carbon dioxide for numerical simulations. *IAHS-AISH Publication*, 355:252–260.

[Hanak et al., 2015] Hanak, D. P., Biliyok, C., and Manovic, V. (2015). Rate-based model development, validation and analysis of chilled ammonia process as an alternative co2 capture technology for coal-fired power plants. *International Journal of Greenhouse Gas Control*, 34:52–62.

[Haszeldine et al., 2018] Haszeldine, R. S., Flude, S., Johnson, G., and Scott, V. (2018). Negative emissions technologies and carbon capture and storage to achieve the paris agreement commitments. https://royalsocietypublishing.org/doi/abs/10.1098/rsta.2016.0447.

[Hekmatmehr et al., 2024] Hekmatmehr, H., Esmaeili, A., Pourmahdi, M., Atashrouz, S., Abedi, A., Ali Abuswer, M., Nedeljkovic, D., Latifi, M., Farag, S., and Mohaddespour, A. (2024). Carbon capture technologies: A review on technology readiness level. https://doi.org/10.1016/j.fuel.2024.130898.

[Hu et al., 2017] Hu, G., Smith, K. H., Nicholas, N. J., Yong, J., Kentish, S. E., and Stevens, G. W. (2017). Enzymatic carbon dioxide capture using a thermally stable carbonic anhydrase as a promoter in potassium carbonate solvents. https://www.sciencedirect.com/science/article/pii/S138589471631138X.

[IEA, 2021] IEA (2021). Phasing out unabated coal: Current status and three case studies. https://www.iea.org/reports/phasing-out-unabated-coal-current-status-and-three-case-studies. Last accessed: 12-02-2025.

[IEA, 2025] IEA (2025). World - emissions. https://www.iea.org/world/emissions. Last accessed: 12-02-2025.

[Kemp, 2019] Kemp, I. C. (2019). *Pinch Analysis and Process Integration: A User Guide on Process Integration for the Efficient Use of Energy*. Butterworth-Heinemann.

[Klein and Nellis, 2017] Klein, S. and Nellis, G. (2017). *Thermodynamics*. Cambridge University Press. ISBN: 978-0-521-19570-6.

[Kothandaraman, 2010] Kothandaraman, A. (2010). Carbon dioxide capture by chemical absorption: A solvent comparison study. https://sequestration.mit.edu/pdf/Anusha_Kothandaraman_thesis_June2010.pdf.

[Lu et al., 2012] Lu, Y., Rostam-Abadi, M., Ye, X., Zhang, S., Ruhter, D., Khodayari, A., and Rood, M. (2012). Development and evaluation of a novel integrated vacuum carbonate absorption process. https://www.osti.gov/servlets/purl/1083750.

[Lu et al., 2011] Lu, Y., Ye, X., Zhang, Z., Khodayari, A., and Djukadi, T. (2011). Development of a carbonate absorption-based process for post-combustion co2 capture: The role of biocatalyst to promote co2 absorption rate. *Energy Procedia*, 4:1286–1293. 10th International Conference on Greenhouse Gas Control Technologies.

[Masson-Delmotte et al., 2018] Masson-Delmotte, V., Zhai, P., Pörtner, H.-O., Roberts, D., Skea, J., Shukla, P., Pirani, A., Moufouma-Okia, W., Péan, C., Pidcock, R., Connors, S., Matthews, J., Chen, Y., Zhou, X., Gomis, M., Lonnoy, E., Maycock, T., Tignor, M., and Waterfield, T. (2018). Global warming of 1.5°c: An ipcc special report on the impacts of global warming of 1.5°c above pre-industrial levels and related global greenhouse gas emission pathways, in the context of strengthening the global response to the threat of climate change, sustainable development, and efforts to eradicate poverty. https://www.ipcc.ch/sr15/.

[Minhas, 2025] Minhas, M. A. (2025). Entrainment flooding and weeping velocities.

[Nakamura et al., 2013] Nakamura, S., Yamanaka, Y., Matsuyama, T., Okuno, S., and Sato, H. (2013). Ihi s amine-based co2 capture technology for coal fired power plant. https://doi.org/10.1016/j.egypro.2013.06.070.

[NOAA, 2025] NOAA (2025). Carbon dioxide now more than 50% higher than pre-industrial levels. https://www.noaa.gov/news-release/carbon-dioxide-now-more-than-50-higher-than-pre-industrial-levels. Last accessed: 10-02-2025.

[Okuno et al., 2019] Okuno, S., Nakamura, S., Hamada, K., Takano, K., and Matsuyama, T. (2019). Development of a design for a carbon capture and storage facility by utilizing a process simulation technology. https://www.ihi.co.jp/en/technology/sdgs/topic01/pdf/c7a0636667b72e742a3d42708e9b837f.pdf.

[Olsson and Schipfer, 2022] Olsson, O. and Schipfer, F. (2022). Decarbonizing industrial process heat: The role of biomass. https://www.ieabioenergy.com/wp-content/uploads/2022/02/Role-of-biomass-in-industrial-heat.pdf.

[Pankow, 2020] Pankow, J. F. (2020 - 2020). *Aquatic chemistry concepts*. CRC Press, Taylor Francis Group, Boca Raton, FL, 2. edition. edition.

[Pashchenko, 2024] Pashchenko, D. (2024). Green hydrogen as a power plant fuel: What is energy efficiency from production to utilization? https://doi.org/10.1016/j.renene.2024.120033.

[Pfaff et al., 2010] Pfaff, I., Oexmann, J., and Kather, A. (2010). Optimised integration of post-combustion co2 capture process in greenfield power plants. https://doi.org/10.1016/j.energy.2010.06.004.

[Qi et al., 2018] Qi, G., Liu, K., House, A., Salmon, S., Ambedkar, B., Frimpong, R. A., Remias, J. E., and Liu, K. (2018). Laboratory to bench-scale evaluation of an integrated co2 capture system using a thermostable carbonic anhydrase promoted k2co3 solvent with low temperature vacuum stripping. https://doi.org/10.1016/j.apenergy.2017.10.083.

[Qin et al., 2011] Qin, F., Wang, S., Kim, I., Svendsen, H. F., and Chen, C. (2011). Heat of absorption of co2 in aqueous ammonia and ammonium carbonate/carbamate solutions. https://doi.org/10.1016/j.ijggc.2010.04.005. The 5thTrondheim Conference on CO2 Capture, Transport and Storage.

[Saipem, 2025] Saipem (2025). Co2 solutions. https://www.saipem.com/en/solutions-energy-transition/reduce-co2-emissions/co2-capture-storage/carbon-capture/co2-solutions. Last accessed: 24-02-2025.

[SINTEF, 2009] SINTEF, E. A. (2009). Towards hydrogen and electricity production with carbon capture and storage. https://cordis.europa.eu/docs/results/19/19672/122320071-6_en.pdf. Project no.: 019672, co-funded by the European Commission within the Sixth Framework Programme (2002-2006).

[SLB Capturi, 2025] SLB Capturi (2025). Just catch. https://www.capturi.slb.com/products/just-catch%E2%84%A2. Last accessed: 04-03-2025.

[Suleman et al., 2022] Suleman, H., Fosbøl, P. L., Nasir, R., Ameen, M., Suleman, H., Fosbøl, P. L., Ameen, M., and Nasir, R. (2022). *Sustainable Carbon Capture: Technologies and Applications*. CRC Press, Milton, 1 edition.

[Sutter et al., 2015] Sutter, D., Gazzani, M., and Mazzotti, M. (2015). Formation of solids in ammonia-based co2 capture processes identification of criticalities through thermodynamic analysis of the co2nh3h2o system. https://www.sciencedirect.com/science/article/pii/S0009250915000160. 19th International Symposium on Industrial Crystallization.

[Sutter et al., 2016] Sutter, D., Gazzani, M., and Mazzotti, M. (2016). A low-energy chilled ammonia process exploiting controlled solid formation for post-combustion co 2 capture. http://dx.doi.org/10.1039/C6FD00044D.

[Thee et al., 2015] Thee, H., Smith, K. H., da Silva, G., Kentish, S. E., and Stevens, G. W. (2015). Carbonic anhydrase promoted absorption of co2 into potassium carbonate solutions. https://doi.org/10.1002/ghg.1455.

[TNO, 2025] TNO, B. . C. T. (2025). Phyllis2: Database for the physico-chemical composition of biomass. https://phyllis.nl/Browse/Standard/ECN-PhylliswoodLast accessed: 03-03-2025.

[UNFCCC, 2022] UNFCCC (2022). The paris agreement. https://unfccc.int/process-and-meetings/the-paris-agreement/the-paris-agreement?gclid=CjwKCAiA3KefBhByEiwAi2LDHFXPgxxSAJSzqJPCsUEqhx9w2H0FY_BT_JzVLpa6LONWbJb6LXY1JhoCVWYQAvD_BwE. Last accessed 13th of February 2022.

[Wacker and Dittmer, 2014] Wacker, C. and Dittmer, R. (2014). Integrally geared compressors for supercritical co2. https://www.sco2symposium.com/papers2014/turbomachinery/79-Dittmer.pdf. Last accessed: 28-04-2025.

[Weather Atlas, 2025] Weather Atlas (2025). Denmark climate. https://www.weather-atlas.com/en/denmark-climate. Last accessed: 29-04-2025.

[Zhang and Lu, 2015] Zhang, S. and Lu, Y. (2015). Kinetic performance of co2 absorption into a potassium carbonate solution promoted with the enzyme carbonic anhydrase: Comparison with a monoethanolamine solution. https://www.sciencedirect.com/science/article/pii/S1385894715006853.

[Zhang et al., 2006] Zhang, Z., Wang, G., Massarotto, P., and Rudolph, V. (2006). Optimization of pipeline transport for co2 sequestration. https://doi.org/10.1016/j.enconman.2005.06.001.

Appendix A

Biomass Flue Gas Composition

The moisture content is assumed to be 42.3 % [DEA, 2018]. Table A.1 presents the weight percentages from the Phyllis database for a typical sample of fir wood chips.

Table A.1: Fir wood properties based on Phyllis database (wood, fir (#239)). [TNO, 2025]

Properties	Unit	Value
Carbon	[wt.%]	29.06
Hydrogen	[wt.%]	3.42
Oxygen	[wt.%]	25.04
Nitrogen	[wt.%]	0.03
Moisture	[wt.%]	42.3
Ash content	[wt.%]	0.15

Assuming the ash content is inert in biomass combustion and the excess air ratio is 1.5, hence 50 % excess air from the stoichiometric combustion. The combustion reaction is presented in Reaction R-APP1.

$$C_{2.42}H_{3.393}N_{0.002142}O_{1.565} + 1.5 \cdot n_s \, (O_2 + 3.76\, N_2) \longrightarrow n_1\, CO_2 + n_2\, H_2O + n_3\, N_2 + n_4\, O_2 \quad \text{(R-APP1)}$$

n is the stoichiometric coefficient for each compound. The stoichiometric coefficient for air is 2.551. Solving these coefficients in an algebraic format gives the stoichiometric coefficients and, hereafter, the molar fraction presented in Table A.2. Additionally, the flue gas composition is determined, including the moisture in the wood chips.

Table A.2: Stoichiometric coefficients for biomass combustion

Compounds	n_i	Flue gas (wet basis) [vol%]	Flue gas (T_{sat} 60 °C) [vol%]
CO_2	2.42	10.93	11.05
H_2O	1.697	18.28	17.44
O_2	1.275	5.76	5.82
N_2	14.39	65.03	65.69

Appendix B

Cooling Water Temperature Calculations

A hot summer day in Denmark typically reaches 28 °C with a relative humidity of 80 % [Weather Atlas, 2025]. A cooling tower condenses water from the air. Utilizing a hot Danish summer day to determine the cooling water temperature helps determine the compressor work needed with the worst-case intercooling temperature.

The dewpoint temperature resembles the cooling water temperature, which is determined by a psychrometric chart. Figure B.1 illustrates a psychrometric chart constructed utilizing the EES software tool. [Klein and Nellis, 2017]

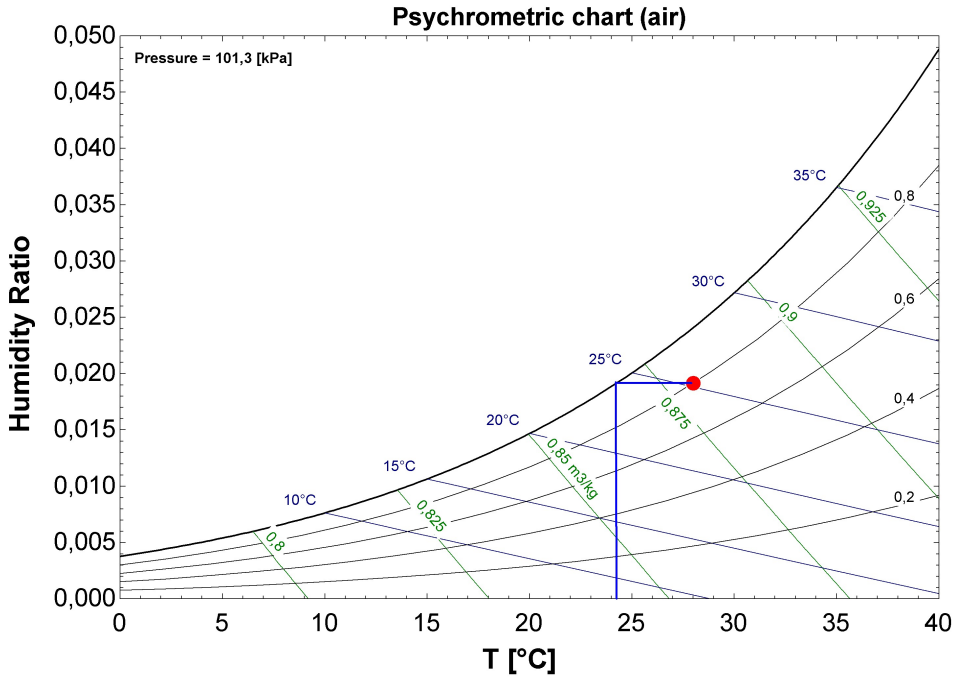

Figure B.1: Psychrometric chart for air at atmospheric pressure

On the figure above, a red dot indicates a hot summer day with an air temperature of 28 °C and a relative humidity of 80 %. The blue lines are constructed to indicate the dewpoint temperature. The condensation point is reached at 24.2 °C, through isobaric cooling of the air. By this, the cooling water temperature is set to 25 °C to ensure a safe margin.

Appendix C

Process Model Flowsheets and Iteration Orders
This chapter presents the process flowsheet and iteration order diagram for the equilibrium models for MEA, PCCA, and CAP, respectively.

C.1 Monoethanolamine Model Flowsheet and Iteration Order

Figure C.1 present the flowsheet of the MEA equilibrium model.

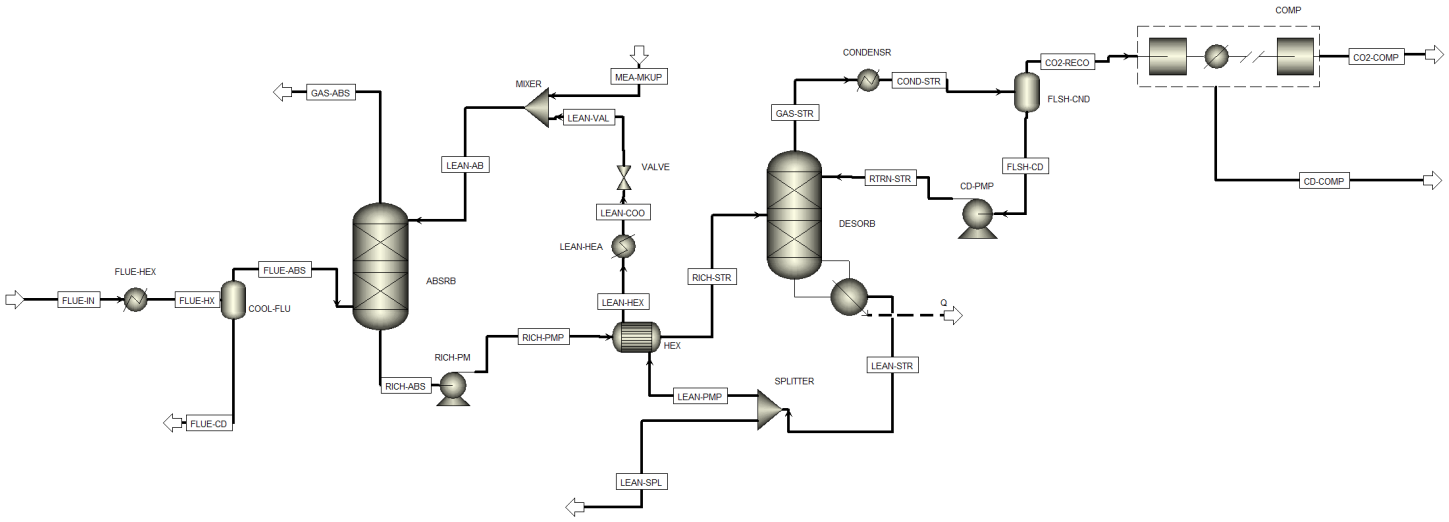

Figure C.1: Process flow diagram of MEA Aspen Plus process model

Figure C.2 is conducted to illustrate the convergence order concerning the loops introduced in the process model and due to the design specification.

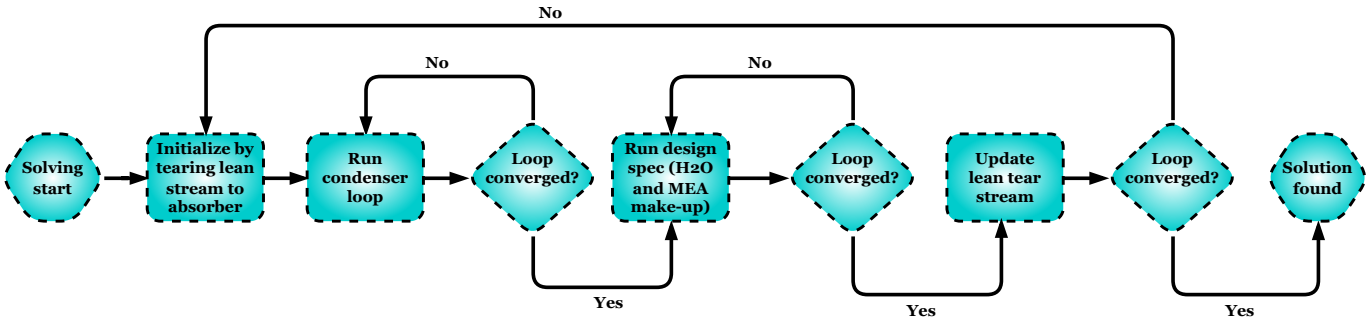

Figure C.2: Iteration order MEA equilibrium model

Here, the tear stream for defining the outer loop is the "LEAN-AB" stream entering the

absorber. This stream is initialized with the starting guesses for the CO_2 loading and the MEA concentration. The design specification loops for H2O and MEA iterate simultaneously. The solution is found when all loops are converged, ending with the "LEAN-AB" tear stream where it all began.

C.2 Potassium Carbonate with Carbonic Anhydrase Model Flowsheet and Iteration Order

The process flowsheet of the PCCA model is presented in Figure C.3.

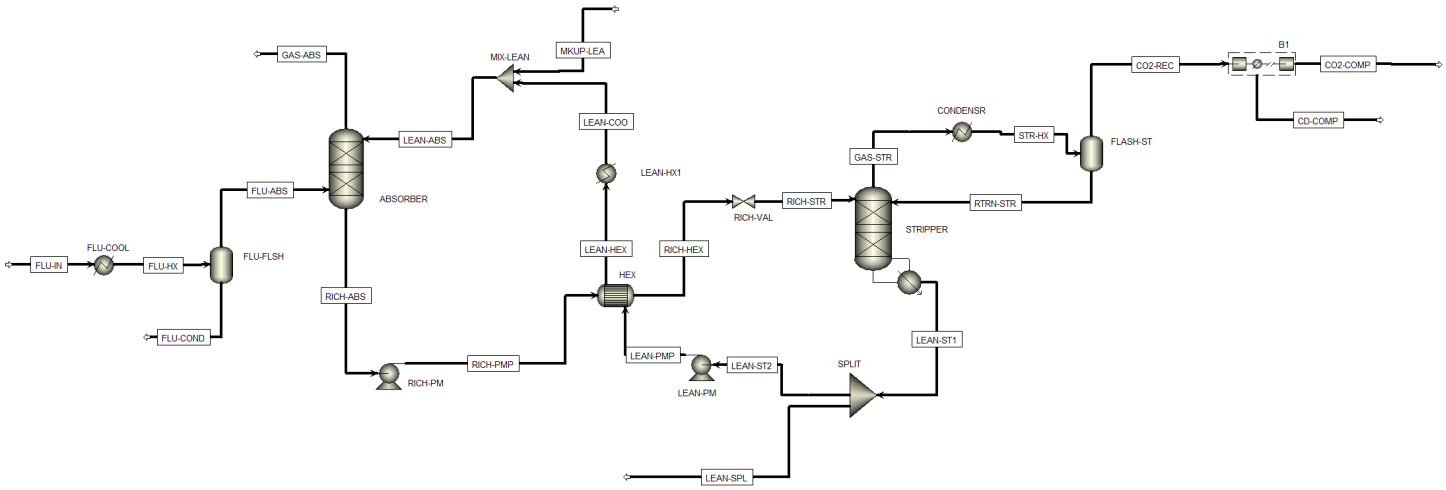

Figure C.3: Process flow diagram of PCCA Aspen Plus process model

Just as for the MEA model, a convergence order flowsheet diagram is conducted. Figure C.4 illustrates the iteration order for the PCCA model.

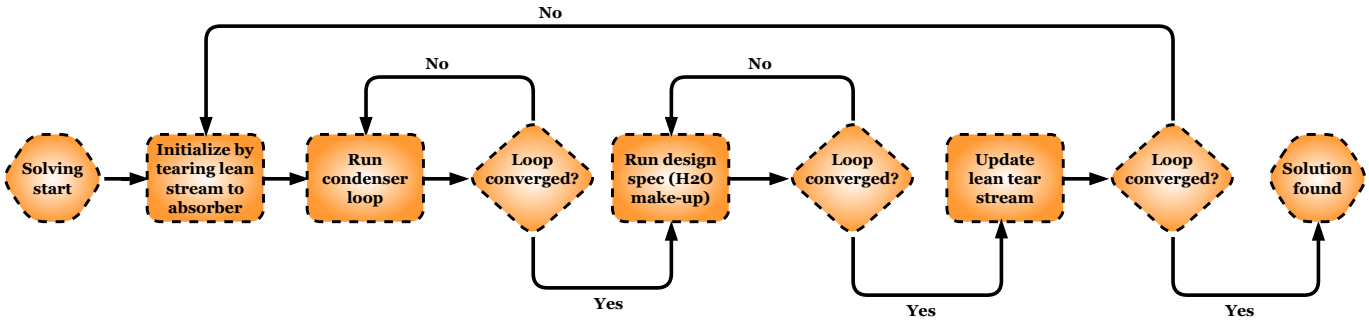

Figure C.4: Iteration order PCCA equilibrium model

The loops are similar to the MEA flowsheet, however, no make-up design specification is

needed for the solvent K_2CO_3. No solid form of K_2CO_3 escapes the system as a result of a 0.0 split fraction in the purge stream ("LEAN-SPL"). The tear stream is still the lean stream entering the absorber, initialized with a starting guess, yet also the end of the simulation at a converged result.

C.3 Chilled Ammonia Process Model Flowsheet and Iteration Order

Figure C.5 shows the CAP equilibrium model flowsheet from Aspen Plus.

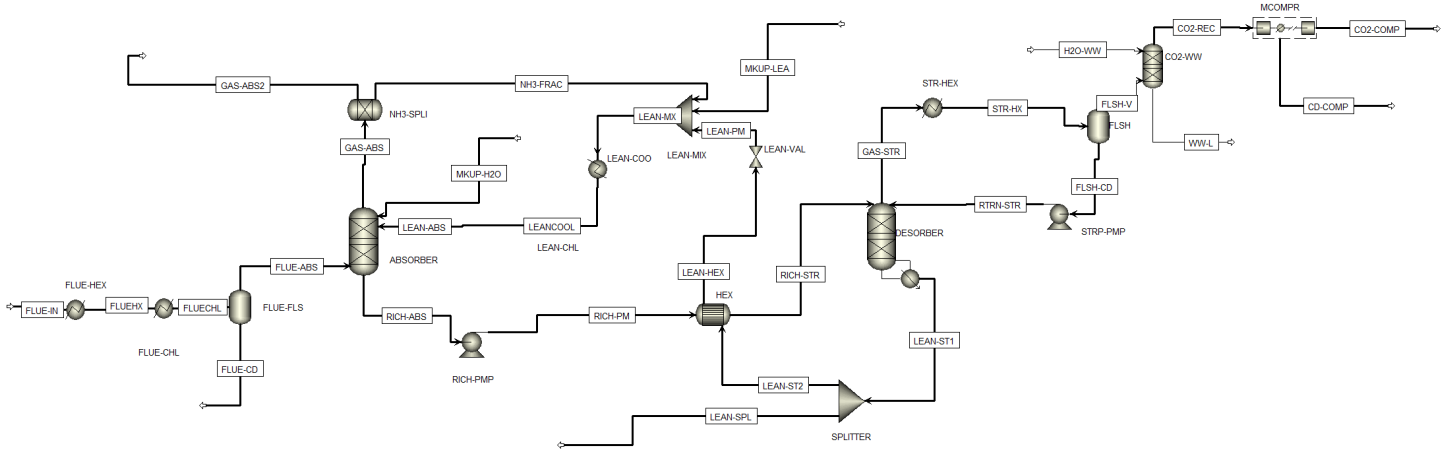

Figure C.5: Process flow diagram of CAP Aspen Plus process model

The figure above illustrate a difference compared to the MEA and PCCA flowsheets as a recovery loop for NH_3 is added and a CO_2 water-wash to eliminate NH_3 from the pure CO_2 stream. Lastly, the converging order for the CAP is illustrated in Figure C.6.

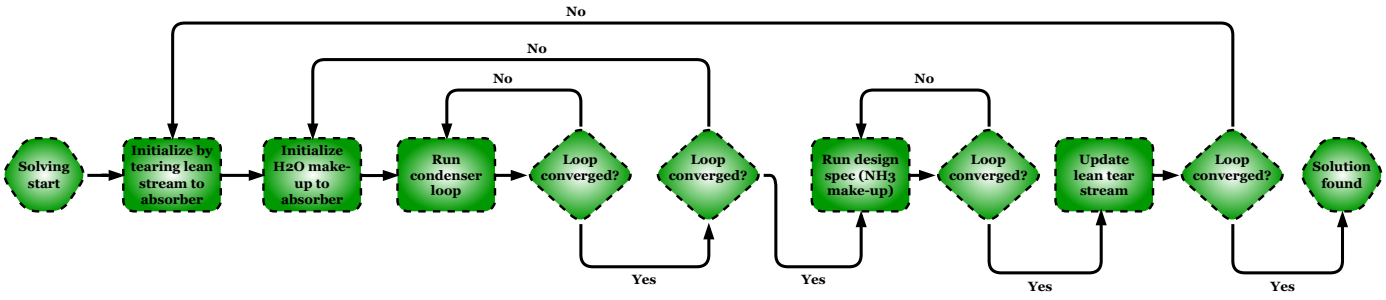

Figure C.6: Iteration order CAP equilibrium model

Another loop is present in the converging order since the CAP includes a loop reflecting the recycling of captured NH_3 back to the lean stream. The make-up water is added in the

absorber, not the lean stream. water escapes the system in the cleansed flue gas and CO_2 recovery stream. As a result, the design specification for the water mass balance creates a loop outside the condenser loop to maintain the mass balance for water in the process simulation.

Appendix D

Stream Results for 90 % Recovery Case on Waste Incineration Point Source

Table D.1: Key stream data from the MEA process model of 90 % fixed CO_2 recovery on waste incineration point source

Stream	FLUE-IN	FLUE-CD	FLUE-ABS	LEAN-ABS	GAS-ABS	RICH-ABS	RICH-STR	LEAN-STR	LEAN-HEX	LEAN-VAL	MEA-MKUP	GAS-STR	CO2-REC	RTRN-STR	CD-COMP	CO2-COMP
Temperature [C]	60.0	20.0	20.0	20.0	50.7	41.7	103.9	122.2	46.7	20.0	20.0	103.1	25.0	25.0	35.1	35.0
Pressure [bar]	1.0	1.0	1.0	1.0	1.0	1.0	2.0	2.0	2.0	1.0	1.0	2.0	1.5	2.0	2.6	110.0
Mass Flows [tonne/hr]	76.5	7.4	69.1	251.4	59.4	261.0	261.0	247.9	247.9	247.9	3.5	18.1	13.1	5.1	0.1	13.0
Mole Flows [kmol/hr]	2680.5	412.0	2268.4	10463.5	2158.6	10279.2	10372.5	10272.9	10271.3	10271.3	192.2	580.2	300.9	279.1	6.1	294.9
Molar Fractions [mol%]																
CO_2	12.20	0.01	14.41	0.00	1.51	0.00	0.90	0.01	0.00	0.00	0.00	50.80	97.80	0.09	0.01	99.81
O_2	7.70	0.00	9.10	0.00	9.56	0.00	0.00	0.00	0.00	0.00	0.00	0.00	0.00	0.00	0.00	0.00
H_2O	17.40	99.99	2.40	88.85	11.07	88.01	87.60	88.62	88.67	88.65	99.93	49.16	2.19	99.77	99.99	0.18
N_2	62.70	0.00	74.09	0.00	77.86	0.00	0.00	0.00	0.00	0.00	0.00	0.00	0.01	0.00	0.00	0.01
MEA	0.00	0.00	0.00	5.38	0.00	0.42	1.88	5.58	5.49	5.48	0.06	0.03	0.00	0.00	0.00	0.00
MEA^+	0.00	0.00	0.00	2.92	0.00	5.81	4.82	2.90	2.94	2.98	0.00	0.00	0.00	0.07	0.00	0.00
H^+	0.00	0.00	0.00	0.00	0.00	0.00	0.00	0.00	0.00	0.00	0.00	0.00	0.00	0.00	0.00	0.00
$MEACOO^-$	0.00	0.00	0.00	2.74	0.00	5.01	4.45	2.77	2.81	2.79	0.00	0.00	0.00	0.00	0.00	0.00
HCO_3^-	0.00	0.00	0.00	0.02	0.00	0.70	0.35	0.12	0.04	0.02	0.00	0.00	0.00	0.07	0.00	0.00
OH^-	0.00	0.00	0.00	0.00	0.00	0.00	0.00	0.00	0.00	0.00	0.00	0.00	0.00	0.00	0.00	0.00
CO_3^{2-}	0.00	0.00	0.00	0.08	0.00	0.05	0.01	0.01	0.04	0.08	0.00	0.00	0.00	0.00	0.00	0.00

Table D.2: Key stream data from the PCCA process model of 90 % fixed CO_2 recovery on waste incineration point source

Stream	FLUE-IN	FLUE-CD	FLUE-ABS	LEAN-ABS	GAS-ABS	RICH-ABS	RICH-STR	LEAN-STR	LEAN-HEX	LEAN-VAL	H2O-MKUP	GAS-STR	CO2-REC	RTRN-STR	CD-COMP	CO2-COMP
Temperature [C]	60.0	25.0	25.0	27.1	63.5	59.3	64.5	78.2	64.3	78.2	25.0	64.5	18.0	18.0	35.1	35.0
Pressure [bar]	1.0	1.0	1.0	1.0	1.0	1.0	0.3	0.3	1.0	1.0	1.0	0.3	0.3	0.3	1.1	110.0
Mass Flows [tonne/hr]	76.5	7.1	69.4	300.2	59.9	309.7	309.7	296.2	296.2	296.2	3.9	18.6	13.4	5.1	0.5	13.0
Mole Flows [kmol/hr]	2680.5	392.7	2287.8	11697.4	2184.5	11506.5	11528.3	11478.8	11478.8	11478.8	218.7	606.1	321.9	284.2	27.0	294.9
Molar Fractions [mol%]																
CO_2	12.20	0.01	14.29	0.00	1.50	0.00	0.19	0.00	0.00	0.00	0.00	48.57	91.43	0.02	0.00	99.81
O_2	7.70	0.00	9.02	0.00	9.45	0.00	0.00	0.00	0.00	0.00	0.00	0.00	0.00	0.00	0.00	0.00
H_2O	17.40	99.99	3.22	73.76	12.12	70.77	70.83	73.26	73.26	73.26	100.00	51.43	8.56	99.98	100.00	0.18
N_2	62.70	0.00	73.46	0.00	76.93	0.00	0.00	0.00	0.00	0.00	0.00	0.00	0.01	0.00	0.00	0.01
K_2CO_3	0.00	0.00	0.00	0.00	0.00	0.00	0.00	0.00	0.00	0.00	0.00	0.00	0.00	0.00	0.00	0.00
H^+	0.00	0.00	0.00	0.00	0.00	0.00	0.00	0.00	0.00	0.00	0.00	0.00	0.00	0.00	0.00	0.00
K^+	0.00	0.00	0.00	16.29	0.00	16.56	16.53	16.60	16.60	16.60	0.00	0.00	0.00	0.00	0.00	0.00
OH^-	0.00	0.00	0.00	0.00	0.00	0.00	0.00	0.01	0.00	0.01	0.00	0.00	0.00	0.00	0.00	0.00
HCO_3^-	0.00	0.00	0.00	3.60	0.00	8.77	8.37	3.67	3.67	3.67	0.00	0.00	0.00	0.00	0.00	0.00
CO_3^{2-}	0.00	0.00	0.00	6.35	0.00	3.90	4.08	6.47	6.47	6.47	0.00	0.00	0.00	0.00	0.00	0.00

Table D.3: Key stream data from the CAP process model of 90 % fixed CO_2 recovery on waste incineration point source

Stream	FLUE-IN	FLUE-CD	FLUE-ABS	LEAN-ABS	MKUP-H2O	GAS-ABS2	RICH-ABS	RICH-STR	LEAN-ST1	LEAN-PM	MKUP-LEA	NH3-FRAC	LEAN-MX	GAS-STR	RTRN-STR	FLSH-V	CO2-REC	CD-COMP	CO2-COMP
Temperature [°C]	60.0	7.0	7.0	10.0	10.0	38.5	25.6	138.1	143.1	39.0	30.0	38.5	49.0	114.6	68.0	68.0	67.8	35.0	35.0
Pressure [bar]	1.0	1.0	1.0	1.0	1.0	1.0	1.0	10.0	10.0	1.0	1.0	1.0	10.0	10.0	10.0	10.0	10.0	13.5	110.0
Mass Flows [tonne/h]	76.5	8.0	68.5	128.1	2.1	57.6	138.6	138.6	125.4	125.4	0.1	2.6	128.1	15.7	2.6	13.1	13.1	0.2	13.0
Mole Flows [kmol/h]	2680.5	442.8	2237.7	6874.8	118.2	2056.4	6728.6	6728.6	6726.4	6719.3	4.2	151.2	6874.8	412.2	82.9	303.8	303.7	8.8	294.9
Molar Fractions [mol%]																			
CO_2	12.20	0.02	14.61	0.00	0.00	1.57	0.00	0.00	0.11	0.00	0.00	0.00	0.00	77.74	0.26	97.00	96.91	0.02	99.80
O_2	7.70	0.00	9.22	0.00	0.00	10.04	0.00	0.00	0.00	0.00	0.00	0.00	0.00	0.00	0.00	0.00	0.00	0.00	0.00
H_2O	17.40	99.98	1.06	89.23	100.00	6.48	86.87	86.87	90.32	91.10	0.00	0.00	89.07	15.80	37.66	2.87	3.07	99.98	0.18
N_2	62.70	0.00	75.11	0.00	0.00	81.73	0.00	0.00	0.00	0.00	0.00	0.00	0.00	0.01	0.00	0.01	0.01	0.00	0.01
NH_3	0.00	0.00	0.00	7.42	0.00	0.19	0.43	0.43	6.45	5.48	100.00	100.00	7.61	6.45	0.07	0.12	0.00	0.00	0.00
NH_4^+	0.00	0.00	0.00	1.71	0.00	0.00	6.66	6.66	1.57	1.76	0.00	0.00	1.68	0.00	31.11	0.00	0.00	0.00	0.00
NH_2COO^-	0.00	0.00	0.00	1.48	0.00	0.00	1.45	1.45	0.52	1.31	0.00	0.00	1.32	0.00	0.45	0.00	0.00	0.00	0.00
HCO_3^-	0.00	0.00	0.00	0.08	0.00	0.00	3.98	3.98	1.04	0.28	0.00	0.00	0.27	0.00	30.22	0.00	0.00	0.00	0.00
OH^-	0.00	0.00	0.00	0.00	0.00	0.00	0.00	0.00	0.00	0.00	0.00	0.00	0.00	0.00	0.00	0.00	0.00	0.00	0.00
CO_3--	0.00	0.00	0.00	0.07	0.00	0.00	0.61	0.61	0.00	0.08	0.00	0.00	0.04	0.00	0.22	0.00	0.00	0.00	0.00
H^+	0.00	0.00	0.00	0.00	0.00	0.00	0.00	0.00	0.00	0.00	0.00	0.00	0.00	0.00	0.00	0.00	0.00	0.00	0.00

Appendix E

Selection Matrix Scores for Remaning Fixed CO_2 Recovery Cases

Figure E.1 presents all the KPI scores attained from the selection matrix analysis. Each KPI result is color-scaled with each column, indicating dark blue as the best score and light blue as the worst for each KPI.

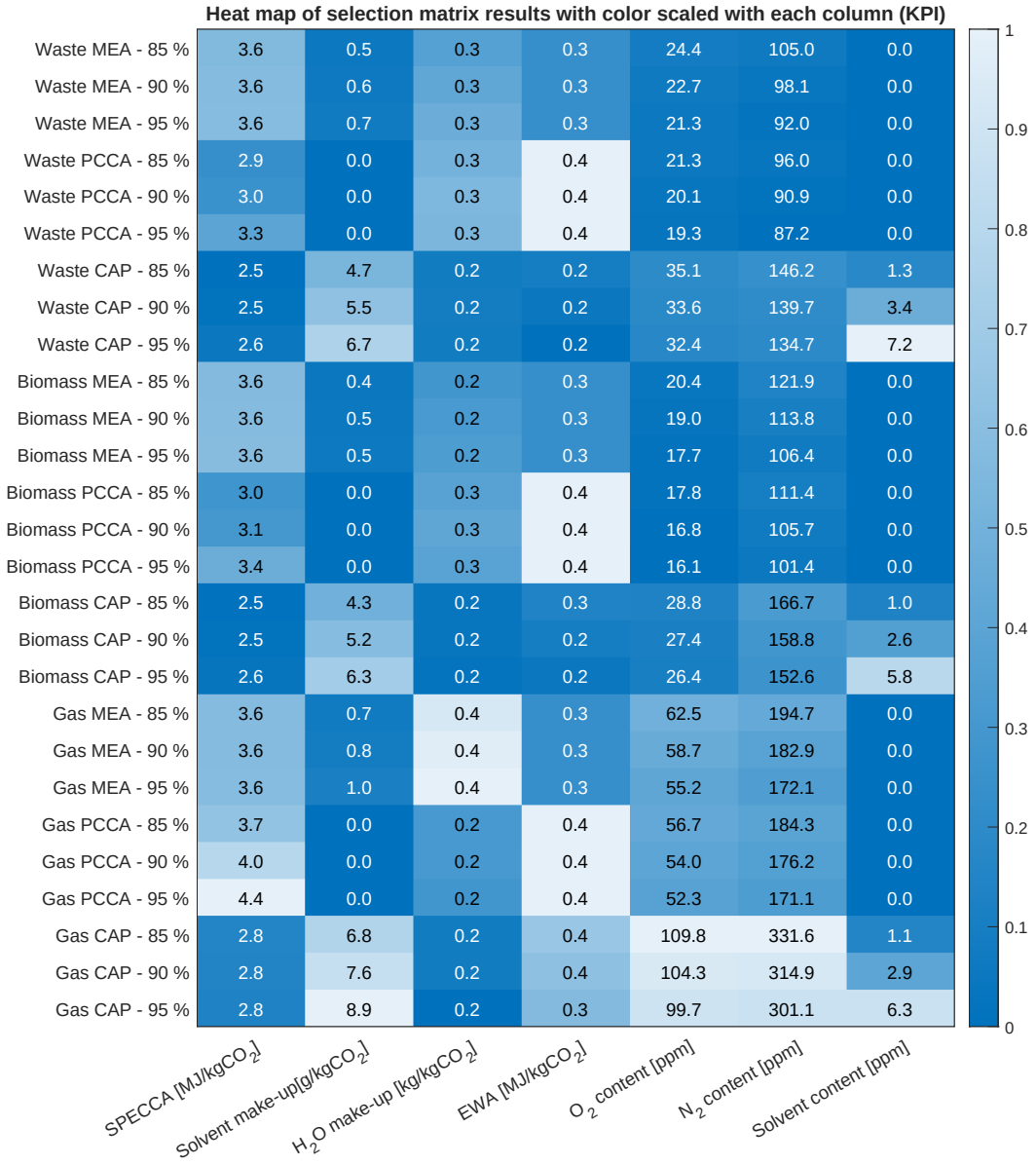

Figure E.1: Heat map of KPI scores across all conducted cases

As observed in the matrix above, the SPECCA value is lowest for the CAP, with MEA having the highest. The CAP needs the reboiler duty at approximately 138 °C where MEA

and PCCA only need heat at 120 and 78 °C, respectively. The SPECCA values show that CO_2 is more tightly bound to the solvent concerning MEA compared to PCCA and CAP. This reflects the higher heat of absorption for MEA than for PCCA and CAP.

The EWA value shows that the PCCA process requires greater electrical power per avoided CO_2 compared to MEA and CAP. CAP scores lowest in EWA value, even with the electrical work needed for chiller operation. The compressor power is significantly lower than the 10 bar desorber operation pressure. The solvent make-up, shown in grams per kg CO_2 avoided, is greatest for CAP, reflecting the highly volatile NH_3 escaping the process, yet the absolute numbers are significantly small compared to the amount for CO_2 captured. It is worth noting that the solvent make-up for MEA is a magnitude lower than CAP, while no make-up is needed for the PCCA process, as no escape of the solid K_2CO_3 is observed.

Water make-up scores show PCCA and MEA require significantly more water make-up to maintain water mass balance. This is reflected in the absorber temperatures, as higher temperatures point to higher absolute humidity, hence water escaping with the cleaned flue gas. As lean stream and flue gas temperature is lower for CAP (10 and 7 °C, respectively), the water make-up necessary is less than that of MEA and PCCA.

The O_2 and N_2 contents in the captured CO_2 are lowest for PCCA than those of MEA and CAP. This reflects that the Henry constants of O_2 and N_2 are lower regarding the PCCA alkaline solvent than for MEA and CAP. Previously explained, the CAP exhibits negligible impact on CO_2 capture, yet for the purity of the CO_2 recovered, KPI, CAP scores lowest among the technologies for this case. Additionally, the solvent content is highest for CAP, yet each technology scores below the CO_2 quality specification of 10 ppm [ABS, 2025] and aligns with the DYNAMIS recommendations for CO_2 quality regarding less than 4 vol% N_2 and below 100 ppm for O_2 [SINTEF, 2009].

Appendix F

High-Temperature Heat Pump

A high-temperature heat pump has been modeled to get an accurate estimate of the inserted utility coverage for the PCCA GCC. Table F.1 shows the input conditions and results from a simple ammonia high-temperature heat pump model.

Table F.1: Ammonia heat pump model inputs and results

Input	Unit	Value
Condeser duty	[MW]	10.0
Hot reservior temperature	[°C]	95
Cold reservior temperature	[°C]	40
Isentropic compressor efficiency	[-]	0.8
Global minimum temperature approach	[°C]	2
Results		
Evaporator duty	[MW]	7.4
Compressor work	[MW]	2.6
COP	[-]	3.9

The temperatures are assumed constant with the minimum temperature approach of 2 °C. The important results from the table above are the compressor work, which shows that 10.0 MW of thermal energy can come from 2.6 MW of electrical work. The pressure-enthalpy and temperature-entropy diagrams for the modelled heat pump are presented in Figures F.1(a) and F.1(b).

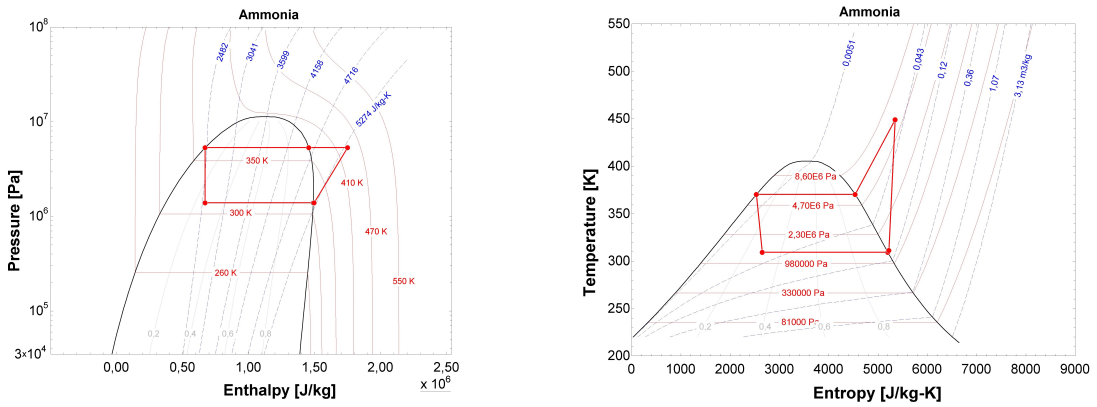

((a)) P-h diagram of ammonia heat pump

((b)) T-s diagram of ammonia heat pump

Figure F.1: Diagrams for ammonia heat pump

The figure above shows that pressure loss is neglected, yet this could impact the COP and the heat flow necessary for hot and cold reservoirs.

Appendix G

Heat Integration Illustrations for Waste-to-Energy Case

The heat integrations for MEA and CAP are different due to the temperature levels. The integration illustration for MEA is seen in Figure G.1.

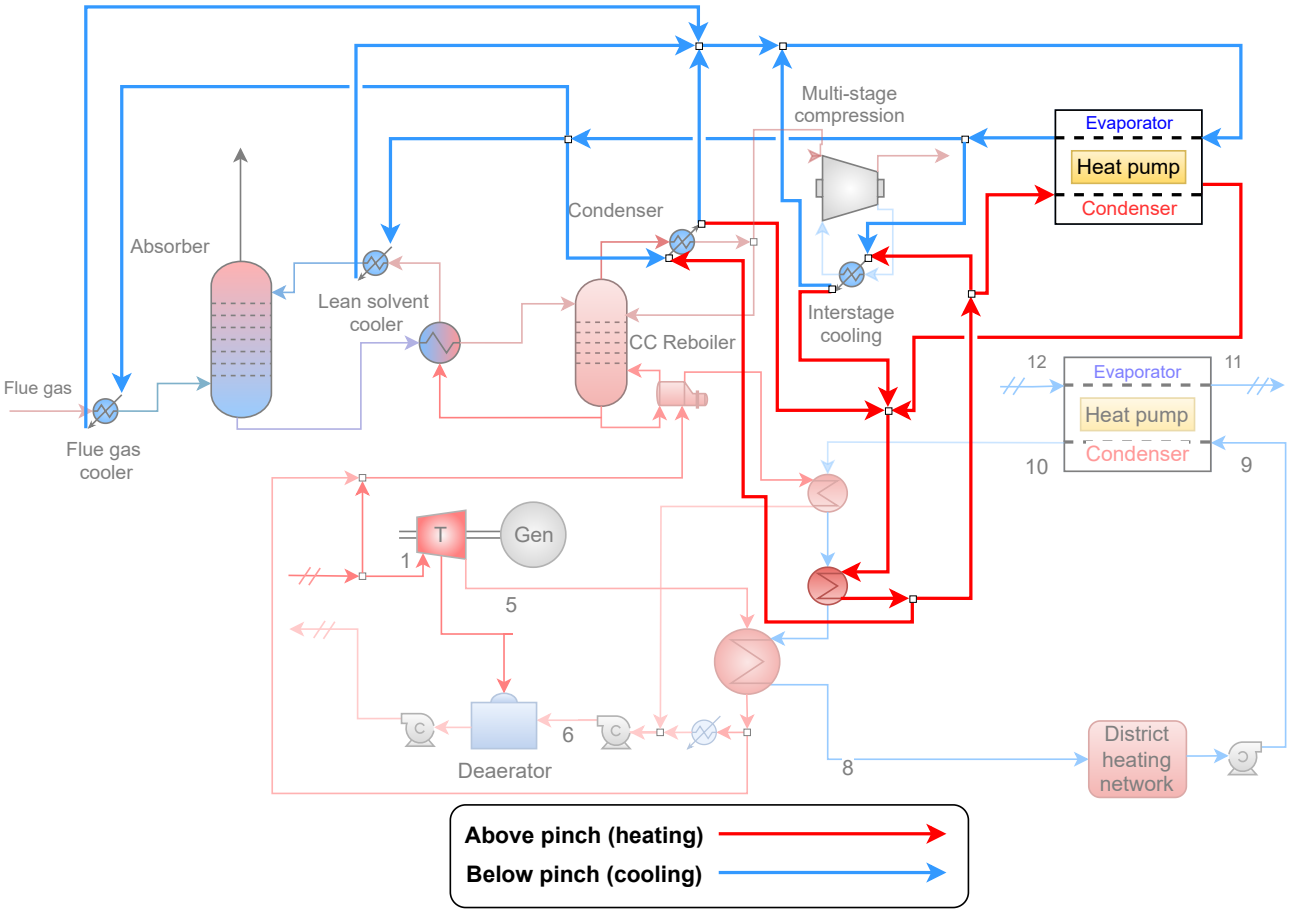

Figure G.1: Illustration of HP with water cycle integration to cover updated hot utility demand for MEA

For MEA, the above and below pinch are shown, and the difference from the PCCA is the steam extraction point. Figure G.2 illustrates the CAP integration with the WtE plant.

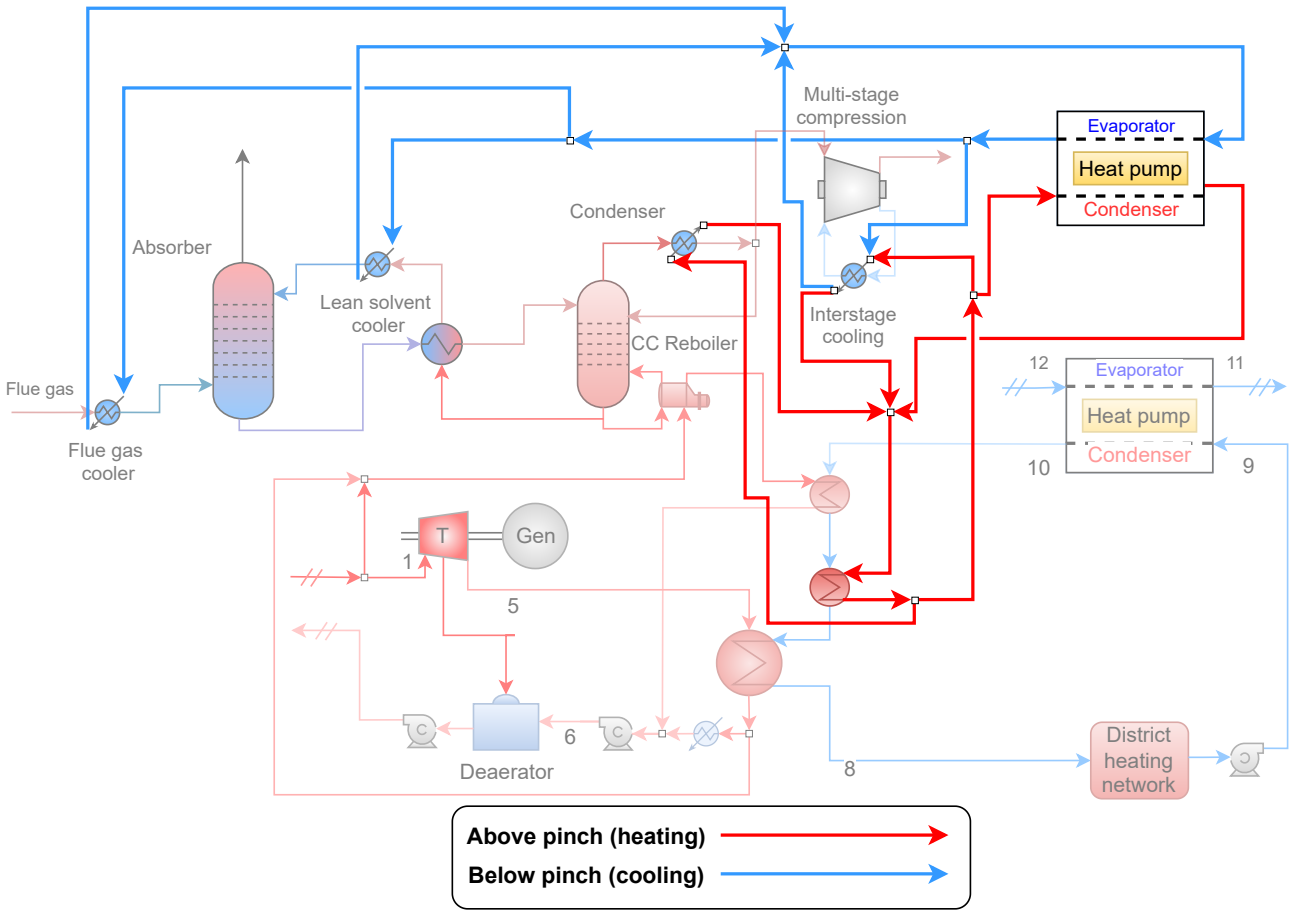

Figure G.2: Illustration of HP with water cycle integration to cover updated hot utility demand for CAP

Here, the condenser temperature is above the pinch temperature (60.4 °C) and can not be incorporated in the cooling cycle with the evaporator, yet can deliver greater energy to the district heating stream, hence the better heat integration option.